Role of local premotor nonspiking interneurons in walking pattern generation of the stick insect *Carausius morosus*

Inaugural-Dissertation

zur

Erlangung des Doktorgrades

der Mathematisch-Naturwissenschaftlichen Fakultät

der Universität zu Köln

vorgelegt von

Géraldine Freiin von Uckermann

aus Paris

Köln, April 2008

Berichterstatter:

Prof. Dr. Ansgar Büschges

Prof. Dr. Peter Kloppenburg

Tag der mündlichen Prüfung: 25.06.2008

On ne fait pas d'omelette sans casser des œufs.

(Französisches Sprichwort)

Abstract

In the course of this thesis, neural mechanisms underlying the generation of single leg stepping in the stick insect *Carausius morosus* were investigated at the premotor level. Local nonspiking interneurons (NSIs) are important premotor elements within the leg muscle control system of insects, which integrate sensory signals from different sources and provide synaptic drive onto motoneurons (MNs).

The single middle leg preparation used allows intracellular recordings from identified NSIs while the active animal performs stepping movements on a treadmill. For identification, NSIs were stained following physiological characterization by iontophoretical dye injection and viewed with a confocal laser scanning microscope. The alternating activity of flexor and extensor tibiae MNs during single middle leg stepping, which characterizes stance and swing phase, respectively, was monitored by extracellular recordings.

In the first part of the thesis, the activity pattern of NSIs driving tibial MNs during single leg stepping was studied and their contribution to the generation of stepping motor output was revealed. With the initiation of stepping, modulations of membrane potential were generated in all NSIs that were closely related to the step cycle. The activity pattern comprised distinct excitatory or inhibitory phasic input, during at least one phase of the step cycle. Most NSI types showed an inversion of membrane potential polarization from one phase of the step cycle to the other. It was shown that the activity pattern of the individual NSIs during stepping was not predictable from the synaptic drive, i.e., excitatory or inhibitory, they provide onto MNs in the resting animal. Artificial alterations of membrane potential and measurements of local input resistance for individual NSIs revealed that phasic excitatory and inhibitory modulations of membrane potential during stepping results from true excitatory and inhibitory synaptic input. Current injections into NSI I1 immediately terminated stepping sequences, indicating an important role of I1 in the control of motor output for stepping. The amplitude of phasic membrane potential modulation of NSIs during stepping varied markedly. The maximum peak-to-peak amplitude of membrane potential modulation

during stepping amounted to 16.9 ± 6.0 mV on average for all NSIs presented in this study and ranged from 5 to 34 mV for individual recordings. The time of peak and trough potential occurrence within a step cycle appears to contribute substantially to the patterning of motor output, since the extensor MN activity was closely correlated with the membrane potential of individual NSIs, e.g., E2/3, E4, E8 and I2. For the first time, it could be shown that the activity of NSIs during stepping can largely be explained by the state dependency of their inputs from the femoral chordotonal organ, one of the main leg sensors. Hence, the results presented here strongly support the notion that the motor response during the „active reaction“ represents a part of the control regime for the generation of single leg stepping.

In the second part of the thesis, the interest was to investigate neural mechanisms underlying adaptivity in locomotor systems. Therefore, it was examined which parameters contribute to alterations in stepping velocity. An important finding was that stepping velocity varies with membrane potential alterations of NSIs activated during stance phase, but not with NSIs activated during swing phase. Furthermore, the results suggest that the stance part of the locomotor network is stronger activated during fast stepping velocities and that the swing part is simultaneously inhibited to the same extent. However, investigation of extensor MN activity failed to show a correlation with stepping velocity. This finding implies that swing phase activity is independent of stepping velocity and, hence, corroborates the notion that the swing part of the premotor network does not contribute to alterations in stepping velocity. Finally, it was investigated whether there is a correlation between swing phase activation and stance phase velocity during single leg stepping. The results indicate that there is no influence between stance and swing phase activation in the single middle leg preparation, at least, not in the way that activation strength of stance would influence the subsequent activation of swing phase.

The insights gained on premotor NSIs within the femur-tibia joint control system of the stick insect raise the assumption of a premotor network organized into functionally different and partly overlapping pools of NSIs. In the single middle leg preparation, individual NSI types appear to control the actual magnitude of stepping motor output (e.g., E2/3, E8, I2) or the stepping velocity (e.g., E1, I1, I2), while others seem to control step phase transitions (e.g., E2/3, E4, I4) or phase duration (e.g., I8, I1, E1).

Zusammenfassung

Es wurden neuronale Mechanismen der Laufrhythmuserzeugung für ein Einzelbein der Stabheuschrecke *Carausius morosus* auf prämotorischer Ebene untersucht. Lokale nichtspikende Interneurone (NSIs) stellen wichtige prämotorische Elemente im Kontrollsystem der Beinmuskulatur von Insekten dar, welche sensorische Signale von verschiedenen Quellen verarbeiten und den motorischen Ausgang kontrollieren.

Im verwendeten Einbeinpräparat kann intrazellulär von identifizierten NSIs abgeleitet werden während das aktive Tier Laufbewegungen auf einem Laufband ausführt. Zur Identifikation wurden die NSIs nach physiologischer Charakterisierung iontophoretisch gefärbt und an einem konfokalen *Laser-Scanning*-Mikroskop betrachtet. Die für Stemm- und Schwingphase eines Laufzyklus charakteristische alternierende Aktivität tibialer Extensor- und Flexor-Motoneurone wurde extrazellulär registriert.

Im ersten Teil der Arbeit wurde das Aktivitätsmuster von NSIs mit Einfluss auf tibiale Motoneurone beim Einbeinlaufen untersucht und ihr Beitrag zur Laufrhythmus-erzeugung aufgedeckt. Mit Beginn einer Laufsequenz wurde in allen NSIs eine Membranpotentialmodulation im Zusammenhang mit dem Schrittzyklus erzeugt. Das Aktivitätsmuster wies deutlich erregende oder hemmende phasische Eingänge während mindestens einer Phase des Schrittzyklus auf. NSIs zeigten mehrheitlich eine Umkehrung ihres Membranpotentialverlaufs von einer Schrittzyklushälfte zur anderen. Es wurde gezeigt, dass das Aktivitätsmuster von NSIs während des Laufens nicht von dem erregenden oder hemmenden Einfluss, den sie im ruhenden Tier auf Motoneurone ausüben, vorhersagbar ist. Durch experimentelle Veränderungen des Membranpotentials und Messungen des lokalen Eingangswiderstandes von NSIs konnte aufgedeckt werden, dass die phasischen Membranpotentialmodulationen aus erregenden und hemmenden synaptischen Eingängen resultieren. Strrominjektionen in NSI I1 führten zu sofortigem Abbruch von Laufsequenzen und deuten somit auf eine bedeutende Rolle von I1 in der Laufrhythmuserzeugung hin. Die Amplitude der phasischen Membranpotential-modulationen von NSIs variierte beträchtlich. Die maximale Amplitude während des Laufens betrug 16.9 ± 6.0 mV Spitze-Spitze im Mittel für alle untersuchten NSIs und

reichte von 5 bis 34 mV in einzelnen Ableitungen. Der Zeitpunkt des Auftretens der maximalen De- und Hyperpolarisation innerhalb des Schrittzyklus scheint eine entscheidende Rolle bei der Gestaltung des motorischen Ausgangs zu spielen, da die Aktivität von Extensor-Motoneuronen maßgeblich vom Membranpotential einzelner NSIs, z.B. E2/3, E4, E8 und I2, abhing. Zum ersten Mal konnte gezeigt werden, dass die Aktivität von NSIs beim Laufen hinreichend mit der Zustandsabhängigkeit ihrer Eingänge vom femoralen Chordotonalorgan, einem der wichtigsten Beinsinnesorgane, erklärt werden kann. Dadurch unterstützen die hier vorgestellten Ergebnisse maßgeblich den Gedanken, dass die motorische Antwort während der „aktiven Reaktion“ einen Teil des Kontrollregimes für die Laufrhythmuserzeugung im Einzelbein darstellt.

Im zweiten Teil der Arbeit lag das Interesse auf neuronalen Mechanismen, welche der Adaptivität lokomotorischer Systeme zugrunde liegen. Es wurde untersucht welche Parameter zu Änderungen der Laufgeschwindigkeit beitragen. Ein wichtiger Befund war, dass Laufgeschwindigkeitsänderungen nur im Zusammenhang mit Membranpotentialmodulationen von NSIs auftreten, die während der Stemmphase aktiviert werden, nicht jedoch bei denjenigen, die während der Schwingphase aktiviert werden. Die Ergebnisse deuten darauf hin, dass der Stemmphasenteil des Kontrollnetzwerks bei hohen Laufgeschwindigkeiten stärker aktiviert wird und zugleich der Schwingphasenteil gleichermaßen gehemmt wird. Es konnte jedoch kein Zusammenhang zwischen der Aktivität von Extensor-Motoneuronen und der Laufgeschwindigkeit festgestellt werden. Dieses Ergebnis zeigt, dass die Schwingphasenaktivität unabhängig von der Laufgeschwindigkeit ist und stützt somit den Befund, dass der Schwingphasenteil des prämotorischen Netzwerks nicht zu Änderungen der Laufgeschwindigkeit beiträgt. Schließlich wurde untersucht, ob ein Zusammenhang zwischen der Aktivierung der Schwingphase und der Stemmphasengeschwindigkeit beim Einbeinlaufen besteht. Es konnte jedoch kein Einfluss der Aktivierungsstärke der Stemmphase auf die Aktivierung der folgenden Schwingphase festgestellt werden.

Die hier gewonnenen Erkenntnisse lassen vermuten, dass das prämotorische Netzwerk aus funktionell verschiedenen, teilweise überlappenden Gruppen von NSIs aufgebaut ist. Einige NSIs kontrollieren offensichtlich die motorische Ausgangsstärke (E2/3, E8, I2) oder die Laufgeschwindigkeit (E1, I1, I2), während andere den Phasenübergang (E2/3, E4, I4) oder die Phasenlänge (I8, I1, E1) zu kontrollieren scheinen.

Contents

1 Introduction 1
1.1 Locomotion 1
1.2 Leg anatomy 2
1.3 Central pattern generators 3
1.4 Afferent signals from sense organs 4
1.5 Motor control 4
1.6 Premotor nonspiking interneurons 5
1.7 Objectives of this thesis 6
2 Material and Methods 8
2.1 Single middle leg preparation 8
2.2 Video analysis of leg kinematics 9
2.3 Extracellular recordings 9
2.4 Intracellular recordings 10
2.5 Identification of premotor nonspiking interneurons 11
2.6 Single leg stepping on a treadmill 12
2.7 Data recording and evaluation 14
3 Results 16
3.1 Leg kinematics during single leg stepping on a treadmill 16
3.2 Activity pattern of nonspiking interneurons during single leg stepping 19
3.2.1 Inhibitory nonspiking interneurons 19
3.2.2 Excitatory nonspiking interneurons 25
3.3 Operating range and synaptic inputs to NSIs during single leg stepping 33
3.4 Comparison of NSI contribution to the generation of the „active reaction“ and their activity during single leg stepping 40
3.5 Correlation between NSI membrane potential and extensor MN activity during single leg stepping 50
3.6 Contribution of NSIs to alterations in stepping velocity in the single middle leg preparation 57

3.7 Correlation between extensor MN activity and stepping velocity in the single middle leg preparation 70
3.8 Correlation between stance phase velocity and swing phase activation during single leg stepping..... 74
4 Discussion..... 79
4.1 Afferent signals in the single middle leg preparation 79
4.2 Physiological properties of identified NSIs during single leg stepping..... 79
4.2.1 Activity pattern of NSIs in relation to step cycle in the single middle leg preparation 80
4.2.2 Amplitude of phasic membrane potential modulation of NSIs during single leg stepping..... 81
4.2.3 Time course of NSI membrane potential modulation during single leg stepping..... 82
4.2.4 Tonic modulation of NSI membrane potential during single leg stepping.... 82
4.2.5 NSI activity pattern during single leg stepping compared to six-legged stepping..... 83
4.3 NSIs as elements in the FT-joint control system of the stick insect middle leg .. 84
4.4 Contribution of NSIs to the generation of motor activity in the single middle leg preparation 85
4.5 Estimated number of premotor NSIs within one thoracic ganglion in insects..... 87
4.6 Correlation between NSI membrane potential and extensor MN activity during single leg stepping..... 89
4.7 Contribution of NSIs to alterations in stepping velocity in the single middle leg preparation 92
4.8 Correlation between extensor MN activity and stepping velocity in the single middle leg preparation 94
4.9 Correlation between stance phase velocity and swing phase activation during single leg stepping..... 94
4.10 Conclusions on the role of NSIs during single leg stepping and outlook to possible future projects 98
Bibliography..... 103
Appendix

Abbreviations

CI_1	common inhibitor 1
CPG	central pattern generator
CT	coxa-trochanter
DCC	discontinuous current-clamp
EMG	electromyogram
E, E-NSI	excitatory nonspiking interneuron
Ext	extensor
fCO	femoral chordotonal organ
FETi	fast extensor tibiae
Flex	flexor
freq	frequency
FT	femur-tibia
I, I-NSI	inhibitory nonspiking interneuron
KAc	potassium acetate
KCl	potassium chloride
max	maximum
MN(s)	motoneuron(s)
NSI(s)	nonspiking interneuron(s)
p-p	peak-to-peak
RMP	resting membrane potential
SETi	slow extensor tibiae
TC	thorax-coxa
t-p	time-to-peak
V	velocity

1 Introduction

Locomotion is an important behavior being part of many other complex behavioral programs, such as searching for food, searching for mating partners or avoiding predators, to give only a few examples. Many different forms of locomotion have evolved through the animal kingdom, such as flying, swimming or walking, the latter representing one of the most important ways to move for terrestrial animals. Understanding the underlying neural mechanisms responsible for locomotor control has been an objective to many researchers for several decades. The focus, thereby, is directed on basic principles and functions of the nervous system, intrinsic properties of its components, as well as on specific tasks, e.g., the control of locomotor speed and direction. These issues become very interesting, not only for researchers, when it comes to the application of scientific findings in robotics or in the development of intelligent prostheses.

1.1 Locomotion

Coordinated rhythmic activity of locomotor organs, e.g., wings, fins or legs, serves to move the animal body into a desired direction, as well as to maintain posture. A locomotor cycle divides into a power stroke for the propulsion of the animal and a return stroke of the locomotor organ. In walking systems these are the stance and swing phases, which lead to a cyclic movement of the stepping leg. During stance phase the leg is on the ground, carrying the body weight and moving backward in relation to the direction taken by the body. During swing phase the leg is lifted off the ground and swung to the starting position of the next stance phase. Walking systems are generally equipped with two, four, six or more limbs. Depending on the coordination pattern among the limbs, different gaits are discriminated. In quadrupeds, for example, the legs can be lifted one after the other (walk), or two legs are lifted at once (trot), or all four legs might leave the ground together (gallop). So, quadrupeds change from walk to trot

to gallop when the speed of locomotion increases (summary in Orlovsky et al. 1999). Thereby, the stride length of stance increases to some extent with locomotor velocity, but it is primarily a decrease in cycle period that is responsible for faster speed (cat: Halbertsma 1983; Yakovenko et al. 2005; crayfish: Clarac and Chasserat 1986; stick insect: Wendler 1964; Graham 1972; Graham and Cruse 1981). The decrease in cycle period, in turn, is generally achieved by a decrease in stance phase duration, while swing phase duration remains relatively constant (stick insect: Wendler 1964; Gabriel and Büschges 2007; locust: Burns 1973; lobster: Ayers and Davis 1974; cat: Halbertsma 1983; reviewed in Orlovsky et al. 1999). Adult stick insects can walk in a tripod, tetrapod or intermediate gait on even ground. During tripod walking, three legs are swung forward quasi simultaneously and three legs, a front and a hind leg together with the contralateral middle leg, remain on the ground performing stance phase. In the tetrapod gait, which often occurs under higher load conditions, four legs are on the ground at the same time and support the body (summary in Graham 1985).

1.2 Leg anatomy

In walking systems, locomotor organs usually are legs and typically consist of several segments connected by joints. A stick insect leg, for example, consists of more than four segments: the coxa, the fused trochantero-femur, the tibia, and the tarsal segments, which are driven by more than a dozen muscles. The three proximal leg joints, thorax-coxa (TC), coxa-trochanter (CT) and femur-tibia (FT), are each moved by sets of antagonistic muscles. Protractor and retractor coxae move the coxa back and forth, levator and depressor trochanteris enable levation and depression of the leg, and flexion and extension of the tibia is achieved by activation of flexor and extensor tibiae. For the generation of coordinated stepping movements, the leg muscles have to be activated in a rapid orderly succession, contracting and relaxing at distinct times (Bässler and Büschges 1998; Pearson 2000a).

1.3 Central pattern generators

The control of motor output is arranged hierarchically. Increasingly complex motor tasks are organized in successively higher centers. Thus, at the simplest level, sensory neurons synapse with motoneurons within the vertebrate spinal cord to mediate simple reflexes, without involvement of higher centers being required. Today, it is clear that rhythmic motor patterns, as during locomotion, are generated by neural networks within the central nervous system, called central pattern generators (CPGs), for a great variety of active locomotor systems (Grillner 1985, 2003; Pearson 1993, 2004; Marder and Calabrese 1996; Marder and Bucher 2001). Albeit CPGs can generate rhythmic motor output even in the absence of sensory feedback or descending inputs from higher brain centers (reviewed in Pearson 1993; Stein et al. 1997), numerous examples show that a functional motor program requires sensory feedback reporting the actual movements from the periphery (Clarac et al. 2000; Pearson 2000a, 2004; Grillner and Wallén 2002; Fouad et al. 2003). With few exceptions, motor output is continually updated and adjusted by sensory feedback.

For stick insects, it was shown that each of the six legs has its own CPG for walking, located in the thoracic ganglia (Cruse 1990; reviewed in Bässler and Büschges 1998). The prothoracic ganglion controls the front legs, the mesothoracic ganglion controls the middle legs and the metathoracic ganglion controls the hind legs, with the CPG lying in the respective hemiganglion of each leg (Wendler 1977; Foth and Bässler 1985a,b; Cruse 1990; Bässler 1993a). The detailed topology of CPGs is not known, although some premotor interneurons have been identified within the network (Büschges 1995a). By means of tactile stimulation of the stick insect’s head or abdomen, as well as by application of the muscarinic agonist pilocarpine to deafferented thoracic ganglia, these networks can be activated and generate rhythmic activity in antagonistic motoneuron pools of each leg joint (Bässler and Wegener 1983; Büschges et al. 1995, 2004). The activity of antagonistic motoneuron pools of each leg joint is alternating, reflecting the output of CPGs for each leg joint. Importantly, no reliable cycle-to-cycle coupling seems to be present between the motoneurons controlling different leg joints, suggesting

that the individual joint CPGs can operate rather independent of each other (Büschges et al. 1995; summary in Bässler and Büschges 1998).

1.4 Afferent signals from sense organs

The coordination of activity within and between the joint CPGs for walking arises from the continuous interaction with sense organs measuring the movement generated during locomotion and feeding it back to the CPGs (Hess and Büschges 1999; Akay et al. 2001, 2004, 2007; Bucher et al. 2003; Ekeberg et al. 2004). To do so, each leg is equipped with several sensors measuring relative position of a leg segment (hair plates and hair rows on coxa and trochanter), strain (femoral and trochanteral campaniform sensilla), as well as joint position and velocity (femoral chordotonal organ: fCO) (Wendler 1964; Bässler 1965, 1993b; Schmitz 1986; Büschges et al. 1994). Each of these sensors contributes to magnitude and timing control and is necessary to modify and adjust the ongoing motor output to actual requirements, for example, variation of walking speed or direction (reviewed in Pearson 2000b; Grillner 2003; Cruse et al. 2004; Büschges 2005; Ritzmann and Büschges 2007a,b; Büschges and Gruhn 2008; Büschges et al. 2008).

1.5 Motor control

One key mechanism, by which sensory signals contribute to the generation of motor output, is the reinforcement of ongoing movements (reviewed in Clarac et al. 2000; Pearson 2000b; Büschges and Gruhn 2008). For example, force signals from the ankle extensor muscle in the cat hind leg, elicited by stance-like activity, were found to reinforce extensor activity and such assist the control of stance phase motor output. Evidence for such control regime, especially for aspects of stance control, is known from all well studied walking systems in vertebrates and invertebrates (cat: Forssberg et al. 1975; Pearson and Collins 1993; humans: Duysens and Tax 1994; Grey et al. 2007; crab: DiCaprio and Clarac 1981; crayfish: Skorupski and Sillar 1986; E1 Manira et al. 1991; locust: Zill 1985; Bässler 1992).

Similarly, elongation of the fCO in the active locomotor system of the stick insect, signaling FT-joint flexion, reinforces flexor activity in the front and middle leg during the reflex reversal (Bässler 1976, 1988). The activity of hind leg motoneurons upon joint flexion differs depending on the influence of other legs and the walking direction (Nothof and Bässler 1990; Hellekes 2008). The reflex reversal in stick insects is the first part of the so-called „active reaction“ and occurs when the resistance reflex, which serves to maintain posture and equilibrium in the inactive animal, is reversed in sign. In posture control, elongating the fCO receptor apodeme by a passive leg flexion leads to inhibition of flexor and activation of extensor motoneurons (MNs), thus representing a negative feedback loop (Bässler 1986a). In the two-partite „active reaction“, however, a flexion of the FT-joint simultaneously excites flexor MNs and inhibits extensor MNs (positive feedback), thereby assisting the generation of stance phase activity (Bässler 1976, 1988). The second part of the „active reaction“ consists of a position dependent inactivation of flexor MNs and activation of extensor MNs (Bässler and Storrer 1980). At present, evidence suggests that this two-partite response to fCO elongation signals could contribute to the generation of leg stance and the subsequent transition into leg swing (Bässler 1986a).

1.6 Premotor nonspiking interneurons

Intracellular studies have demonstrated that the sensorimotor reflex pathways in arthropods involve both monosynaptic and polysynaptic connections, the latter including nonspiking interneurons (Burrows 1989; Bässler 1993b). In motor control systems, Mendelson (1971) was the first to describe nonspiking interneurons in the ventilatory system of hermit crabs and lobsters, which elicited spiking in two antagonistic pools of MNs upon depolarization and hyperpolarization. A number of premotor nonspiking interneurons have also been reported in other crustacean species (e.g., lobster: Graubard 1978; crab: Simmers and Bush 1980; crayfish: Heitler and Pearson 1980; Takahata et al. 1981). In many insects, it could be shown that local nonspiking interneurons (NSIs) are important premotor elements within leg muscle control systems (e.g., cockroach: Pearson and Fourtner 1975; locust: Burrows and

Siegler 1978; Wolf and Büschges 1995; stick insect: Büschges et al. 1994). NSIs integrate sensory signals from different sources, namely from local leg sensors, intersegmental pathways, descending pathways, and CPGs, and provide synaptic drive onto motoneurons (summary in Bässler and Büschges 1998; Büschges et al. 2001). The activity of individual NSIs can be supporting or opposing with respect to the actual motoneuronal output for a given motor program (Kittmann et al. 1996). A detailed insight into how identified NSIs contribute to the generation of the „active reaction“ and its associated motor output was provided by studies in the stick insect primarily (Driesang and Büschges 1996). Further investigations of the participation of NSIs in the reflex reversal revealed that the sign of the reflex results from a balance between the antagonistic contributions of individual NSIs (Bässler 1993b; Büschges and Wolf 1995). Thus, the visible motor output always represents the overall differences of all contributing sensorimotor pathways converging onto MNs (reviewed in Bässler and Büschges 1998).

1.7 Objectives of this thesis

Up to now, the question remained open whether premotor NSIs serve similar functions in the leg muscle control system during the generation of stepping, as it was inferred from their contribution to the generation of the „active reaction“. To address this issue, a preparation was needed that enables investigation of identified NSIs and their activity pattern during the generation of stepping, as well as a comparison to their contribution to the „active reaction“. Since the network of NSIs is the origin of the motor output for the „active reaction“ and for active leg movements, it is necessary to address this issue at the level of premotor interneurons, instead of studying the visible motor output solely (Büschges et al. 1994; Kittmann et al. 1996). This issue might also answer if the „active reaction“ can be considered as a functional module in the control of motor output for walking in the stick insect (summary in Bässler 1993b).

The „active reaction“ was studied in restrained preparations of decerebrated stick insects where the motor output is released by fCO stimulation only (Bässler 1986a,b). A

similar situation seems to be given in the single middle leg preparation of the stick insect. In this preparation, stepping movements of the middle leg involve only two of the proximal leg joints, the CT- and the FT-joint, and the largest change in joint angle occurs in the FT-joint (Bässler 1993a; Fischer et al. 2001). Previous studies showed that afferent movement signals from the CT-joint do not affect tibial MNs, indicating that movement signals from the FT-joint, provided by the fCO, play the most relevant role in the control of extensor and flexor MNs (Akay et al. 2001). The single middle leg preparation is thus likely to be appropriate for studying the question whether the role of identified local premotor NSIs in the generation of stepping is similar to the generation of the „active reaction“ and, consequently, if the „active reaction“ represents part of the walking motor output in the stick insect. To do so, the kinematics of middle leg stepping movements were analyzed at first. Subsequently, identified premotor NSIs were recorded in the mesothoracic segment during stepping. Furthermore, „active reactions“ were elicited during recording from identified NSIs in the single middle leg preparation. Simultaneously, the activity of tibial MNs was monitored by extracellular recordings. The semi-intact single leg preparation of the stick insect provides the additional advantage of allowing endogenous variation of motor output in respect to cycle period, speed, or strength (Bässler 1993a; Fischer et al. 2001). Hence, this preparation also enabled an analysis of premotor NSI activity in regard to alterations in stepping velocity.

Five main topics were addressed in the course of the present study:

1) How do premotor NSIs contribute to the generation of stepping motor output?
2) Does the activity of NSIs during stepping comply with their contribution to the generation of the „active reaction“?
3) How tight is the control of motoneuron activity through the premotor network?
4) Does the premotor network play a role in the control of stepping velocity?
5) Is the activation strength of swing phase influenced by the preceding stance phase?

2 Material and Methods

All experiments were performed under dimmed daylight conditions and room temperature (20 - 22°C) on adult female stick insects of the species *Carausius morosus (BRUNNER)*, from a breeding colony maintained at the University of Cologne.

2.1 Single middle leg preparation

Using the single middle leg preparation, all legs except the middle leg studied were amputated at the middle of the coxa, thereby excluding coordinating influences from sensory organs of the other legs (Fischer et al. 2001). The animal was attached dorsal side up along the edge of a foam platform using dental cement (Protemp II, ESPE, Seefeld, Germany). To avoid obstruction of coxa-trochanter (CT) joint movements, a little piece was cut out of the foam so that the coxa would not get caught or twisted. To prevent pro- and retraction of the leg, the thorax-coxa (TC) joint was blocked mechanically with dental cement and deafferented later. The platform was then placed under a stereomicroscope on a vibration isolating table in a Faraday cage for the rest of the experiment. The thorax of the animal was opened by a sagittal cut along the dorsal midline, spanning from the middle of the meso- to the middle of the metathorax. Both sides of the cuticle were folded apart and fixed with insect pins. The gut, fat, and connective tissue were removed in order to expose the mesothoracic ganglion and the lateral nerves. Tracheae were left intact wherever possible. To exclude indirect sensory influences, lateral nerves nl2, nl4 and nl5 (nomenclature according to Marquardt 1940; Graham 1985) ipsilateral to the remaining leg, as well as all lateral nerves on the contralateral side, were crushed with fine forceps. To stabilize the mesothoracic ganglion, it was lifted onto a movable waxed steel platform. The surrounding connective tissue was pinned down with small cactus spines (*Nopalea dejecta*). To improve electrode penetration, small crystals of a proteolytic enzyme (Pronase E, Merck, Darmstadt, Germany) were placed on the ganglionic sheath for 60 - 90 s, then the

enzyme was thoroughly washed out. Throughout the experiment the thorax was filled with saline (pH 7.2; composition according to Weidler and Diecke 1969).

2.2 Video analysis of leg kinematics

For the analysis of leg kinematics, the animal was mounted on a platform as described for the single middle leg preparation with the exception that the thorax was not dissected. At the distal ends of the femur and tibia, the leg was marked with orange fluorescent pigments dissolved in a shellac/alcohol solution (catalog no. 56200 “gold-orange”, Dr. Georg Kremer Farbmühle, Aichstetten, Germany). A high-speed video camera (Marlin F-033C, Allied Vision Technologies, Stadtroda, Germany) was positioned in front of the animal and aligned to its longitudinal axis, so that the plane of movement of femur and tibia was perpendicular to it. This allowed an analysis of joint angles. The leg was illuminated with blue LED arrays (24 V ac/dc, Conrad Electronic, Germany), to cause better fluorescence of the labels, and the leg movement was videotaped (100 frames/s) during stepping. The pictures were fed into a personal computer through a FireWire interface, stored as video files, and analyzed using the motion tracking software WINanalyze (Version 1.9, Mikromak service, Berlin, Germany). For definition of joint angles, the fluorescent markers on the femur and tibia were used, as well as the position of the immobilized coxa.

2.3 Extracellular recordings

Activity of extensor tibiae motoneurons (MNs) was recorded extracellularly from lateral nerve nl3, containing all three axons innervating the extensor tibiae muscle (FETi: Fast Extensor Tibiae, SETi: Slow Extensor Tibiae, and CI_1: Common Inhibitor 1; Bässler & Storrer, 1980), with a monopolar hook electrode (custom built, modified after Schmitz et al. 1988, 1991). The nerve was electrically isolated from the surrounding medium with silicon-gel (Baysilone-Paste hochviskos, Bayer AG, Leverkusen, Germany). A non-insulated silver wire of 0.25 mm diameter was used as reference electrode and

placed in the saline. The extracellular recordings were amplified and bandpass filtered (400 Hz - 3 kHz).

Flexor tibiae activity was recorded via an electromyogram (EMG) of the flexor tibiae muscle. For this purpose, two thin copper wires (50 µm diameter, insulated except for the tips) were inserted closely together through the cuticle of the proximal femur and fixed with dental cement. Because of the innervation by several excitatory MNs (up to 25 in the species *Carausius morosus*; Storrer et al. 1986; Debrodt and Bässler 1989; Goldammer 2008), it was not possible to discriminate single motor units in the EMG recordings of the flexor tibiae muscle. The signals were amplified and bandpass filtered (50 Hz - 3 kHz). All pre- and filter-amplifiers were custom built.

2.4 Intracellular recordings

Intracellular recordings of premotor nonspiking interneurons (NSIs) were made from their neuropilar arborizations in the mesothoracic hemiganglion, ipsilateral to the remaining leg. Recordings were made from NSIs that fulfilled the following criteria: (1) Manipulation of the membrane potential by injection of a current pulse influenced the activity of one or both postsynaptic excitatory extensor MNs. (2) Imposed flexion and extension of the tibia, resulting in stimulation of the femoral chordotonal organ (fCO), induced reproducible responses in the recorded interneuron. (3) No action potentials (spikes) were observed or could be elicited during the recording (for definition and identification of nonspiking neurons see: Hengstenberg 1977; Burrows 1981; Wilson 1981; Siegler 1985; Büschges 1990).

Neurons were impaled using sharp microelectrodes filled with 5% tetramethyl-rhodaminedextran (3000 MW, anionic, lysine fixable, Molecular Probes, Eugene, OR, USA; 5% in 3 M KAc/100 mM KCl) as tip solution and 3 M KAc/100 mM KCl shaft solution (electrode resistance 15 - 25 MΩ). Microelectrodes were pulled on a P-97 filament puller (Flaming/Brown Micropipette Puller, Sutter Instruments, Novato, CA, USA) using thin walled borosilicate glass (GB100-TF8P, Science Products, Hofheim,

Germany). Recordings were done in the bridge or discontinuous current-clamp (DCC) mode of an intracellular amplifier (SEC-10L, npi electronics, Tamm, Germany). A switching frequency of >12 kHz was used during recordings in the DCC mode and the electrode potential was monitored on an oscilloscope (Type 5103N, Tektronix, USA). A chloride-coated silver wire was used as reference electrode and placed in the saline. The signals were amplified with the intracellular amplifier with low-voltage headstage (both npi electronics, Tamm, Germany) and low pass filtered (~2.7 kHz).

Following physiological characterization, dye was iontophoretically injected into the cell at the end of the experiment (2.0 - 3.5 nA depolarizing current pulses of 400 ms duration at 1 Hz for 15 - 25 min). After an incubation time of 30 min to allow dye diffusion, the mesothoracic ganglion was removed from the thoracic cavity and fixed in 4% paraformaldehyde in 0.1 M phosphate buffer with 5% TritonX. After washing in TrisHCl (3 times, 15 min each), the ganglion was dehydrated with an ascending ethanol series (50%, 70%, 90%, 100%; 10 min each) and cleared in methylsalicylate. For morphological identification, NSIs were viewed with a Zeiss 510 confocal laser scanning microscope and compared to a catalog with *camera lucida* drawings of known interneurons (catalog compiled by A. Büschges).

2.5 Identification of premotor nonspiking interneurons

The different types of known premotor NSIs E1 - 8, I1, I2, I4 and I8 of the FT-joint control system in the stick insect were identified by their physiological properties and morphological characteristics, according to established criteria (Büschges 1990, 1995b; Büschges et al. 1994). All types of NSIs examined were characterized previously (Büschges 1990: E1 - 6, I1, I2; Sauer et al. 1996: E7, I4; Stein and Sauer 1998: E8; Akay 2002: I8). Morphological characteristics were soma location, course of the primary neurite, and branching pattern in the neuropil. Physiological properties were the effect of depolarizing or hyperpolarizing current injection on the postsynaptic extensor MN activity and the characteristic time course of membrane potential upon fCO stimulation (Büschges 1990, 1995b; Büschges et al. 1994). Excitatory (E) and inhibitory

(I) NSIs were distinguished according to their synaptic drive onto extensor MNs. The second digit in the nomenclature according to Büschges (1990) terms the type of NSI and is associated to its characteristics.

In the experiments presented in this study, stimulation of the fCO was performed by moving the treadmill belt with the resting leg on top of it. In the starting position, the FT-angle was approximately 100°. Moving the treadband towards the animal caused an imposed flexion of the leg and elongation of the fCO receptor apodeme. Tearing the treadband away from the animal caused an imposed leg extension and relaxation of the fCO receptor apodeme.

Two types of E-NSIs, E2 and E3, are morphologically quite similar (Büschges 1990) and differ only little concerning the response to fCO stimulation, i.e., a position dependency observed in E3 as compared to E2. Unfortunately, the position dependency of E3 varies in magnitude in the semi-intact preparation and could therefore not be used for differentiation (Büschges 1990; Sauer et al. 1996). Consequently, all NSIs that showed morphological properties of E2 or E3 were taken together as E2/3 (cf. Büschges and Wolf 1995; Stein and Sauer 1998).

Intracellular recordings were discarded when no effect on extensor MNs was present. The physiological results presented in this study are based on a total of 55 recordings from identified NSIs with effect on tibial MNs (recorded in 45 animals): three recordings from E1, nine from E2/3, five from E4, seven from E5, seven from E6, two from E7, seven from E8, three from I1, nine from I2, two from I4 and one from I8. More than 1600 step cycles were analyzed. For the quantitative evaluation of the data, the number of recordings and step cycles used are given in each case.

2.6 Single leg stepping on a treadmill

A custom made passive, low friction treadmill that allowed the animal to perform stepping movements was placed under the remaining leg, perpendicularly to the

longitudinal axis of the animal. The treadmill consisted of two styrofoam drums (40 mm diameter, width 28 mm), each mounted on a micro DC-motor (DC1516, Faulhaber, Schönaich, Germany), with a center distance of 50 mm. A belt made of light crepe paper was placed around the styrofoam drums. One of the DC-motors served as a tachometer recording the belt velocity, and the other motor was used to reduce the belt friction without moving the belt itself (details in Gabriel et al. 2003). The treadmill was height adjusted when the animal was mounted on the experimental platform, so that the femur-tibia and tibia-treadmill angles of the middle leg studied were about 90° (cf. Figure 2.1 A). By then, the animal usually was in the inactive mode.

Stepping was elicited either by a brief puff of air or by tactile stimulation of the abdomen or antennae with a soft paintbrush (Bässler 1983). Upon stimulation, the animal showed signs of arousal, such as searching movements of the antennae or bending of the abdomen, and then started to perform stepping movements. Stimulation was stopped as soon as the animal started a sequence of stepping movements. Sometimes stepping was initiated spontaneously. A typical stepping sequence was characterized by the alternating activity of flexor and extensor tibiae MNs (Figure 2.1 B). The swing phase was designated by the fast extensor (FETi) MN activity, as the extension movements during stepping are exclusively generated by the fast extensor part (summary in Bässler et al. 2007). The stance phase was demarcated by the flexor activity and the registered treadmill belt velocity. In the experiments without flexor EMG recording, the time of stance phase can be seen from the treadmill trace. Stance phase starts shortly before the raising edge of the treadmill trace (cf. Gabriel 2005). The end of stance phase corresponds to the last maximum of the treadmill trace before the velocity decreases back to zero (cf. Borgmann et al. 2007). The falling edge is determined by the inertia of the treadmill and does not contain any information about the status of the leg. At the transition from one phase to the other, short pauses between extensor and flexor MN activity can occur as previously reported (Fischer et al. 2001).

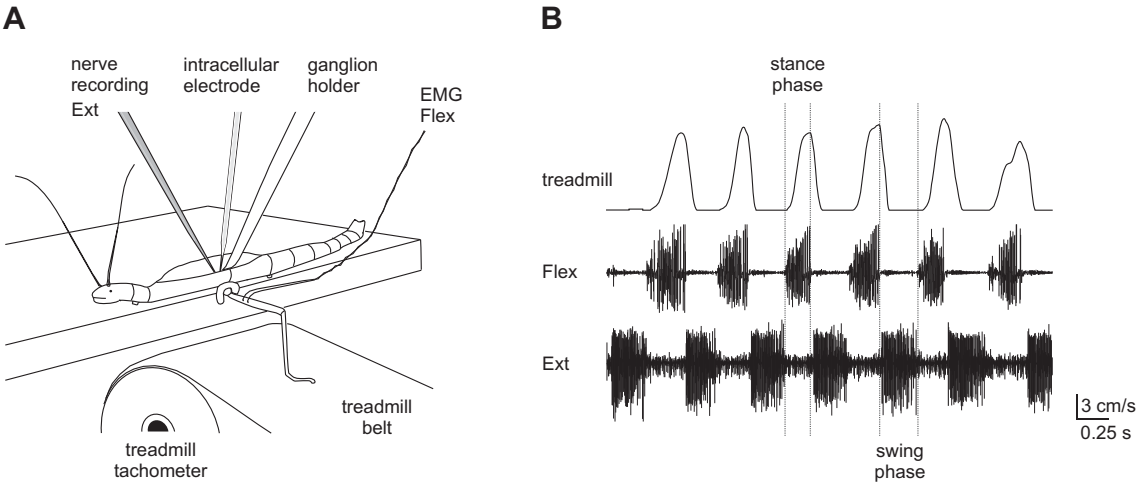

Figure 2.1: A Schematic drawing of the single middle leg preparation of the stick insect *Carausius morosus* used in the present study. The ganglion holder and the intracellular electrode were used for recording from nonspiking interneurons, the extracellular electrode for recording extensor (Ext) activity from nerve nl3, the wires of the electromyogram (EMG) for recording flexor (Flex) activity from the flexor muscle, the treadmill belt and tachometer to register belt velocity. **B** A typical stepping sequence with six steps is exemplified. The flexor MNs are active during stance phase and the fast extensor MN is active during swing phase.

2.7 Data recording and evaluation

Electrophysiological signals and the voltage output of the treadmill tachometer were digitized and recorded on a personal computer using a Micro1401 A/D converter and Spike2 software (both Cambridge Electronic Design, Cambridge, UK). The second DC-motor of the treadmill was connected to the voltage-current converter and a custom Spike2 sequencer program (written by J. P. Gabriel) was used to apply a continuous current to the motor. For the A/D conversion, a sampling rate of 6.25 kHz was used for the tachometer signal and the intracellular recordings, and 12.5 kHz for extracellular recordings and 5-fold amplified intracellular recordings. At these sampling rates, no loss of information could be detected compared to the signal displayed on the oscilloscope.

Recorded data was analyzed using Spike2 software and scripts written by the author. For instance, to enable the analysis of the time-to-peak of instantaneous FETi spike frequency (1/interspike interval), a Spike2 script was written that evaluated the necessary values in consideration of the following criterion. To ensure that the peak of FETi spike frequency was set correctly, the two interspike intervals neighboring the shortest interspike interval of a burst needed to be similarly short.

For each NSI recording, the maximum peak-to-peak amplitude (p-p) of the membrane potential modulation during stepping was determined. To do so, each recording was analyzed for both the maximum hyperpolarization and the maximum depolarization, which occurred in the course of all stepping sequences of one experiment. Subtraction of these two values gave the maximum p-p amplitude for an individual recording.

Regression analysis was used to analyze linear correlation between two variables. The correlation coefficient was determined and tested for significance with the Fisher test (Sachs 1971). Mean values were compared to zero or among each other using a t-test. Means, samples and correlation coefficients were regarded as significantly different from zero or from each other at $P < 0.05$. The following symbols show the level of statistical significance: (n.s.) not significant $P > 0.05$; (*) $0.01 \leq P < 0.05$; (**) $0.001 \leq P < 0.01$; (***) $P < 0.001$. Values are shown as mean ± standard deviation (SD). "N" gives the number of experiments and "n" gives the sample size.

Statistical analysis and plots were rendered using Excel 2002 (Microsoft) and Origin 6.0 (Microcal). Layout editing was performed with Corel Draw 11 (Corel Corporation).

3 Results

3.1 Leg kinematics during single leg stepping on a treadmill

At first, the kinematics of single middle leg stepping movements were analyzed to test whether the single middle leg preparation is an appropriate preparation to study the question in focus.

The cyclic leg movement during stepping on a treadmill is illustrated as a stick figure (Figure 3.1 A). During stance phase, the leg is moved towards the body by a flexion of the FT-joint (red dashed arrow). During swing phase, the leg is first lifted and extended (long black arrow), then the extended leg is moved downward again (short black arrow) and thereby the step cycle is completed. The positions of the fluorescent joint markers, which were used for the motion tracking analysis, are depicted as they changed over space during several steps (Figure 3.1 B). Joint angles were defined as symbolized by the two-headed arrows. During stepping there were major changes in FT-angle, whereas the amplitude of movement in the CT-joint was modest in comparison. The TC-joint was not modified as the coxa is restrained in the single leg preparation. The joint angles are shown as they changed over time during six steps of a typical stepping sequence (Figure 3.1 C). The CT-angle peaked two times, once at the beginning and once at the end of stance phase. During stance, the CT-angle altered only little in between the two peaks. The minimum CT-angle appeared at the middle of swing phase. The FT-angle was maximum at the transition from swing to stance. During leg flexion in stance phase, the FT-angle decreased gradually and reached its minimum at the transition from stance to swing. With the beginning of swing phase, the FT-angle increased until the end of swing. Alterations in the FT-angle were similar during stance and swing, respectively, since both the maximum and the minimum occurred right at the transitions. During one step cycle, the FT-joint reached angular peak-to-peak (p-p) amplitudes twice as big as the CT-joint (Table 3.1). The same was true for the change in joint angle during swing phase. During stance phase, however, the p-p amplitude of FT-angle was a multiple of

the change in CT-angle. The animal performed steps with different velocities within one stepping sequence as can be seen from the treadmill trace.

Table 3.1: CT- and FT-angle p-p amplitude during single middle leg stepping on a treadmill, given as mean ± SD. Three animals and 89 step cycles were analyzed (N = 3, n = 89).

	animal 1	**animal 2**	**animal 3**
n	27	35	27
CT [°]	48 ± 8.5	43.2 ± 5.3	36.3 ± 3.9
FT [°]	90.6 ± 11.8	80.3 ± 10.3	70.8 ± 10.7

To describe joint coordination geometrically, in a time independent manner, the interplay of the two joints during the step cycle was plotted as CT-angle *versus* FT-angle (Figure 3.1 D). The y-axis was inverted to facilitate comparison to Figure 3.1 (A) and (B). The slightly curved part of the plot, resulting during stance phase (red dashed arrow), is caused by the distal part of the tibia moving virtually parallel to the treadband (see Figure 3.1 B). Based on this property of joint geometry, the leg movement during stance phase could sufficiently be explained by an initial activation of depressor coxae MNs, keeping the leg down and the tarsus against the treadband, accompanied by the activity of flexor tibiae MNs being regulated in the course of stance phase. Swing phase (black arrows) appears as a two-partite movement, which closes the loop. A short pause in a stepping sequence would not disturb the cyclic pattern of joint coordination, since the movement would be continued out of the stopping position, as has also been reported for the pattern of interleg coordination in intact walking animals (Wendler 1977).

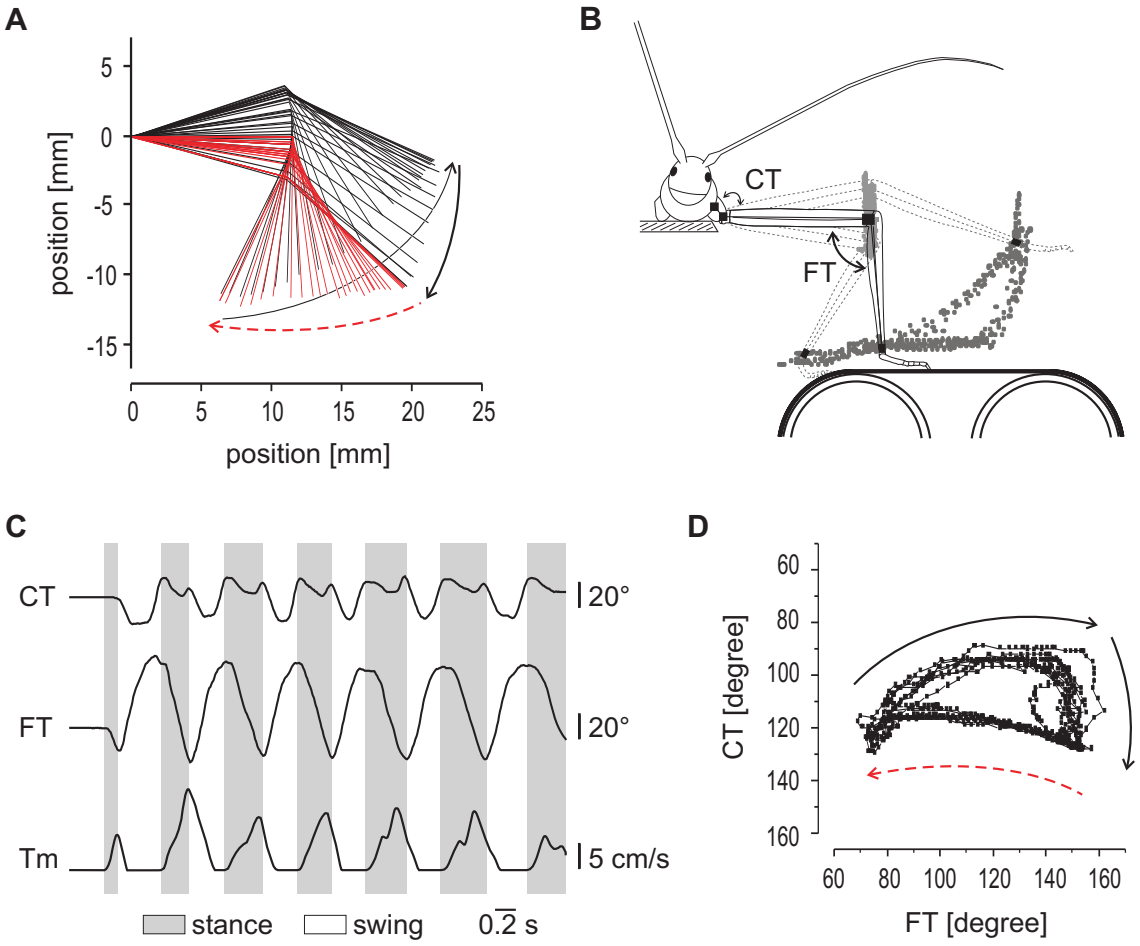

Figure 3.1: Leg kinematics during single middle leg stepping on a passive treadmill. **A** Stick figure of the leg movement. The leg was flexed and moved towards the body during stance phase (red dashed arrow). During swing phase, the leg was first lifted and extended and then put down again (black arrows). **B** Scheme of the stepping stick insect with labeled joints and the fluorescent dots moving over space in the course of a stepping sequence. The joint angles were defined as symbolized by the two-headed arrows. **C** The CT- and FT-angles are shown changing over time in the course of a typical stepping sequence, along with the simultaneously registered belt velocity of the treadmill (Tm). The FT-joint reached angular p-p amplitudes twice as big as the CT-joint within one step cycle. During stance phase, the FT-angle p-p amplitude was a multiple of the alteration in CT-angle. **D** CT- and FT-angle during stepping plotted against one another. The y-axis was inverted for better comparability to (A) and (B). Black arrows mark swing and the red dashed arrow marks stance phase. All data shown resulted from the same stepping sequence, exemplified in (C).

3.2 Activity pattern of nonspiking interneurons during single leg stepping

In the following, the activity pattern of individual types of identified premotor NSIs during single middle leg stepping will be described, first for the known types of inhibitory interneurons I1, I2, I4 and I8, then for the excitatory types of NSIs E1 - 8.

3.2.1 Inhibitory nonspiking interneurons

NSI I1 provides inhibitory synaptic drive onto both excitatory extensor MNs. Injection of depolarizing current into I1 inhibits the activity of SETi and FETi, while injection of hyperpolarizing current releases SETi from inhibition (Büschges 1990). During single middle leg stepping, NSI I1 (N = 3, n = 133) exhibited a strong modulation of membrane potential around the resting membrane potential (RMP). An episode from one recording is exemplified in Figure 3.2 (A). The RMP of the recording shown was -60 mV and the mean RMP of all recordings from NSI I1 was -52 ± 9.2 mV. The membrane potential of NSI I1 depolarized rapidly and with large amplitude during stance, which is the phase of stepping where the FT-joint undergoes flexion. The level of depolarization was constant throughout stance. NSI I1 was hyperpolarized with the induction of leg swing. The level of hyperpolarization was kept during swing. The maximum p-p amplitude of modulation in NSI I1 during stepping was large, being 25 mV in the recording shown and 19 ± 5.3 mV on average for all recordings. The extended presentation of two steps (Figure 3.2 B) shows that the depolarization of NSI I1 seen during stance started by the time of the last FETi spike of the preceding swing phase. At the transition from stance to swing, the membrane potential repolarized rapidly and hyperpolarized below RMP during leg swing. For a more detailed view on the time course of membrane potential at the transition from swing to stance, as well as during the individual phases, 13 sweeps were superimposed and the average was calculated. These sweeps were aligned at the time of the transition from swing to stance (Figure 3.2 C), or, respectively, normalized to the duration of each of both

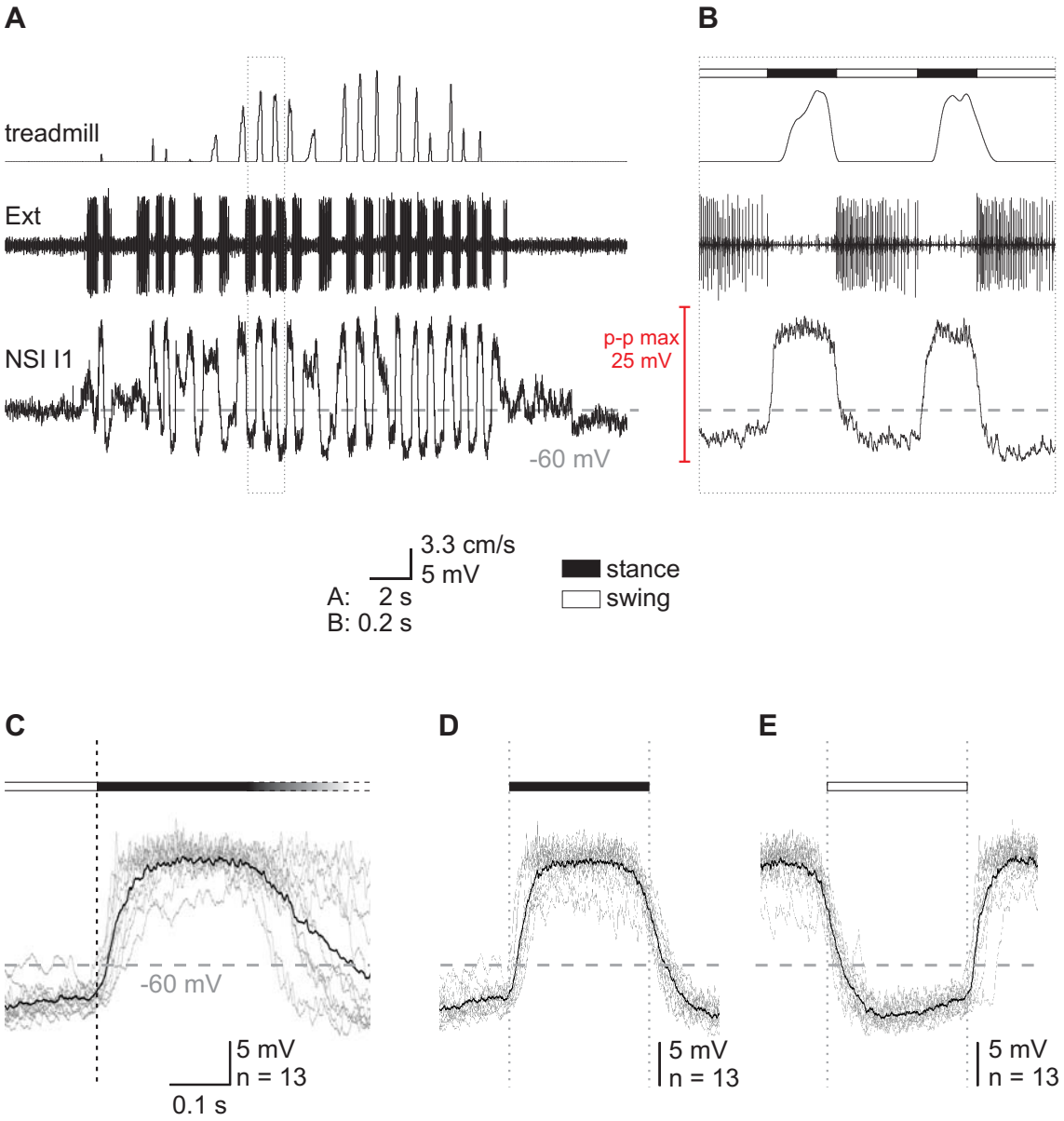

Figure 3.2: Activity pattern of NSI I1 during stepping. **A** Intracellular recording from I1 along with treadmill belt velocity and activity of extensor MNs (Ext; nerve recording) in the course of a stepping sequence. **B** Extended presentation of two steps from (A). The modulation of membrane potential reached a maximum p-p amplitude of 25 mV during stepping and the RMP was -60 mV. Stance and swing phase are labeled with a black or white bar, respectively. Overlays of 13 sweeps (grey) from the intracellular recording along with the calculated average (black), aligned at the time of the transition from swing to stance (**C**), or, respectively, normalized to the duration of stance (**D**) and swing phase (**E**). From the overlays it becomes obvious that I1 was depolarized during stance and hyperpolarized during swing.

phases, i.e., stance (Figure 3.2 D) and swing (Figure 3.2 E). From the overlays, as well as from the original recording, it becomes obvious that the membrane potential of I1 started to repolarize from depolarization shortly before the start of leg swing, thereby removing inhibition from the extensor MNs.

NSI I2 exerts inhibitory synaptic drive onto extensor MNs and excitatory drive onto flexor MNs (Büschges 1990, Büschges and Wolf 1995). Moreover, in the course of this study, it could be observed that I2 always strongly affected CT-joint MN activity, which enabled up and down movements of the leg, upon current application. During injection of depolarizing current the leg was moved downwards, while injection of hyperpolarizing current led to a lifting of the leg. During stepping, NSI I2 (N = 9, n = 326) showed a strong modulation of membrane potential around RMP. An episode from one I2 recording is exemplified in Figure 3.3 (A). The RMP of the recording presented was -65 mV and the mean RMP of all I2 NSIs recorded was -55.1 ± 5.8 mV. In the I2 recording shown, the maximum p-p amplitude during stepping reached 18 mV. The p-p amplitude of all I2 NSIs recorded was 18.1 ± 6.1 mV on average. In the extended presentation of two typical steps (Figure 3.3 B), the detailed time course of membrane potential of I2 differed visibly from I1. The peak depolarization of I2 was reached towards the end of swing phase. Throughout stance, the membrane potential slowly repolarized and finally hyperpolarized well below RMP at the transition from stance to swing. For a more detailed analysis, 38 sweeps were superimposed and aligned at the time of transition from swing to stance (Figure 3.3 C). The overlay supports the observation that NSI I2 reached its maximal depolarization in late swing, which is the time in the step cycle by when depressor MNs become active to put the leg back on the ground. The sweeps were also normalized to the duration of stance and swing phase, respectively. These overlays illustrate that I2 remained at a depolarized level throughout stance (Figure 3.3 D), followed by a hyperpolarization with subsequent depolarization from its minimal membrane potential during swing (Figure 3.3 E).

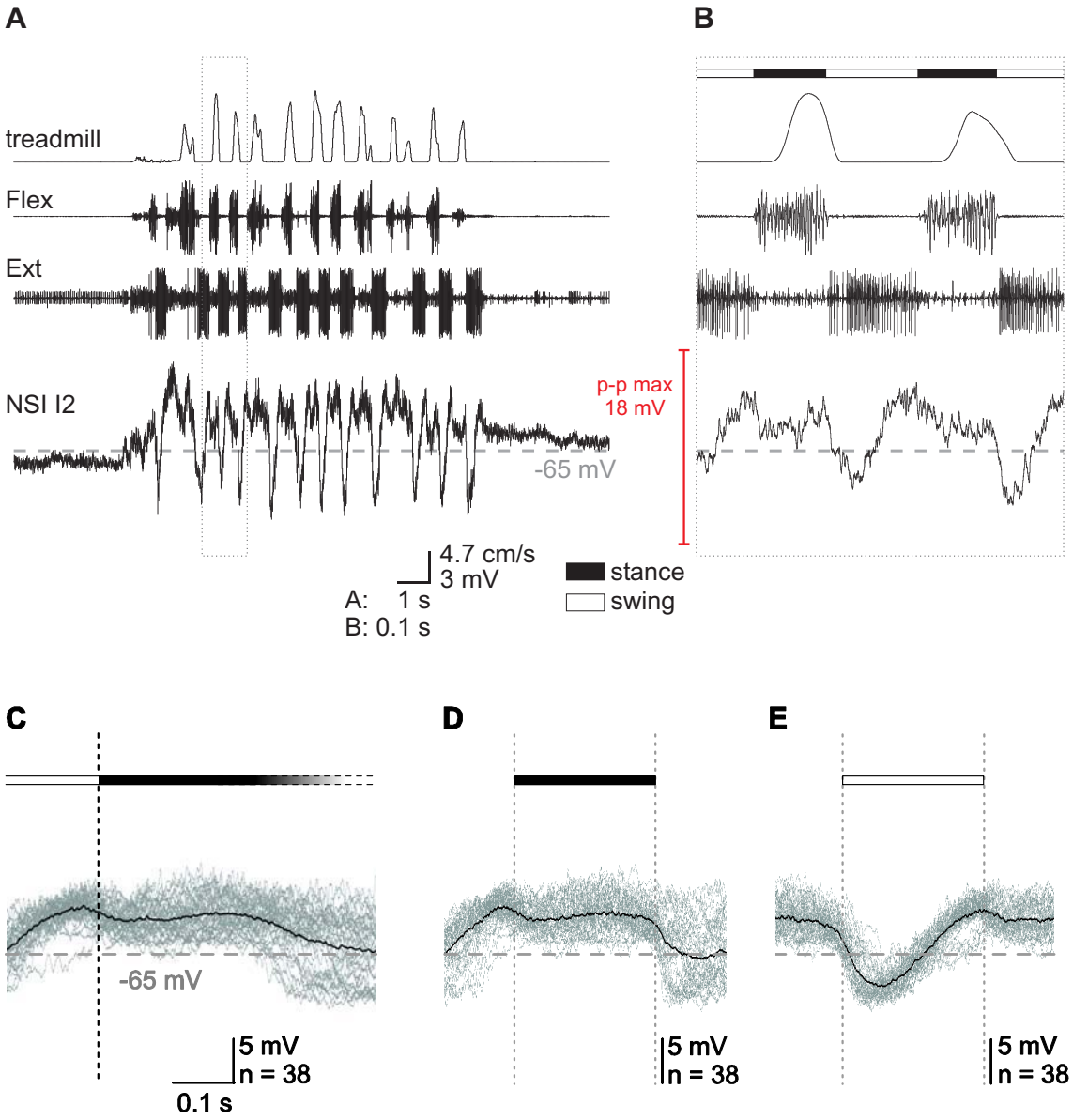

Figure 3.3: Activity pattern of NSI I2 during stepping. **A** Intracellular recording from I2 along with treadmill belt velocity, activity of flexor MNs (Flex; EMG) and extensor MNs (Ext; nerve recording) in the course of a stepping sequence. The RMP was -65 mV and the maximum p-p amplitude during stepping was 18 mV in this recording. **B** In the extended presentation of two steps, it is visible that I2 was hyperpolarized strongest by the time of highest FETi activity during swing. Stance and swing phase are labeled with a black or white bar, respectively. 38 sweeps from the intracellular recording (grey), together with the calculated average (black), were aligned at the time of transition from swing to stance (**C**) or normalized to the duration of stance (**D**) and swing phase (**E**), respectively. From the overlays it becomes obvious that the membrane potential of I2 was depolarized during stance and hyperpolarized below RMP during swing.

NSI I4 provides inhibitory synaptic drive onto SETi. Injection of depolarizing current into I4 decreases the spontaneous SETi activity. The same stimulus increases the activity of the inhibitory extensor MN CI_1 and provides excitatory synaptic drive onto depressor and flexor MNs (Büschges 1995a; Sauer et al. 1996). In contrast to the activity pattern seen in NSIs I1 and I2, the modulation of membrane potential differed for NSI I4 (N = 2, n = 33). An episode from one I4 recording is exemplified in Figure 3.4. Throughout the stepping sequence, the membrane potential was modulated above RMP and a small tonic depolarization seemed to underlie. The membrane potential depolarized throughout swing and repolarized during stance. In the I4 recording shown, the maximum p-p amplitude was 16 mV and the RMP was -58 mV. The other recording showed a p-p amplitude of 17 mV and a RMP of -50 mV.

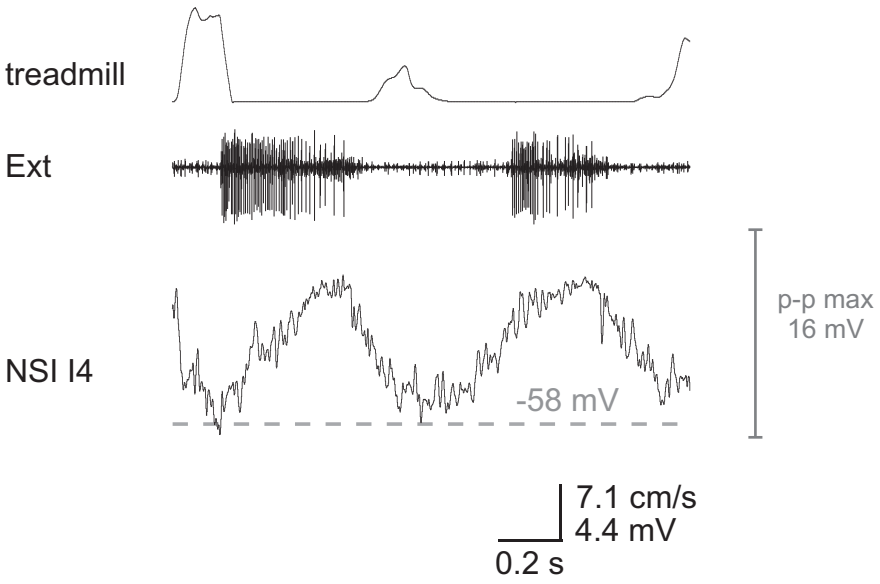

Figure 3.4: Activity pattern of NSI I4 during stepping. Episode from a stepping sequence showing treadmill belt velocity, extensor MN activity (Ext; nerve recording) and an intracellular recording from I4. NSI I4 was depolarized during swing and repolarized during stance. The RMP was -58 mV and the maximum p-p amplitude amounted to 16 mV in this recording.

NSI I8 provides inhibitory synaptic drive onto SETi. Injection of depolarizing current terminates spontaneous SETi activity (Akay 2002). During stepping, I8 (N = 1, n = 4) was rapidly depolarized at the beginning of swing and the membrane potential kept depolarized until the beginning of stance, even if there was a pause between FETi activity and the beginning of stance phase (Figure 3.5, see asterisks). The membrane potential started to repolarize only with the transition to stance. During stance, I8 was still a little depolarized compared to RMP (-49 mV). The maximum p-p amplitude was 10 mV.

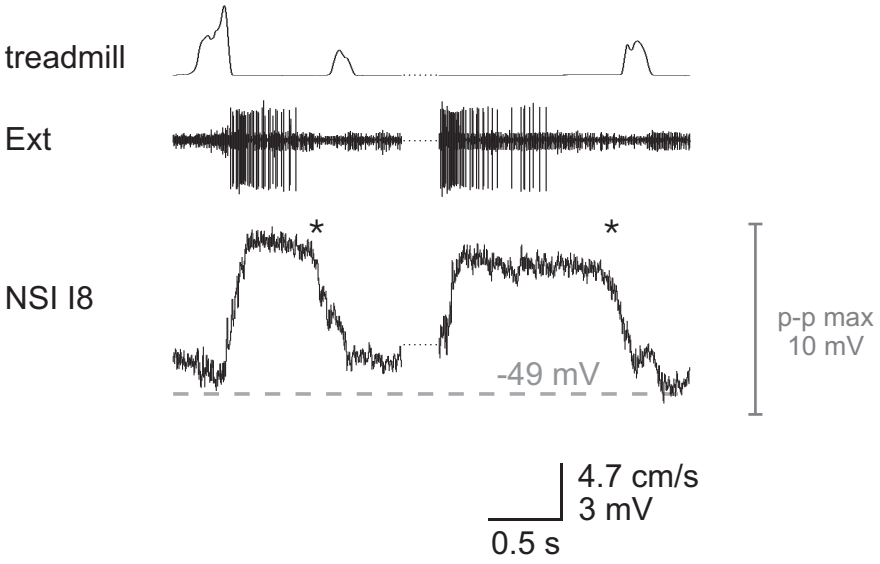

Figure 3.5: Activity pattern of NSI I8 during stepping. Episodes showing treadmill belt velocity, extensor MN activity (Ext; nerve recording) and an intracellular recording from I8 during stepping. I8 was depolarized during swing and started to repolarize with the beginning of stance (*). The RMP was -49 mV and the maximum p-p amplitude amounted to 10 mV in this recording.

3.2.2 Excitatory nonspiking interneurons

The NSIs E1 - 8 all provide excitatory drive onto at least one of the extensor MNs. Injection of depolarizing current into NSIs E4, E5, E6 and E8 excites the activity of both MNs, SETi and FETi (Büschges 1990; Sauer et al. 1996; Stein and Sauer 1998). NSI E4 furthermore excites levator and protractor MNs, as well as the inhibitory MN CI_1, and inhibits activity of depressor and retractor MNs (Büschges 1995a).

During single leg stepping, type E2/3 NSIs (N = 9, n = 239) exhibited a strong modulation of membrane potential around RMP. E2/3 was strongly depolarized during swing and as strongly hyperpolarized during stance when the FT-joint is flexed. An episode from one recording is exemplified in Figure 3.6 (A). The RMP of the recording shown was -54 mV and the mean RMP of all recordings from E2/3 was -55.2 ± 9.2 mV. There was a close relation between the actual membrane potential in NSI E2/3 and the FETi activity. This is exemplified in the last bit of the stepping sequence, which shows irregularly long and extended extensor activity when the leg remained on the treadmill and pushed it away (see treadmill trace). As seen in the expanded presentation of two steps, the peak depolarization occurred within swing phase (Figure 3.6 B). The maximum p-p amplitude was 16 mV for the recording shown and 17.1 ± 6.9 mV on average for all E2/3 recordings. For a more detailed view on the transition from swing to stance phase, 17 sweeps from the intracellular recording (grey) were superimposed together with the calculated average (black) and aligned at the time of the transition from swing to stance (Figure 3.6 C). At the beginning of stance, NSI E2/3 was strongly hyperpolarized and the membrane potential kept hyperpolarized well beyond RMP throughout stance phase, as becomes obvious from the average course of membrane potential normalized to the phase duration (Figure 3.6 D). The start of membrane potential depolarization in E2/3 was located around the transition from stance to swing and the peak depolarization occurred within the first third of leg swing (Figure 3.6 E).

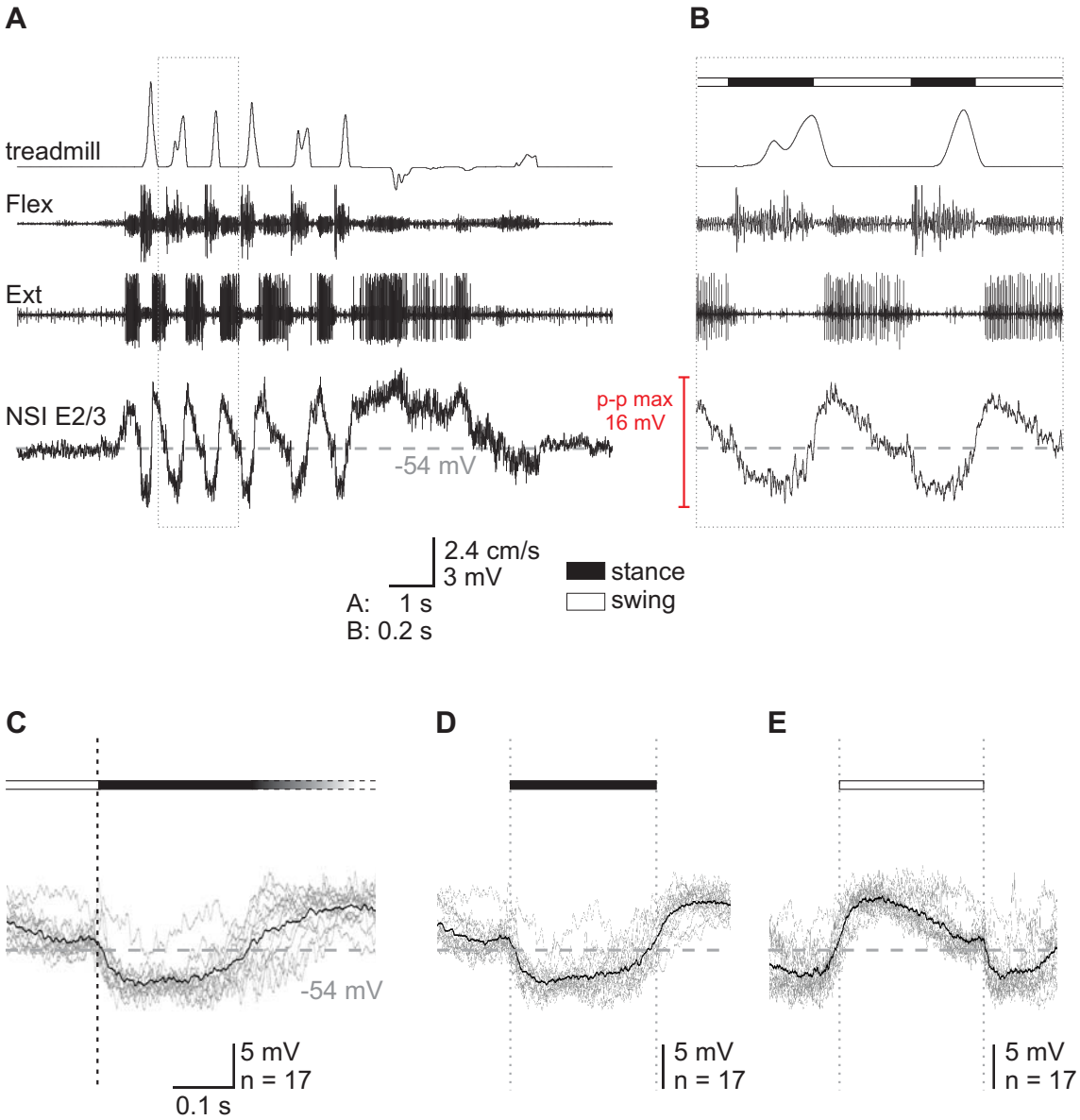

Figure 3.6: Activity pattern of NSI E2/3 during stepping. **A** Intracellular recording from E2/3 along with treadmill belt velocity, activity of flexor MNs (Flex; EMG) and extensor MNs (Ext; nerve recording) in the course of a stepping sequence. The RMP was -54 mV. **B** Extended presentation of two steps. Stance and swing phase are labeled with a black or white bar, respectively. The modulation of membrane potential reached a maximum p-p amplitude of 16 mV during stepping in this recording. The small units visible in the flexor EMG during swing resulted from a crosstalk of extensor activity. **C** Transition from swing to stance: 17 sweeps from the intracellular recording (grey) superimposed and aligned at the time of the transition. The calculated average is drawn in black. The sweeps were also normalized to the duration of stance (**D**) or swing phase (**E**), and superimposed. From the overlays it becomes obvious that E2/3 was hyperpolarized during stance and depolarized during swing.

NSI E8 (N = 7, n = 280) showed modulations of membrane potential during stepping, which were qualitatively similar to those of E2/3. An episode from one E8 recording is exemplified in Figure 3.7. The membrane potential strongly hyperpolarized during stance and strongly depolarized during swing. A maximum p-p amplitude of 30 mV was reached in this recording. The p-p amplitude of all E8 NSI recordings was 18.4 ± 7.8 mV on average. The RMP in the recording shown was -45 mV and the mean RMP of all E8 NSIs was -57.1 ± 8.8 mV.

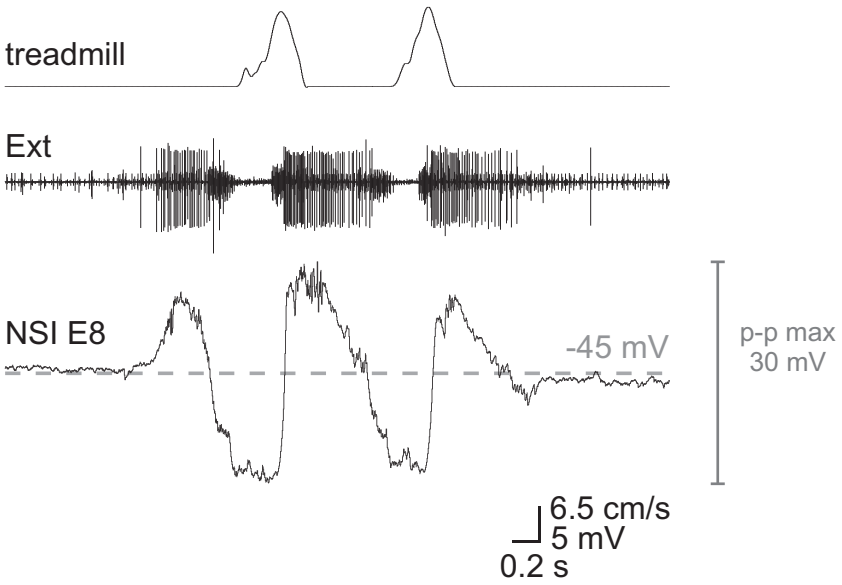

Figure 3.7: Activity pattern of NSI E8 (intracellular recording) during stepping along with treadmill belt velocity and activity of extensor MNs (Ext; nerve recording). The activity pattern of E8 was qualitatively very similar to NSI E2/3. E8 was hyperpolarized during stance and depolarized during swing. The modulation of membrane potential reached a maximum p-p amplitude of 30 mV in this recording. The RMP was -45 mV.

During stepping, NSI E5 (N = 7, n = 99) showed modulations of membrane potential qualitatively similar to those of types E2/3 and E8. An episode from one E5 recording is exemplified in Figure 3.8. NSI E5 was hyperpolarized during stance and depolarized during swing. In most recordings, the peak depolarization was reached towards the middle of swing phase. The maximum p-p amplitude amounted to 14 mV in this recording and to 17 ± 2.3 mV on average for all E5 recordings. The RMP was -58 mV in the recording shown and the mean RMP of all E5 NSIs was -51.7 ± 4.6 mV.

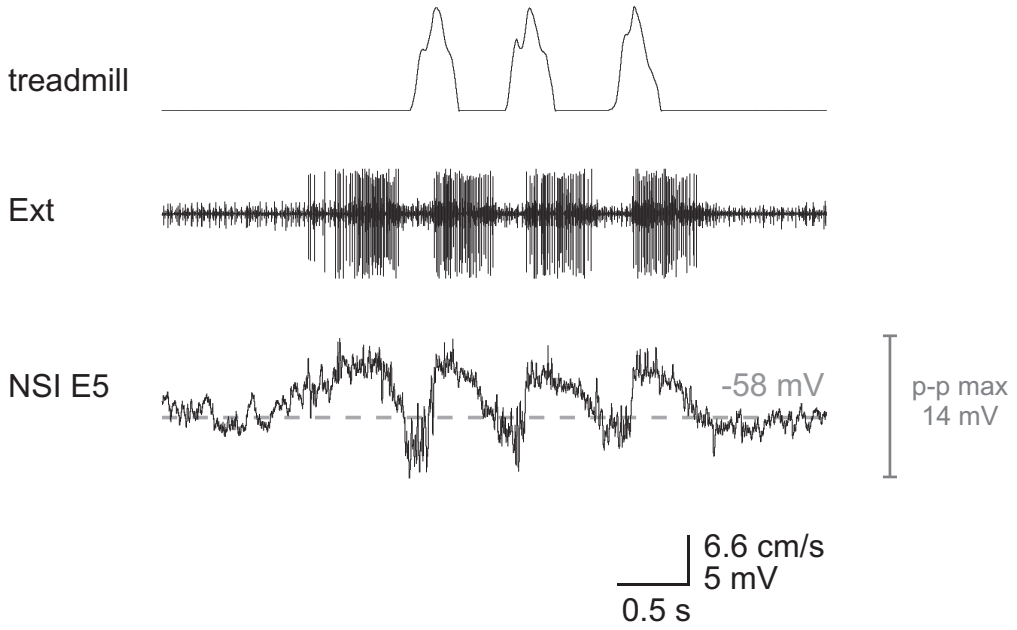

Figure 3.8: Activity pattern of NSI E5 during stepping. Intracellular recording from E5 along with treadmill belt velocity and activity of extensor MNs (Ext; nerve recording). E5 was hyperpolarized during stance and depolarized during swing. The RMP was -58 mV and the maximum p-p amplitude reached 14 mV in this recording.

NSI E4 (N = 5, n = 284) exhibited strong modulations of membrane potential during stepping. An episode from one E4 recording is exemplified in Figure 3.9 (A). The membrane potential was modulated at a relatively depolarized level compared to RMP (-55.6 mV), and rode on top of a small tonic depolarization. The mean RMP of all E4 recordings was -55.9 ± 6.6 mV; a similar value has been previously reported (Sauer et al. 1995). The maximum p-p amplitude during stepping amounted to 15 mV in the recording shown and to 19.8 ± 7.3 mV on average for all E4 recordings (Figure 3.9 B). For a more detailed view on the transition to stance phase, 24 sweeps were superimposed and aligned at the time of the transition from swing to stance (Figure 3.9 C). During stance phase, the membrane potential was depolarized compared to RMP, but no additional phasic modulation occurred (Figure 3.9 D). At the start of leg swing, E4 was rapidly depolarized to peak. Then, the membrane potential gradually repolarized throughout the ongoing swing phase (Figure 3.9 E). Thereby, the activity pattern of E4 differed from the activity of the E-NSIs described until now.

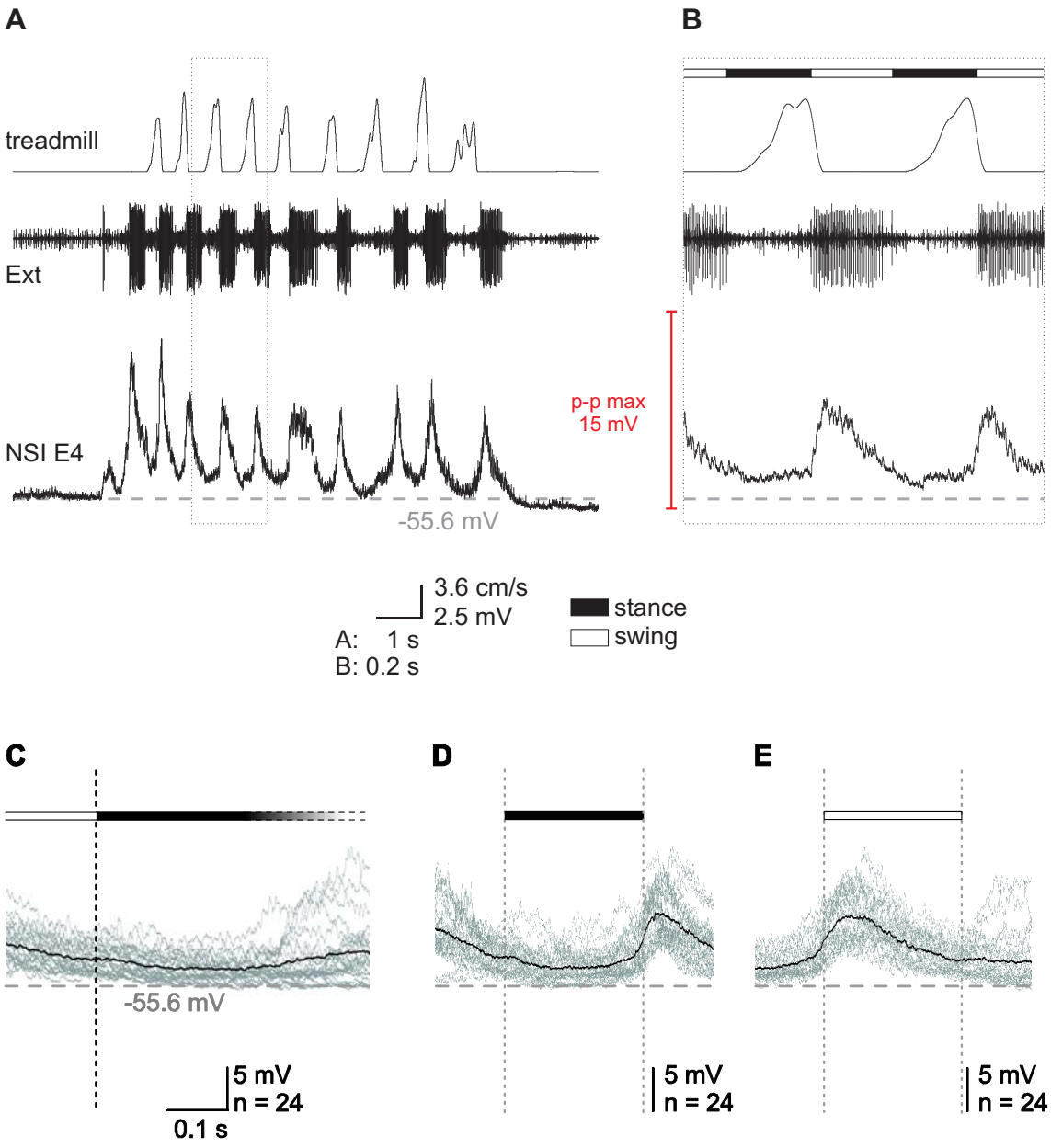

Figure 3.9: Activity pattern of NSI E4 during stepping. **A** Intracellular recording from E4 along with treadmill belt velocity and activity of extensor MNs (Ext; nerve recording). There was a strong phasic modulation of membrane potential during stepping on top of a small tonic depolarization. **B** Extended presentation of two steps. Stance and swing phase are labeled with a black or white bar, respectively. The maximum p-p amplitude reached 15 mV in this recording and the RMP was -55.6 mV. **C** Transition from swing to stance: 24 sweeps from the intracellular recording (grey) are aligned at the time of the transition together with the calculated average (black). The sweeps were also normalized to the duration of stance (**D**) and swing phase (**E**), respectively, and superimposed. From the overlays it can be seen that E4 was depolarized at a constant level throughout stance phase compared to RMP. The peak depolarization was reached shortly after the transition to swing. During the ongoing swing phase the membrane potential repolarized.

The activity pattern of NSI E1 during stepping stood in contrast to the activity pattern described for NSIs E2/3, E5 and E8. The membrane potential of E1 (N = 3, n = 128) depolarized during stance and hyperpolarized during swing. An episode from one E1 recording is exemplified in Figure 3.10 (A). E1 showed strong modulations of membrane potential during stepping. The p-p amplitude was 12.7 ± 2.5 mV on average and reached a maximum of 13 mV in the recording shown (Figure 3.10 B). From the presentation of three extended steps, as well as from the overlay of 37 sweeps from the intracellular recording, aligned at the time of the transition from stance to swing, it can be seen that the depolarization of E1 started shortly after the last FETi spike of the preceding swing phase burst (Figure 3.10 B, C). Sometimes, E1 was hardly depolarized above RMP during stance (Figure 3.10 D). During swing, E1 was strongly hyperpolarized (Figure 3.10 E). The RMP was -43 mV in the present recording and the mean RMP of all E1 recordings was -41 ± 7.2 mV.

The activity of NSI E7 (N = 2, n = 24) resembled E1 qualitatively by showing a depolarization during stance and a hyperpolarization during swing. However, in contrast to the other NSI types, E7 showed only very small modulations of membrane potential during stepping. An episode from one E7 recording is exemplified in Figure 3.11. The RMP was -40 mV and the maximum p-p amplitude amounted to 5 mV in the recording presented. The other recording showed a p-p amplitude of 7 mV and a RMP of -53 mV.

E6 NSIs (N = 7, n = 133) were found to be depolarized during stance and hyperpolarized during swing. Thereby, the activity qualitatively resembled E1 and E7. However, the amplitude of modulation was much bigger than in E7. An episode from one E6 recording is exemplified in Figure 3.12. The maximum p-p amplitude amounted to 20 mV in the recording presented and to 16.3 ± 5.7 mV on average for all E6 NSIs. At the beginning of stance, there was a sharp depolarization of large amplitude. In the course of the ongoing stance phase, E6 was further depolarized until the end of stance. The membrane potential repolarized quickly with the transition to swing and was hyperpolarized during swing. The RMP was -68 mV in the recording shown and the mean RMP of all E6 recordings was -63 ± 9.3 mV.

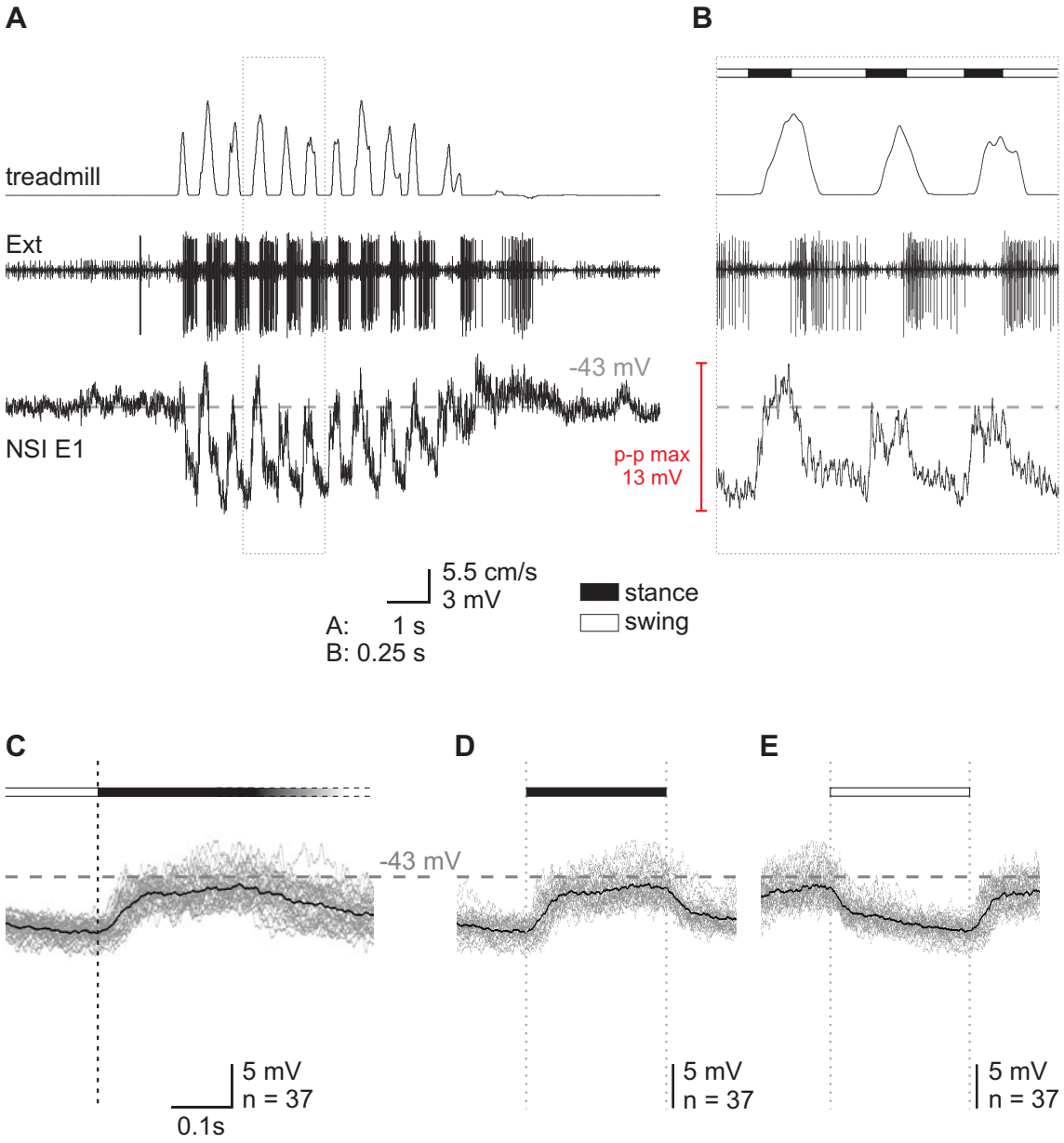

Figure 3.10: Activity pattern of NSI E1 during stepping **A** Intracellular recording from E1 along with treadmill belt velocity and activity of extensor MNs (Ext; nerve recording) in the course of a stepping sequence. **B** Extended presentation of three steps. Stance and swing phase are labeled with a black or white bar, respectively. The maximum p-p amplitude of membrane potential modulation during stepping amounted to 13 mV and the RMP was -43 mV. **C** Transition from swing to stance: 37 sweeps from the intracellular recording (grey) are aligned at the time of the transition and shown with the calculated average (black). The sweeps were also normalized to the duration of stance (**D**) and swing phase (**E**), respectively, and superimposed. From the overlays it becomes obvious that E1 was depolarized during stance, even if RMP was not always exceeded, and hyperpolarized during swing.

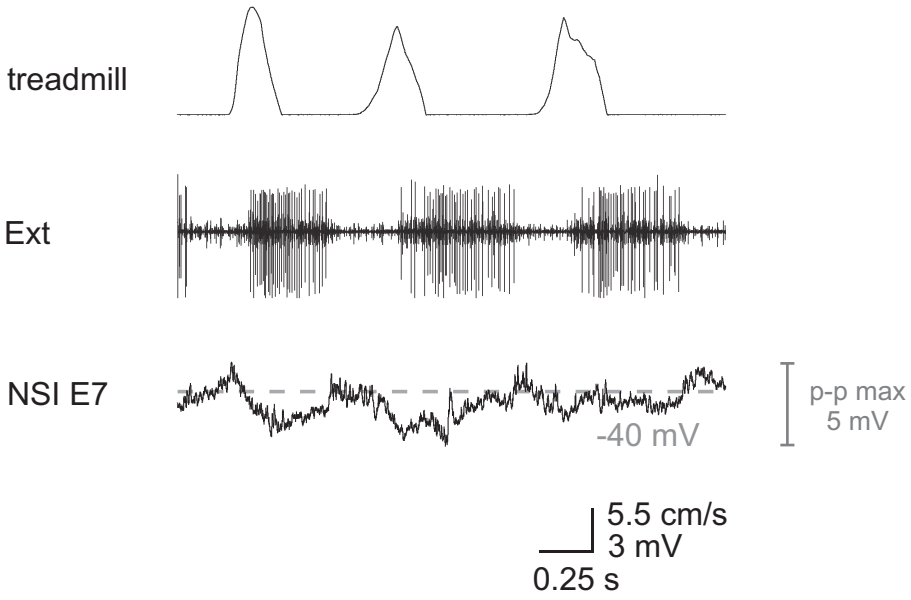

Figure 3.11: Activity pattern of NSI E7 during stepping. Intracellular recording from E7 along with treadmill belt velocity and activity of extensor MNs (Ext; nerve recording). E7 was depolarized during stance and hyperpolarized during swing. The modulation of membrane potential was very small. The maximum p-p amplitude was 5 mV. The RMP was -40 mV.

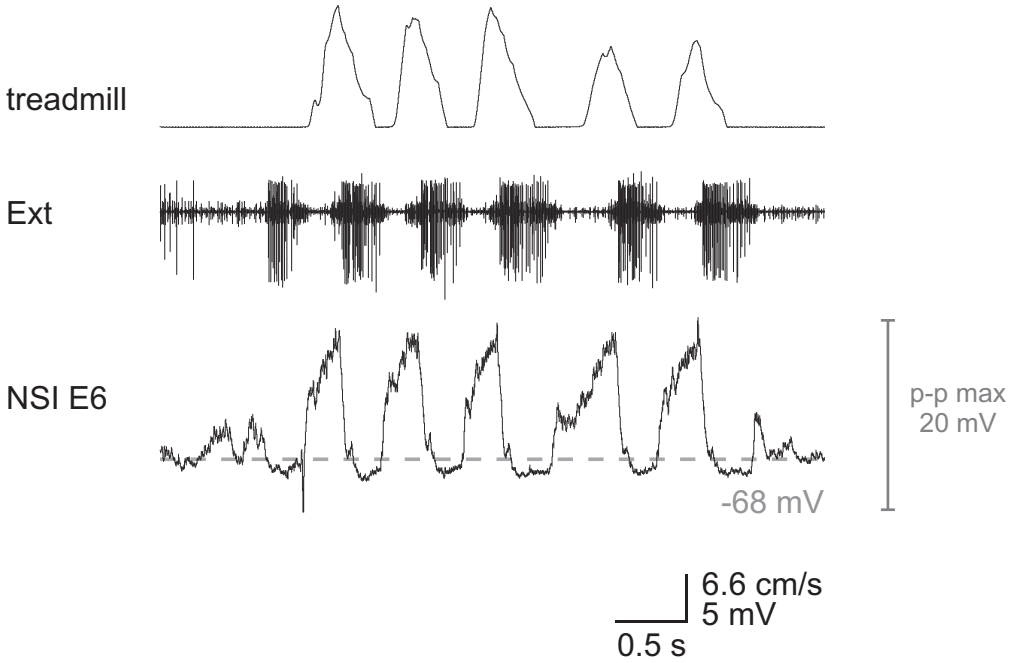

Figure 3.12: Activity of NSI E6 during stepping. Intracellular recording from E6 along with treadmill belt velocity and activity of extensor MNs (Ext; nerve recording) in the course of a stepping sequence. E6 was strongly depolarized during stance and hyperpolarized during swing. The RMP was -68 mV and the maximum p-p amplitude reached 20 mV in this recording.

3.3 Operating range and synaptic inputs to NSIs during single leg stepping

The amplitudes of membrane potential modulation during single leg stepping are summarized for all types of NSIs, together with the RMP values, to give an overview of the operating range for the NSIs analyzed (Figure 3.13). The mean RMP of all NSIs recorded amounted to -54.6 ± 8.6 mV (N = 55) and ranged from -33 to -78 mV for individual recordings. On average, the maximum depolarization for all NSIs amounted to -44.0 ± 8.1 mV (range: -29 to -65 mV). The maximum hyperpolarization for all NSIs amounted to -60.9 ± 8.7 mV on average (range: -43 to -84 mV). The maximum p-p amplitude on average for all NSIs was 16.9 ± 6.1 mV (range: 5 to 34 mV). Within each column all intracellular recordings from one NSI type are presented. In addition to the RMP values, those of the maximum depolarization and maximum hyperpolarization that occurred during stepping were also displayed, together with mean values and standard deviations (SD) in each case. Based on these values, the collectivity of NSIs fell into two main groups.

The first group contained NSIs, whose membrane potential during stepping was not only strongly but also very symmetrically modulated around the overall mean RMP. The mean RMP of NSIs in the first group amounted to -56.9 ± 8.5 mV (N = 35) and ranged from -42 to -78 mV for individual recordings. These NSIs showed depolarizations and hyperpolarizations of the same amplitude. On average, the maximum depolarization for NSIs in the first group amounted to -46.3 ± 8.3 mV (range: -30 to -65 mV). The maximum hyperpolarization for NSIs in the first group amounted to -63.9 ± 8.6 mV on average (range: -47 to -84 mV). The maximum p-p amplitude for the first group was 17.6 ± 6.2 mV on average (range: 6.5 to 34 mV). The membrane potential of NSIs in the second group was mainly modulated at levels being more depolarized than the overall mean RMP. The mean RMP of NSIs in the second group was more positive than in the first group and amounted to -50.7 ± 7.3 mV (N = 20), with a range of -33 to -62 mV for individual recordings. On average, the maximum depolarization for NSIs in the second group amounted to -40.1 ± 6.1 mV

(range: -29 to -50 mV). The maximum hyperpolarization for NSIs in the second group amounted to -55.6 ± 6.1 mV on average (range: -43 to -66 mV). The maximum p-p amplitude in the second group was 15.6 ± 5.6 mV on average (range: 5 to 30 mV). Apart from that difference, both groups showed several similarities. Each group contained two out of four identified inhibitory NSIs (I1, I2 or I4, I8; Büschges 1990; Sauer et al. 1996; Akay 2002), two out of four NSIs known to provide excitatory drive onto both extensor MNs SETi and FETi (E6, E8 or E4, E5; Büschges 1990; Stein and Sauer 1998), and at least one NSI influencing antagonistic MN-pools innervating muscles of different leg joints (I2 or E4, I4; Büschges 1990; Sauer et al. 1996).

To test for the synaptic inputs that NSIs of both groups receive during stepping, individual intracellular recordings were performed in the discontinuous current clamp mode (DCC). Through injection of constant de- or hyperpolarizing current, the RMP can experimentally be changed to another value, closer to or further away from the reversal potential of an excitatory or inhibitory current elicited by synaptic inputs. Therefore, the amplitude of voltage deflection during the phase of excitatory or inhibitory synaptic inputs also changes, depending on the electromotive force that acts on the participating ions.

Figure 3.14 shows NSI I1 at an imposed hyperpolarized or depolarized level, respectively, while the animal performed stepping. (The same neuron was shown during stepping without application of current in Figure 3.2; RMP -60 mV.) When the membrane potential of NSI I1 was held at a hyperpolarized level of -90 mV during a stepping sequence, the amplitude of depolarization was much bigger than in the situation without current application, indicating that I1 received excitatory synaptic input (Figure 3.14 A). An excitatory current, such as resulting from inflowing Na^+-ions or a mixture of cations, causes a larger depolarizing voltage deflection when the neuron is experimentally hyperpolarized, because the imposed membrane potential is further away from the reversal potential of excitation (which is more depolarized than the RMP). Reversely, the depolarizing voltage deflection was smaller when the neuron was experimentally depolarized to a level of -50 mV during a stepping sequence and thus closer to the reversal potential of excitation (Figure 3.14 Ai). An excitation can also be

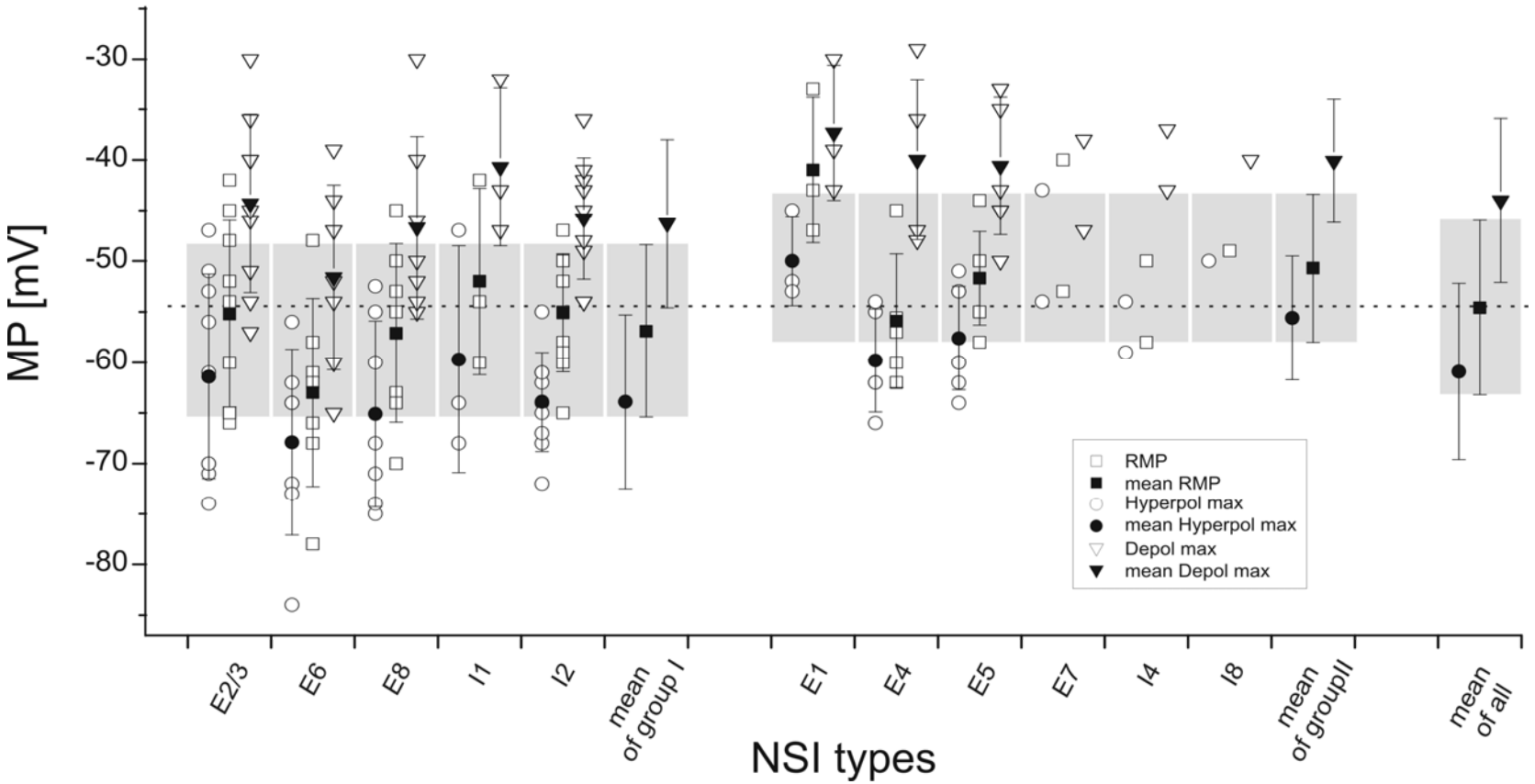

Figure 3.13: Operating range data for all NSI types analyzed. Each column shows the data of all recordings from the NSI type in question. From left to right there are in each column the values for maximum hyperpolarization, RMP, and maximum depolarization, each with the column's mean ± SD. On the right of each group there is the mean ± SD of all values of the group in question. The far right column contains the mean ± SD of all values displayed. Dashed line: mean RMP of all recordings; grey areas: mean RMP ± SD of the respective group.

caused by cessation of a persistent outward current. However, in this case the input resistance would increase, which could not be observed (see below). At the depolarized level of -50 mV, the amplitude of hyperpolarization was clearly bigger than in the situation without current application, indicating that I1 also received inhibitory synaptic input. An inhibitory current is either caused by an inflow of Cl^--ions or by an outflow of K^+-ions. The reversal potential of both currents is more negative than RMP. If the neuron is experimentally depolarized through constant application of depolarizing current, the hyperpolarizing voltage deflection will be larger, because the imposed membrane potential is further away from the reversal potential of the inhibition and thus the electromotive force is bigger. Reversely, if the neuron is experimentally hyperpolarized and thus closer to the reversal potential of the inhibition, the inhibitory current will cause a smaller voltage deflection, because of the smaller electromotive force. Apparently, the reversal potential of the inhibition was not yet reached at the imposed hyperpolarized membrane potential of -90 mV, since there was still a hyperpolarizing voltage deflection visible during the phase of inhibitory current (Figure 3.14 A). An inhibition can also be caused by cessation of a persistent inward current. However, in this case the input resistance would increase, which could not be observed (see below).

To determine whether a depolarization is due to synaptic excitation or to release from inhibition (or reversely, whether a hyperpolarization is due to synaptic inhibition or to cessation of an excitatory persistent inward current), the input resistance of individual types of NSIs was measured by injecting series of negative current pulses in the bridge or current-clamp mode of the intracellular amplifier. Individual responses resulting from a measurement of the local input resistance of NSI I1 are shown (Figure 3.14 B). One of each condition (rest, swing, stance, and again rest) is marked with a grey bar. To facilitate the comparison of voltage deflections at rest and throughout the step cycle, the grey bars all have the same size. Following Ohm's law ($R = U / I$), the amplitude of the voltage deflection (U) upon current (I) injection is a measure of the membrane resistance (R), which is the so-called input resistance. Thus, when the voltage deflection upon injection of current pulses decreases the input resistance is decreased, because synaptic inputs (excitatory or inhibitory) cause an opening of ion channels. At the same

time, the conductance (g), which is the reciprocal of resistance ($g = 1/R$) and a measure of the ease with which current flows through a conductor, is increased. During stepping, the local membrane resistance was decreased in both phases of the step cycle, being smallest during swing phase (Figure 3.14 B). The input resistance was 8.5 ± 0.6 MΩ (3 responses for each phase) at rest before the stepping sequence (range: 7.9 to 9.0 MΩ), 5.2 ± 0.5 MΩ during swing phase (range: 5.0 to 5.8 MΩ), 5.6 ± 1.0 MΩ during stance phase (range: 5.0 to 6.7 MΩ) and 7.9 ± 0.4 MΩ at rest after the stepping sequence (range: 7.5 to 8.1 MΩ). The decrease of the local input resistance indicates a change in conductance, due to synaptic inputs during both stance and swing phase. The conductance was largest during swing. These results confirm that NSI I1 receives true excitatory, as well as true inhibitory synaptic inputs.

NSIs I2, E1 and E5 were tested for their synaptic inputs as well. For these NSIs the same observations as for I1 were made when the membrane potential was experimentally altered to different values. The depolarizing voltage deflection in the phase of excitatory current became smaller when the membrane potential was experimentally depolarized and, reversely, the amplitude of voltage deflection became much bigger when the membrane potential was experimentally hyperpolarized. Analogously, the hyperpolarizing voltage deflection in the phase of inhibitory current became bigger when a depolarization was imposed and smaller when a hyperpolarization was imposed. A measurement of the local input resistance of NSI E1 during stepping also showed decreased voltage deflections during both stance and swing, confirming the presence of true excitatory and inhibitory synaptic inputs. Despite their different operating ranges, NSIs I1, I2, E1 and E5 all seem to receive alternating excitatory and inhibitory synaptic inputs.

Through the application of constant de- or hyperpolarizing current it was also tested how strong the output activity of MNs was connected to the actual membrane potential of a premotor interneuron. In the case of the inhibitory NSI I1 (Figure 3.2 and Figure 3.14), the mean number of steps per stepping sequence clearly changed when the membrane potential was experimentally altered. Stepping sequences could easily be

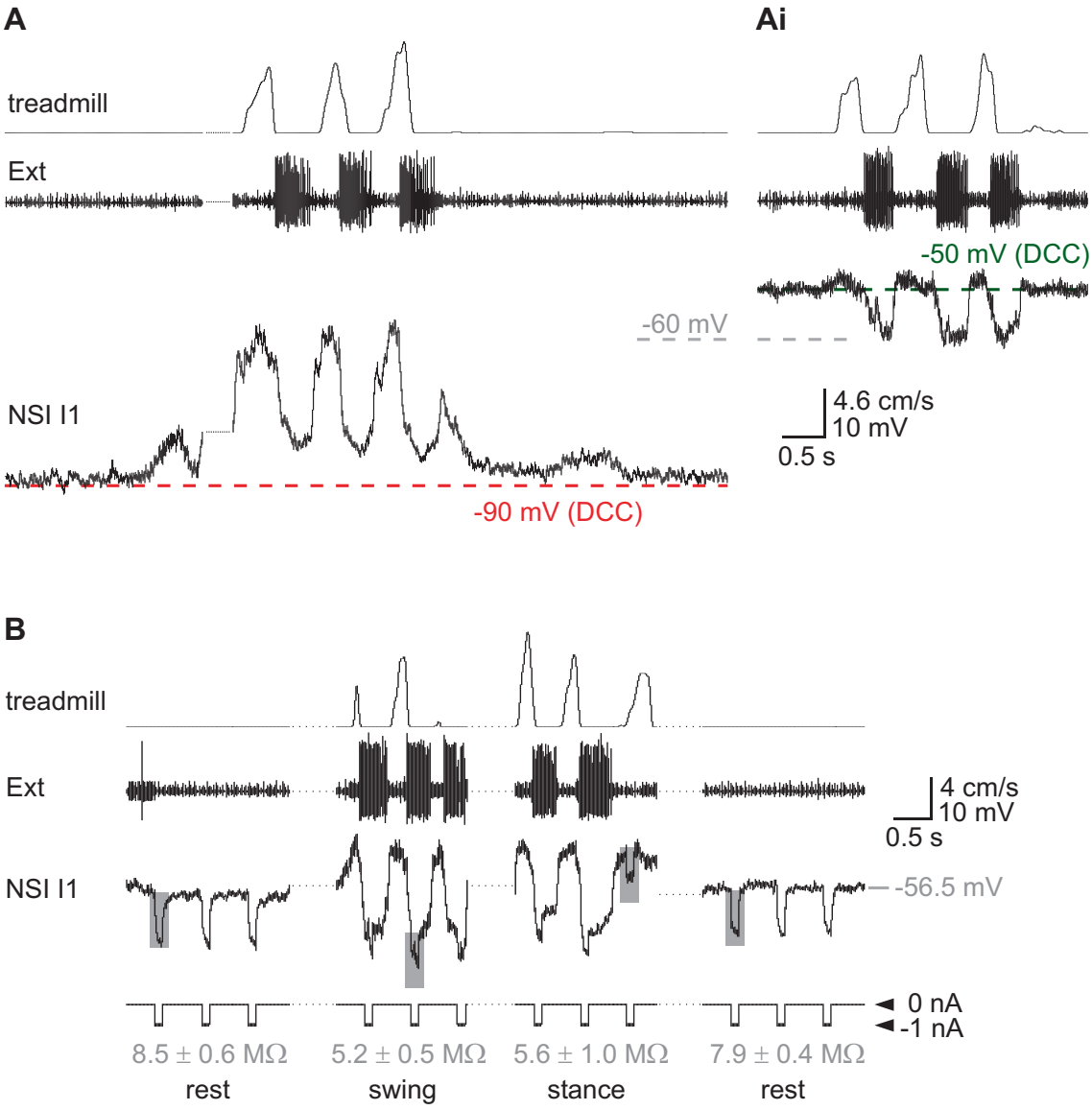

Figure 3.14: Synaptic inputs to NSI I1 during stepping. **A** The membrane potential of NSI I1 was experimentally altered in the DCC mode of the amplifier. The neuron was first hyperpolarized to -90 mV and then depolarized to -50 mV (RMP -60mV). **B** Measurement of local input resistance by injection of hyperpolarizing current pulses of -1 nA. Together with the measurement of input resistance during stepping it becomes obvious that this neuron receives both true inhibition and excitation.

elicited at RMP (-60 mV) and showed a mean of 7.3 ± 5.4 steps per sequence (range: 2 to 18 steps; 7 sequences). Various imposed hyperpolarizations, resulting in membrane potentials between -78 mV and -98 mV, reduced the number of steps per sequence to a mean of 5.5 ± 2.8 steps (range: 2 to 10 steps; 8 sequences). Several imposed depolarizations, resulting in membrane potentials between -49 mV and -41 mV, strongly affected the performance of stepping and the mean value decreased to 3.5 ± 2.1 steps (range: 1 to 6 steps, 4 sequences). Eventually, stepping could be completely terminated by injecting a pulse of depolarizing current into NSI I1 during a stepping sequence (Figure 3.15). The exact time of pulse application within a stepping sequence seemed to be less important. Whenever within a step cycle (end of stance, begin of swing, end of swing or begin of stance) a depolarizing current pulse was applied, the stepping sequence was immediately terminated in five out of six cases.

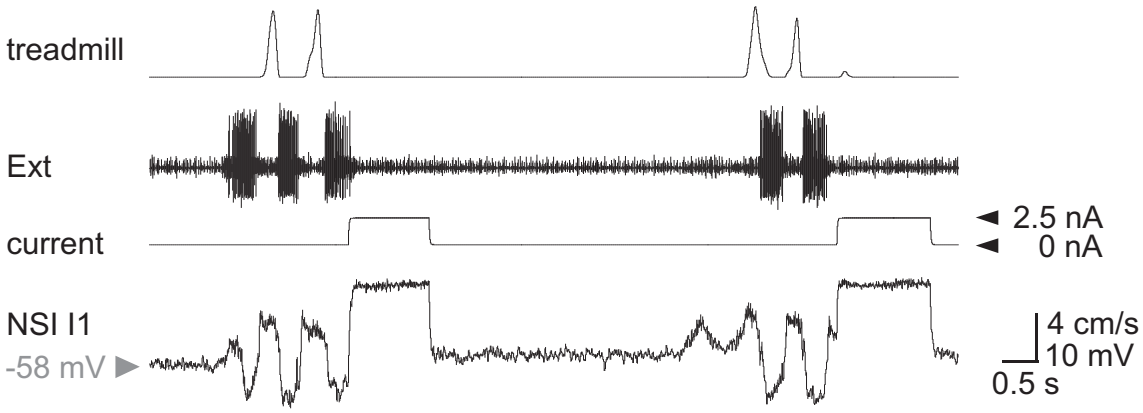

Figure 3.15: Application of current pulses to NSI I1 during stepping. Injection of a depolarizing current pulse within a stepping sequence immediately terminated stepping.

3.4 Comparison of NSI contribution to the generation of the „active reaction“ and their activity during single leg stepping

In the course of this study, activity of identified NSIs was recorded during stepping and during the generation of the „active reaction“. Together with the earlier findings on the “active reaction” from Driesang and Büschges (1996), this allows comparing the contribution of NSIs to both motor programs, thereby taking up on Bässler’s hypothesis. By drawing conclusions from behavioral observations and studies at the motoneuronal level, it was hypothesized that the „active reaction“ could represent a functional module within the control of walking motor output (Bässler 1986a). To prove this hypothesis, it is necessary to study the neurons which generate the „active reaction“. Driesang and Büschges (1996) studied the underlying reflex pathways and found that the „active reaction“ was generated through the activity of premotor NSIs, which operate within distributed and partly antagonistic pathways. They described the contribution of NSIs E1 - 6, I1 and I2 to the generation of the “active reaction” (Driesang and Büschges 1996). Individual NSI types either support or oppose the visible output of an ongoing motor program, which always reflects the sum of the excitatory and inhibitory drive converging onto MNs.

Stimulation of the fCO in the inactive animal results in the generation of a resistance reflex. The MN response to fCO stimulation, especially to elongation stimuli, is reversed when the animal becomes active. That means that an elongation of the fCO receptor apodeme through imposed leg flexion no longer excites extensor MNs and inhibits flexor MNs, but instead inhibits extensor MNs and simultaneously excites flexor MNs. This response to fCO elongation represents the first part of the so-called „active reaction“. In the second part, a position dependent inactivation of flexor MNs occurs simultaneously to activation of extensor MNs. An example of the characteristic MN activity during the resistance reflex in the inactive animal and during the “active reaction” in the active animal is shown in Figure 3.16. Stimulation of the fCO was performed by moving the treadmill belt with the leg on top of it, thereby imposing a leg flexion or extension, respectively (see chapter 2.5). Application time and direction of

fCO stimuli can be seen from the treadmill trace. During upward deflection of the treadmill trace the fCO was elongated and during downward deflection of the treadmill trace the fCO was relaxed. A resistance reflex was elicited through both fCO elongation and fCO relaxation. In the inactive animal, fCO elongation excited extensor MNs and inhibited flexor MNs, whereas fCO relaxation inhibited extensor MNs and excited flexor MNs. The "active reaction" was elicited solely upon fCO elongation in the active animal and led to inhibition of extensor MNs and excitation of flexor MNs, followed by a position dependent inactivation of flexor MNs and activation of extensor MNs. Sometimes, activity of the inhibitory MN CI_1 became visible in the nerve recording during the inhibition of the extensor MNs SETi and FETi.

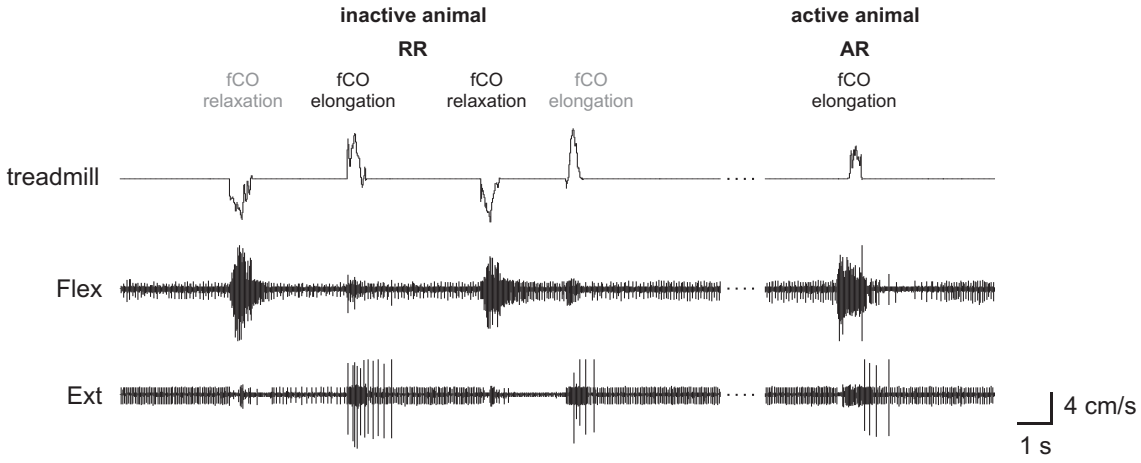

Figure 3.16: Characteristic MN activity during the resistance reflex and the "active reaction". The resistance reflex (RR) occurred upon fCO stimulation in the inactive animal. Both fCO elongation and fCO relaxation led to a characteristic response of tibial MNs. In the inactive animal, fCO elongation excited extensor MNs and inhibited flexor MNs, whereas fCO relaxation inhibited extensor MNs and excited flexor MNs. The "active reaction" (AR) was elicited solely upon fCO elongation in the active animal. In the first part of the "active reaction" extensor MNs were inhibited and flexor MNs excited. In the second part a position dependent inactivation of flexor MNs occurred and extensor MNs were activated simultaneously. The treadmill trace shows the treadmill belt movement during imposed leg flexion and extension, respectively. Flex: activity of flexor MNs (EMG recording). Ext: activity of extensor MNs (nerve recording).

„Active reactions“ were elicited during recording from individual NSI types, e.g., E2/3, E5, E6 and I2. The observed time course in membrane potential corresponded to earlier descriptions (Driesang and Büschges 1996). Furthermore, „active reactions“ were also elicited during recording from NSIs E7 and E8. In the following, the activity of E7 and E8 will be presented since their contribution to the „active reaction“ had not been investigated until now.

An episode from one E7 recording where resistance reflex, “active reaction”, and stepping were elicited subsequently is shown in Figure 3.17 (A). The resistance reflex was elicited at the beginning of the recording when the animal was resting, i.e., inactive. After a sequence of activity, possibly resulting from searching movements of the leg or arousal of the animal due to a brief puff of air, imposed leg flexion elicited the generation of the “active reaction”. Subsequently, the animal performed a stepping sequence. Following stepping, “active reactions” were elicited again. Dotted squares in (A) indicate episodes from the recording that were extended to exemplify NSI activity during the resistance reflex (Figure 3.17 B), the “active reaction” (Figure 3.17 C), and during stepping (Figure 3.17 D). E7 showed a hyperpolarization upon fCO elongation in the inactive animal together with the activation of extensor MNs, which became apparent as FETi burst followed by increased SETi activity, and a depolarization upon fCO relaxation accompanied by a decrease in extensor MN activity due to the inhibition (Figure 3.17 B). The time course of membrane potential of E7 during the resistance reflex corresponded to earlier descriptions (cf. Sauer et al. 1996). In the active animal, the membrane potential of E7 slowly depolarized upon fCO elongation and the inhibition of extensor MNs became apparent from the CI_1 activity in the nerve recording (Figure 3.17 C). During stepping, E7 showed a depolarization during stance and a hyperpolarization during FETi activity in swing phase (Figure 3.17 D), as described in chapter 3.2.2.

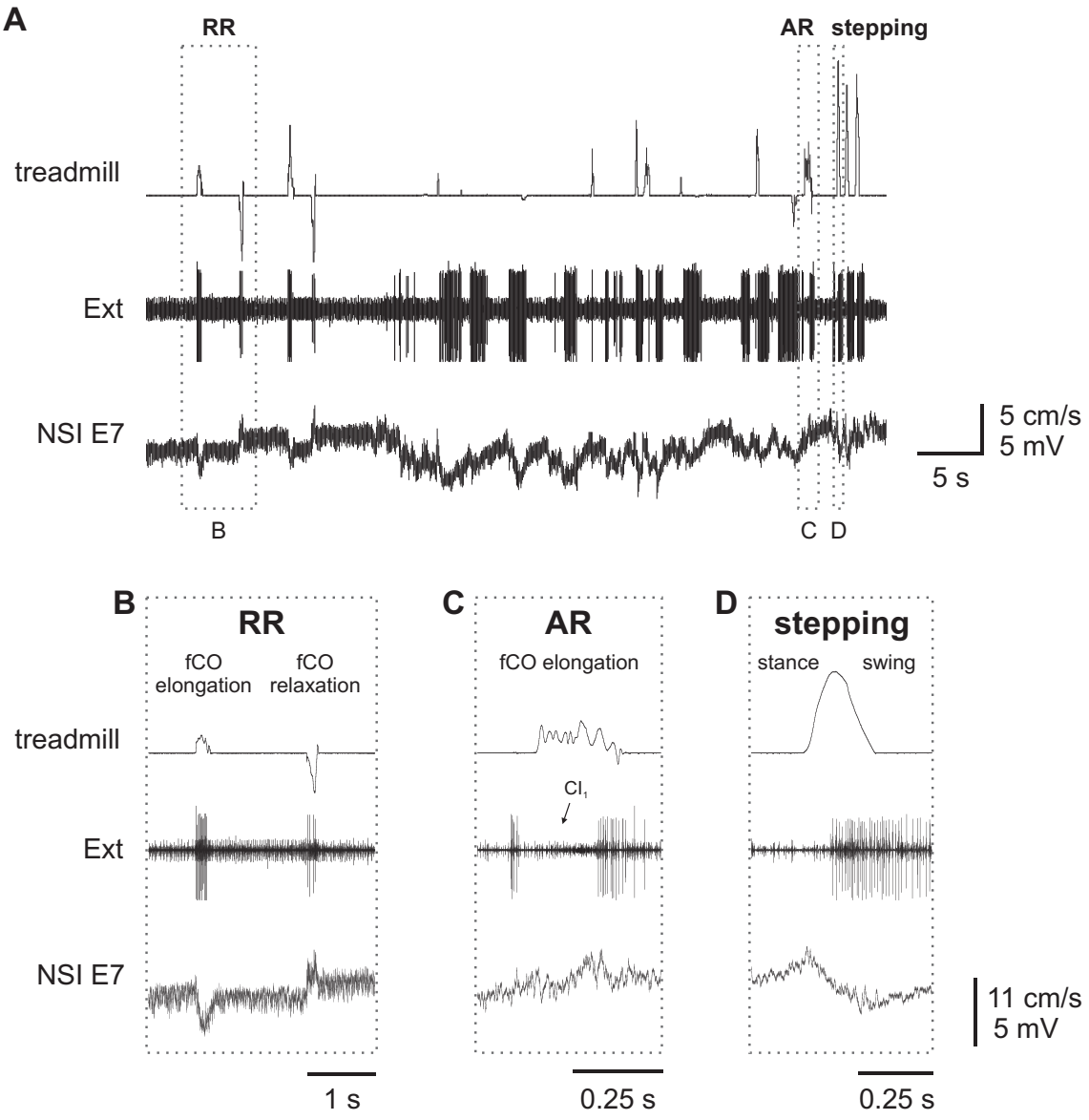

Figure 3.17: A Episode from a recording to exemplify the activity of NSI E7 during the resistance reflex (RR), the "active reaction" (AR), and stepping. The treadmill trace shows application time and direction of the fCO stimulus and the recorded belt velocity during stepping. Ext: activity of extensor MNs from the nerve recording. Areas surrounded by a dotted square indicate episodes from the recording that are extended in (B)-(D). **B** E7 showed a hyperpolarization upon fCO elongation during the resistance reflex in the inactive animal together with the activation of extensor MNs, apparent as FETi burst followed by increased SETi activity, and a depolarization accompanied by a decrease in extensor MN activity upon fCO relaxation. **C** The membrane potential of E7 slowly depolarized upon fCO elongation during the "active reaction" in the active animal. Inhibition of extensor MNs became apparent from the CI_1 activity. **D** During stepping, E7 showed a depolarization during stance and a hyperpolarization during FETi activity in swing phase.

Three out of ten „active reactions“ elicited in the course of two recordings from E7 are exemplified in Figure 3.18 (A). NSI E7 showed a depolarization of its membrane potential upon imposed leg flexion, i.e., fCO elongation, during the generation of the „active reaction“. Thus, E7 opposed the generation of the „active reaction“ with respect to the visible motor output, i.e., the inactivation of extensor MNs and simultaneous activation of flexor MNs. In Figure 3.18 (A), the inactivation of extensor MNs appears as cessation of spontaneous SETi activity and increased CI_1 activity, whereas the activation of flexor MNs upon fCO stimulation was visible by the onset of large units. The time of stimulus onset is depicted by the single dashed line with arrowhead and two dashed lines flag the stimulus duration. To enable analysis of the time course of membrane potential during „active reactions“ from different recordings, the offset at the time of stimulus onset was removed from the membrane potential for all sweeps. The time course of membrane potential during the „active reaction“ is shown in Figure 3.18 (B) where six sweeps from one E7 recording were aligned at the time of stimulus onset and superimposed. The sweeps (grey) are shown together with the calculated average (black). In the active animal, E7 showed a small but reproducible depolarization of membrane potential upon imposed leg flexion. This becomes obvious also from the average of the same six sweeps normalized to stimulus duration (Figure 3.18 C), as well as from the average of ten sweeps from two recordings normalized to stimulus duration (Figure 3.18 D).

Figure 3.19 (A) shows an episode from one E8 recording with resistance reflex, “active reaction”, and stepping. Subsequent to a resistance reflex, an “active reaction” was elicited by imposed leg flexion. Only little later, the animal performed a stepping sequence. Directly after the stepping sequence, oscillations of membrane potential of E8 were observed. Similar oscillations were also observed in other recordings, as well as in other NSI types, and often occurred subsequent to a stepping sequence or sometimes subsequent to fCO stimulation. The depolarizations were in relation to rhythmic SETi activity and their frequency was characteristic for the motor program of rocking described by Pflüger (1977). Areas surrounded by dotted squares indicate episodes from the recording that were extended to exemplify NSI activity during the resistance reflex (Figure 3.19 B), the “active reaction” (Figure 3.19 C), and during stepping (Figure 3.19

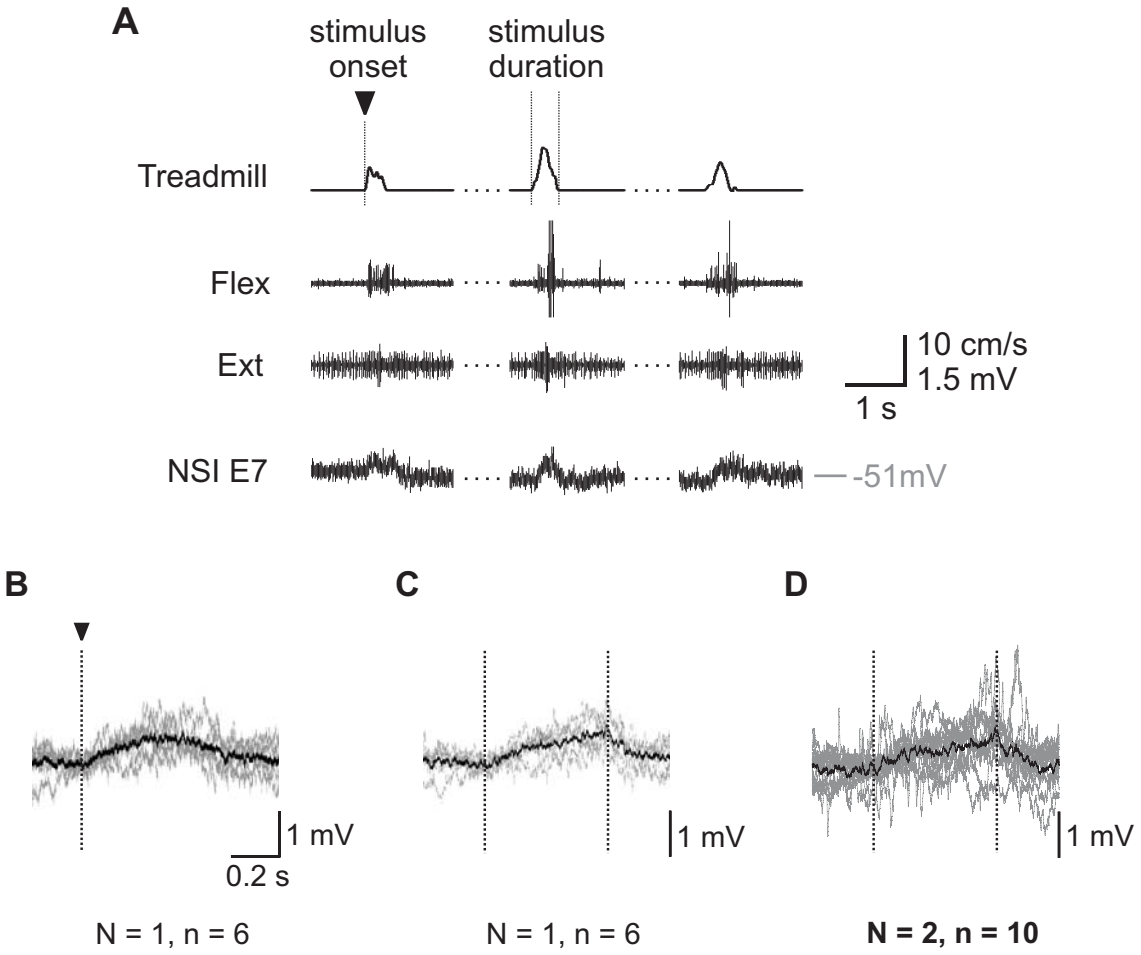

Figure 3.18: Contribution of NSI E7 to the generation of the „active reaction". **A** Activity of E7, flexor MNs (Flex; EMG recording) and extensor MNs (Ext; nerve recording) along with the treadmill trace during three "active reactions" from one recording. E7 showed a small but distinct depolarization of membrane potential upon fCO stimulation in the active animal and thus opposed the MN activity, i.e., the inactivation of extensor MNs (Ext) and activation of flexor MNs (Flex). **B** Six sweeps were aligned at the time of stimulus onset and superimposed. **C** The same sweeps were also normalized to stimulus duration and superimposed. **D** Ten sweeps from two experiments (N = 2, n = 10) were normalized to stimulus duration and superimposed. The depolarization of E7 during the „active reaction" becomes obvious from all three overlays. To enable analysis of the time course of membrane potential during „active reactions" from different experiments, the offset at the time of stimulus onset was removed from the membrane potential for all sweeps. The sweeps (grey) are shown together with the calculated average (black). The single dashed line with arrowhead depicts the time of stimulus onset. Two dashed lines flag the stimulus duration.

D). During the resistance reflex, E8 showed a hyperpolarization upon both fCO elongation and relaxation (cf. Stein and Sauer 1998) and the extensor MNs showed the characteristic activity. A FETi burst followed by increased SETi activity was elicited upon fCO elongation, while extensor MN activity was inhibited upon fCO relaxation (Figure 3.19 B). E8 hyperpolarized during the "active reaction" and CI_1 activity was visible during the inhibition of extensor MNs (Figure 3.19 C). During stepping, E8 showed a hyperpolarization during stance and a depolarization during FETi activity in swing phase (Figure 3.19 D), as described in chapter 3.2.2.

Four out of seven „active reactions" elicited in two recordings from NSI E8 are exemplified in Figure 3.20 (A). E8 showed hyperpolarizations of its membrane potential upon imposed leg flexion in the active animal. The hyperpolarization of E8 contributed to the generation of the active reaction in terms of a cessation of its excitatory inputs to the extensor MNs. Thus, E8 supported the generation of the „active reaction" with respect to the activity of extensor MNs. Together with the subsequent depolarization of E8 both extensor MNs were active. The time of stimulus onset is depicted by the single dashed line with arrowhead and two dashed lines flag the stimulus duration. To enable analysis of the time course of membrane potential during „active reactions" from different recordings, the offset at the time of stimulus onset was removed from the membrane potential for all sweeps. From the average (black) of five sweeps (grey) from one recording, aligned at stimulus onset and superimposed, it becomes visible that E8 hyperpolarized strongly upon imposed leg flexion in the active animal (Figure 3.20 B). The same becomes obvious from the averages (black traces) of the overlays normalized to stimulus duration with five sweeps (grey) from one recording (Figure 3.20 C) or seven sweeps (grey) from two recordings (Figure 3.20 D), respectively. Thereby, the situation in E8 contrasted the findings described for E7.

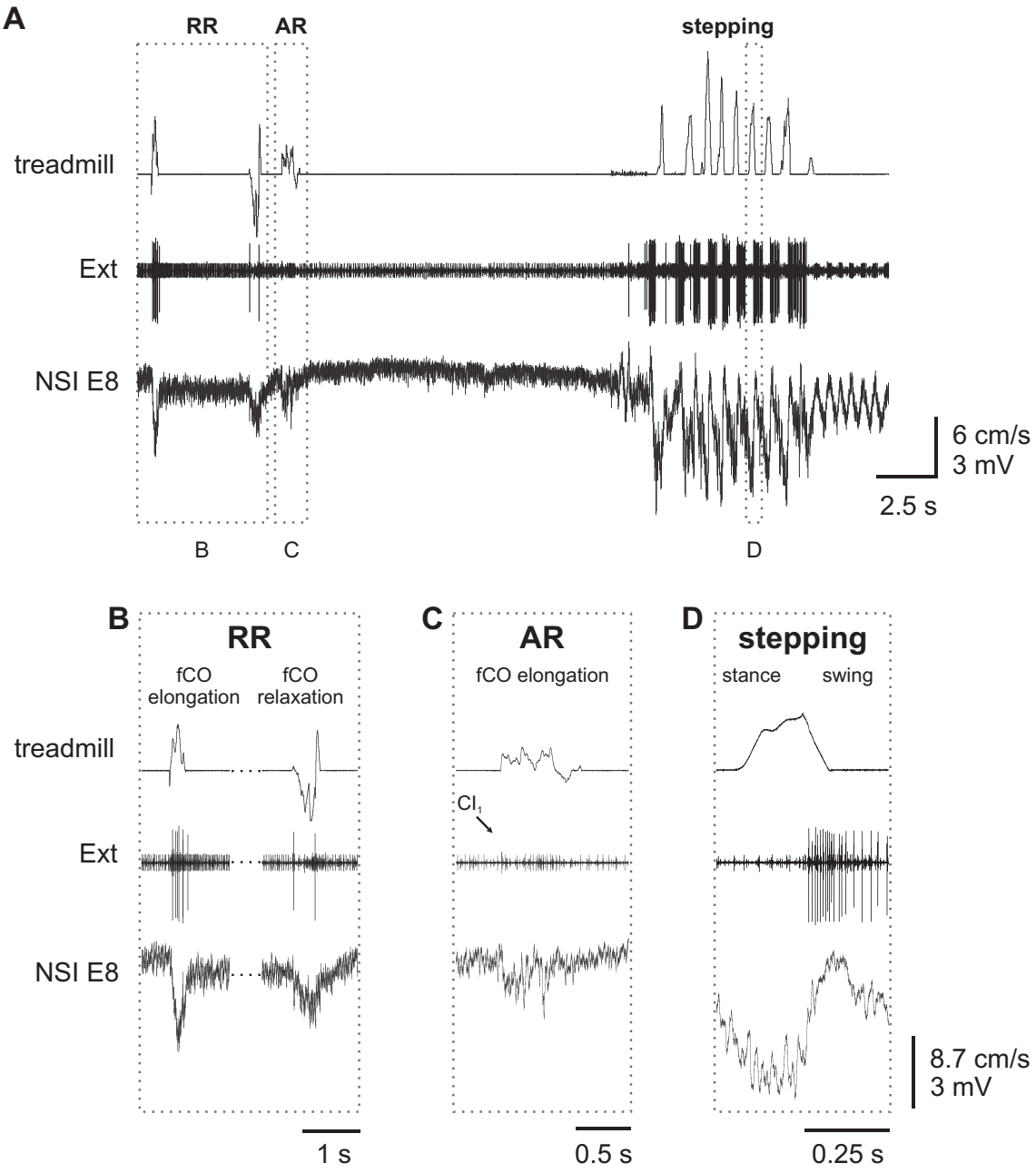

Figure 3.19: A Episode from a recording to exemplify the activity of NSI E8 during the resistance reflex (RR), the "active reaction" (AR), and stepping. The treadmill trace depicts application time and direction of fCO stimulus and the recorded belt velocity during stepping. Ext: activity of extensor MNs from the nerve recording. Areas surrounded by a dotted square indicate episodes from the recording that are extended in (B)-(D). **B** During the resistance reflex, E8 showed a hyperpolarization upon fCO elongation together with the activation of extensor MNs and upon fCO relaxation accompanied by inhibition of extensor MNs. **C** During the "active reaction", the membrane potential of E8 hyperpolarized upon fCO elongation. Inhibition of extensor MNs became apparent from the CI_1 activity. **D** During stepping, E8 showed a hyperpolarization during stance and a depolarization during FETi activity in swing phase.

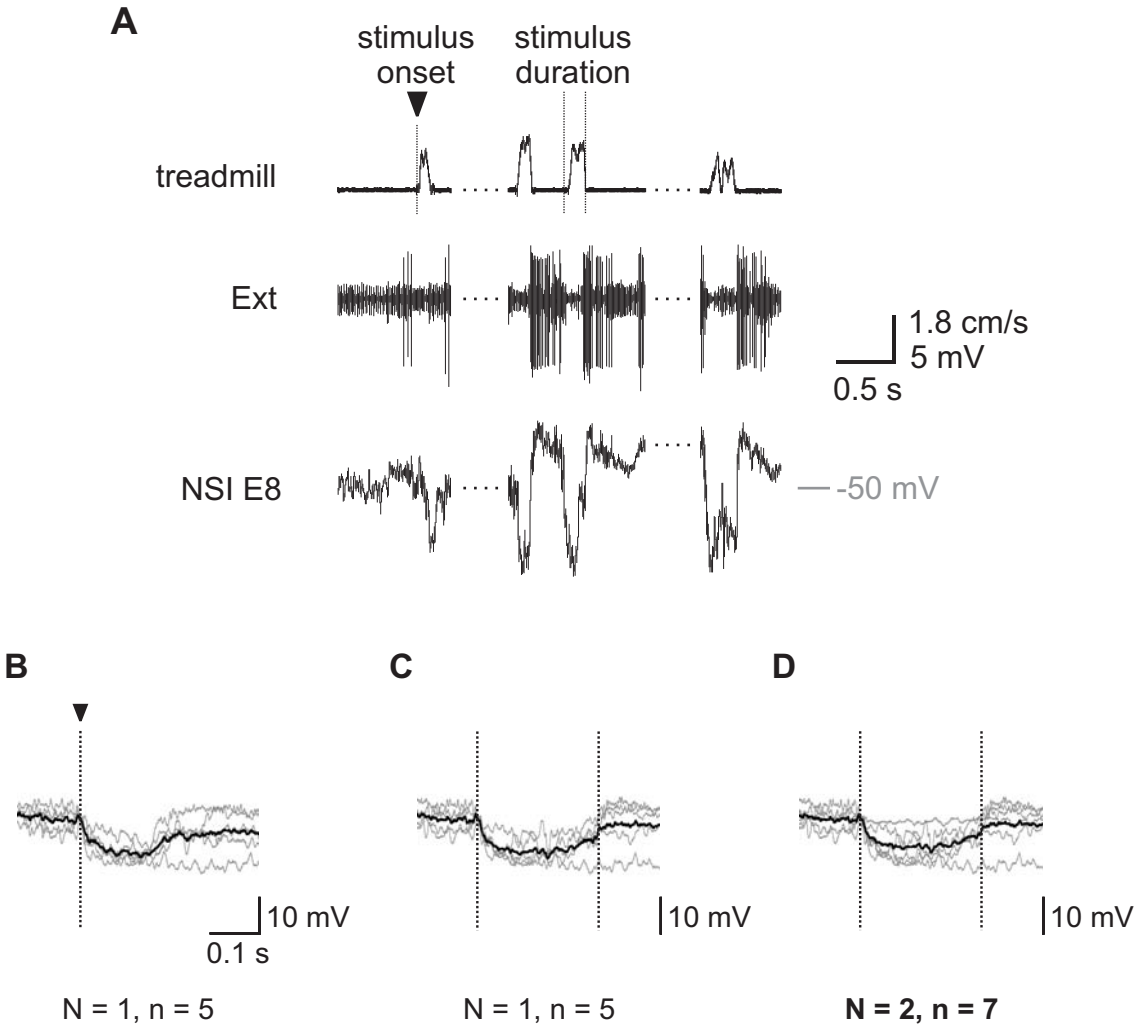

Figure 3.20: Contribution of NSI E8 to the generation of the „active reaction". **A** E8 showed a hyperpolarization of membrane potential upon fCO stimulation in the active animal and thus supports the MN activity, i.e., the inactivation of extensor MNs (Ext). **B** Five sweeps were aligned at the time of stimulus onset and superimposed. **C** The same five sweeps were normalized to stimulus duration and superimposed. **D** Normalized and superimposed sweeps from two experiments (N = 2, n = 7). The hyperpolarization of E8 during the „active reaction" becomes obvious from all three overlays. To enable analysis of the time course of membrane potential during „active reactions" from different experiments, the offset at the time of stimulus onset was removed from the membrane potential for all sweeps. The sweeps (grey) are shown together with the calculated average (black). The single dashed line with arrowhead depicts the time of stimulus onset. Two dashed lines flag the stimulus duration.

In summary, there are two qualitatively different possible contributions of NSIs to the generation of the „active reaction“ (Driesang and Büschges 1996). On the one hand, there are NSIs that support the visible motor output, i.e., NSIs E2/3, E5, E6, I1, I2 and E8, and on the other hand, there are NSIs that oppose the actual motor output, i.e., NSIs E1, E4 and E7 (Table 3.2). [A simplified scheme is given in the appendix that exemplifies supporting and opposing activity of NSIs during the generation of resistance reflex, “active reaction” and single leg stepping.]

Albeit contrasting each other, the contribution to the generation of the „active reaction“ of both E7 and E8 were complying with their contribution to the generation of stepping, described in chapter 3.2. NSI E7, which was found to depolarize upon imposed flexion of the leg in the active animal, also showed a depolarization in stance phase, i.e., the phase of leg flexion, during stepping. Thus, E7 opposed the ongoing motor output in both cases. In analogy, the same was true for NSI E8, which was not only found to support the ongoing motor output by hyperpolarizing upon imposed leg flexion in the active animal, but also during stance phase of stepping where it also showed a hyperpolarization. Comparing the activity of all individual NSI types during the generation of the motor output for the „active reaction“ and for stepping resulted in great compliance, not only for E7 and E8 (Table 3.2).

Table 3.2: Contribution of NSI types to the generation of stepping and to the „active reaction“. NSI activity either supported (+) or opposed (-) the visible motor output.

	E1	**E2/3**	**E4**	**E5**	**E6**	**E7**	**E8**	**I1**	**I2**	**I4**	**I8**
stepping	-	+	-	+	-	-	+	+	+	-	-
„active reaction“ [(1)]	-	+	-	+	+	-	+	+	+		

[(1)] Contribution of NSIs E1 - 6, I1, I2 to the generation of the “active reaction” were taken from Driesang and Büschges (1996) and were corroborated by own findings on individual NSIs. Contribution of NSIs E7 and E8 to the generation of the “active reaction” was revealed in the course of the present study.

3.5 Correlation between NSI membrane potential and extensor MN activity during single leg stepping

Subsequent to the description of premotor NSI activity during stepping, the analysis of synaptic input, and the comparison of NSI contribution to the generation of motor programs such as stepping and the „active reaction“, it will now be analyzed how tight premotor NSIs control the activity of tibial MNs during stepping. The NSIs in question are characterized by their effect upon extensor MNs. The slow extensor MN (SETi) is spontaneously active and the fast extensor MN (FETi) is exclusively activated for fast movements, for example, for the generation of swing phase during stepping. During swing phase, individual SETi spikes can not longer be differentiated with certainty as they are often overlaid by FETi spikes. To enable analysis of a correlation between the extensor MN activity and the drive provided by individual NSIs, the instantaneous FETi spike frequency during stepping was plotted as a function of membrane potential. For this purpose, two regression analyses were performed at a time for each NSI type. One time, the instantaneous FETi spike frequency during stepping was plotted *versus* the membrane potential during swing phase, and additionally, it was plotted *versus* the membrane potential during the whole step cycle (stance and swing phase). In the following, the regression analyses for the individual NSI types will be presented. For each NSI type two plots will be shown. The first plot exemplifies the regression analyses for one single recording from a given NSI type (the original recording was presented in chapter 3.2) and shows the data points for swing and stance phase, along with the regression lines for swing phase or swing and stance phase together. The second plot shows the pairs of regression lines resulting from all regression analyses performed for the NSI type in question.

For individual NSIs, e.g., NSI E2/3, it became visible already earlier in this study that there was a close correlation between the actual membrane potential and the FETi activity (Figure 3.6 A). The strong correlation between the membrane potential of E2/3 and FETi activity became also apparent quantitatively in the regression analyses. In both cases, the regression line showed a significant positive correlation for E2/3. The

correlation coefficient was R = 0.77 for stance and swing phase analyzed together and R = 0.44 for the analysis of swing phase (Figure 3.21 A). Both regression lines are shown along with those from four other experiments (Figure 3.21 Ai). In all five experiments, FETi spike frequency was highly correlated with the membrane potential of E2/3 and all five pairs of regression lines showed a positive correlation.

The activity pattern of NSI E8 resembled qualitatively that of NSI E2/3 during stepping. A close correlation between FETi activity and membrane potential of E8 NSIs during stepping was also found in both cases, during the whole step cycle and during swing phase (Figure 3.21 B). The correlation coefficients were R = 0.89 for stance and swing phase analyzed together and R = 0.48 for the analysis of swing phase. Both regression lines are shown together with those from four other E8 recordings (Figure 3.21 Bi). In all five experiments, FETi spike frequency was highly correlated with the membrane potential of E8 and all five pairs of regression lines showed a positive correlation.

A close correlation between FETi activity and membrane potential during stepping was also found for E4 NSIs in both cases, during the whole step cycle and during swing phase (Figure 3.21 C). The correlation coefficients were R = 0.86 for stance and swing phase analyzed together and R = 0.46 for the analysis of swing phase. Both regression lines are shown along with those from four other experiments (Figure 3.21 Ci). In all five experiments, FETi spike frequency was highly correlated with the membrane potential of E4 and all five pairs of regression lines showed a positive correlation.

The original recording from I2 showed that this NSI was hyperpolarized strongest by the time of highest FETi spike activity during swing (Figure 3.3). The regression analyses showed a negative correlation with a significant correlation coefficient in both cases, indicating that FETi activity was strongly correlated with the actual membrane potential of I2 throughout the whole step cycle (Figure 3.21 D). The correlation coefficients were R = -0.83 for stance and swing phase analyzed together and R = -0.66 for the analysis of swing phase. Both regression lines are shown together with those from four other experiments (Figure 3.21 Di). In all five experiments, FETi spike

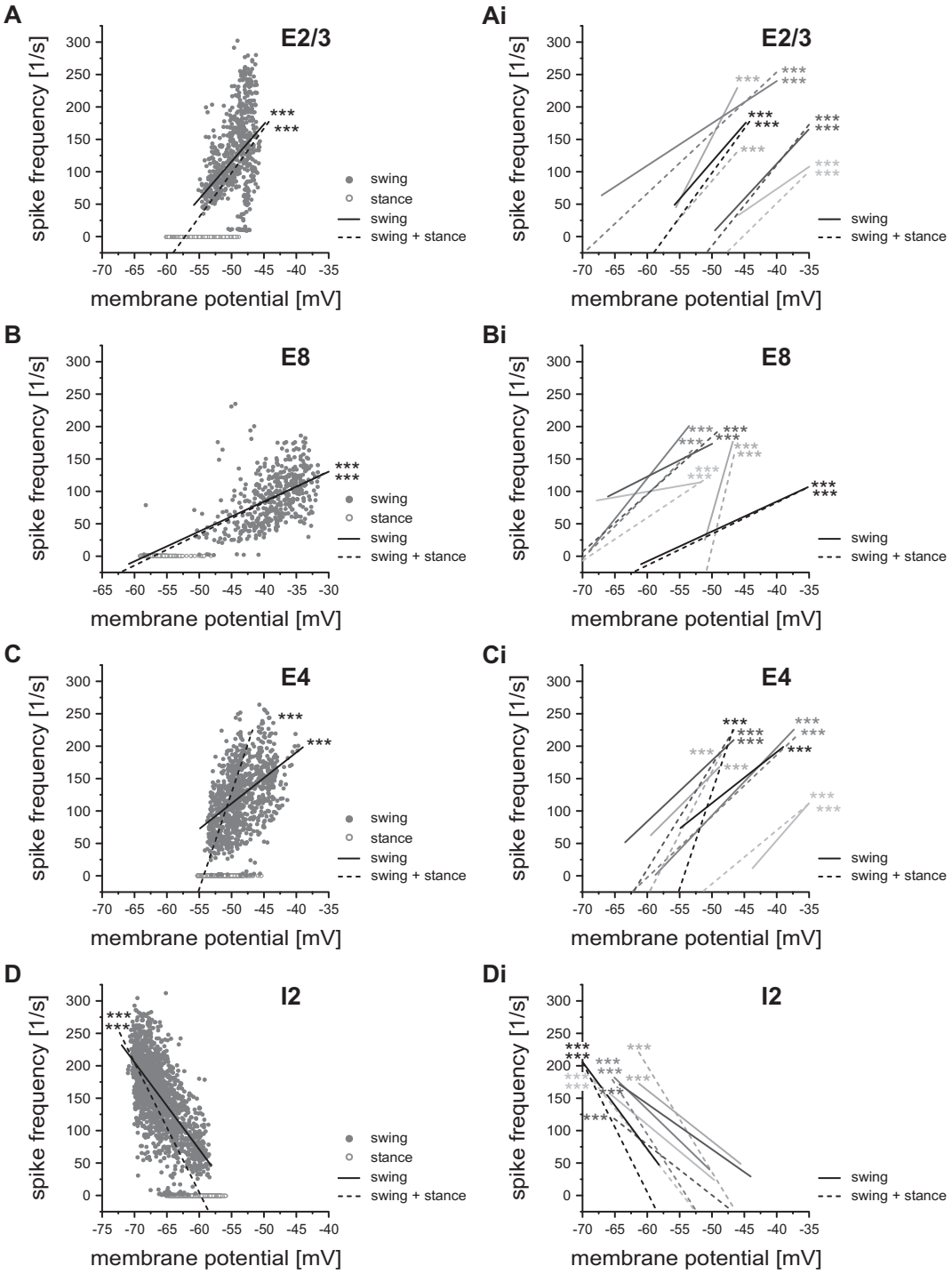

Figure 3.21: FETi spike frequency *versus* membrane potential of NSIs E2/3, E8, E4 and I2. **A** E2/3 showed a positive correlation in both cases (R = 0.77 dashed line and R = 0.44). **Ai** E2/3: 5/5 pairs showed a positive correlation. **B** E8 showed a positive correlation in both cases (R = 0.89 dashed line and R = 0.48). **Bi** E8: 5/5 pairs showed a positive correlation. **C** E4 showed a positive correlation in both cases (R = 0.86 dashed line and R = 0.46). **Ci** E4: 5/5 pairs showed a positive correlation. **D** I2 showed a negative correlation in both cases (R = -0.83 dashed line and R = -0.66). **Di** I2: 5/5 pairs showed a negative correlation. The stars mark the level of significance: (***) P < 0.001.

frequency was highly correlated with the membrane potential of I2 and all five pairs of regression lines showed a negative correlation.

When FETi spike frequency was plotted against the membrane potential of NSI I1 during the whole step cycle a significant negative correlation resulted (Figure 3.22 A; R = -0.72). However, in the regression analysis for the time of swing phase a positive correlation between FETi spike frequency and the membrane potential resulted (Figure 3.22 A; R = 0.32). Both regression lines are shown together with those from four other experiments (Figure 3.22 Ai). In all three experiments, FETi spike frequency was highly correlated with the membrane potential of I1, but only two out of three pairs showed the same algebraic sign of correlation in both cases.

A close correlation between FETi activity and membrane potential of E5 NSIs during stepping was found in both cases, during the whole step cycle (R = 0.72) and during swing phase (R = 0.52), for the experiment presented (Figure 3.22 B). Both regression lines are shown together with those from four other experiments (Figure 3.22 Bi). Only one more experiment showed a significant positive correlation in both cases. The remaining three pairs out of five differed concerning their respective algebraic sign and two of the regression lines, resulting from the analysis of swing phase, showed no significance. Altogether, regression analysis for NSI E5 resulted in a significant correlation between FETi spike frequency and membrane potential in only three out of five experiments, and only two of these showed a positive correlation in both cases.

NSI E1 showed a negative correlation for the analysis of stance and swing phase together (R = -0.43) and a positive correlation for the analysis of swing phase (R = 0.09) (Figure 3.23 A). Both regression lines are shown along with those from two other experiments (Figure 3.23 Ai). All three pairs differed concerning the respective algebraic sign of correlation. One of the regression lines, resulting from swing phase analysis, showed no significance.

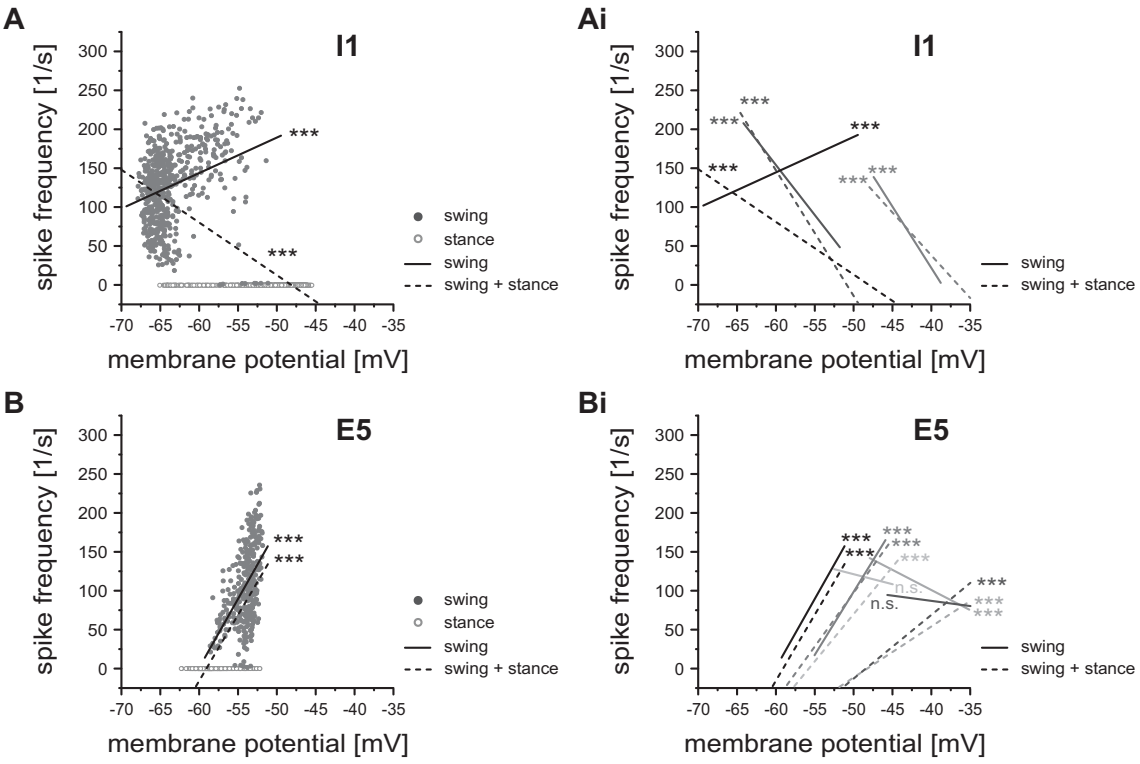

Figure 3.22: FETi spike frequency *versus* membrane potential of NSIs I1 and E5. **A** NSI I1 showed a negative correlation for the analysis of stance and swing phase together (dashed line) and the correlation coefficient was R = -0.72. For swing phase analysis I1 showed a positive correlation with a coefficient of R = 0.32. **Ai** I1: 2/3 pairs showed a negative correlation in both cases. One pair differed concerning the respective algebraic sign of correlation. **B** NSI E5 showed a positive correlation in both cases with correlation coefficients of R = 0.89 (dashed line) and R = 0.48. **Bi** The regression analysis for E5 resulted in a significant correlation between FETi spike frequency and membrane potential in only 3/5 experiments, and only two of these showed a positive correlation in both cases. The stars mark the level of significance: (***) P < 0.001; (n.s.) not significant P > 0.05.

NSI E6 showed a negative correlation for the analysis of stance and swing phase together (R = -0.71) and a positive correlation for the analysis of swing phase (R = 0.13) (Figure 3.23 B). Both regression lines are shown along with those from four other experiments (Figure 3.23 Bi). Two pairs out of five were significantly correlated and showed positive correlations in both cases. Three pairs out of five differed concerning the respective algebraic sign of correlation and two of these regression lines, resulting from the analysis of swing phase, showed no significance.

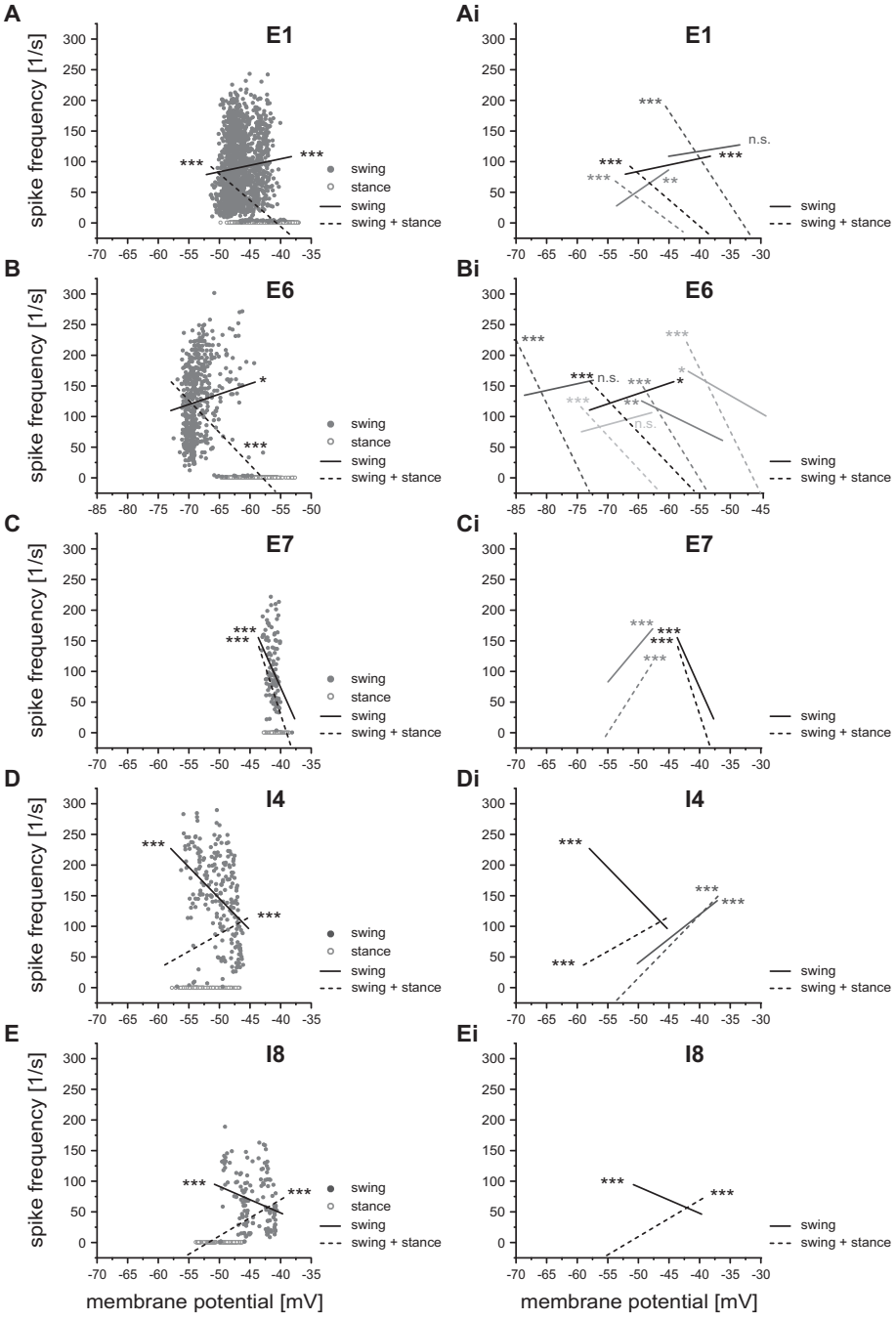

Figure 3.23: FETi spike frequency *versus* membrane potential of NSIs E1, E6, E7, I4 and I8. **A** For E1 correlations differed in sign (R = -0.72; R = 0.32). **Ai** E1: 3/3 pairs differed in sign. **B** For E6 correlations differed in sign (R = -0.71; R = 0.13). **Bi** E6: 2/5 pairs showed a negative correlation in both cases; 3/5 pairs differed in sign. **C** E7 showed negative correlations in both cases (R = -0.44; R = -0.34). **Ci** E7: One pair consisted of negative regression lines and the second pair of positive regression lines. **D** For I4 correlations differed in sign (R = 0.18; R = -0.4) **Di** I4: One pair differed in sign; the other pair was positively correlated in both cases. **E** For I8 correlations differed in sign (R = 0.51; R = -0.26). **Ei** I8: The regression lines differed in sign. The stars mark the level of significance: (***) $P < 0.001$; (**) $0.001 \leq P < 0.01$; (*) $0.01 \leq P < 0.05$; (n.s.) not significant $P > 0.05$.

In the experiment presented, the regression analyses for NSI E7 showed negative correlations in both cases (Figure 3.23 C). The correlation coefficients were R = -0.44 for stance and swing phase analyzed together and R = -0.34 for the analysis of swing phase. Both regression lines are shown along with those from another experiment (Figure 3.23 Ci). Both pairs of regression lines showed a high correlation. Albeit both regression lines of a pair showed the same algebraic sign, one pair showed a negative correlation and the second pair a positive correlation.

NSI I4 showed a positive correlation for the analysis of stance and swing phase together (R = 0.18) and a negative correlation for the analysis of swing phase (R = -0.4) (Figure 3.23 D). Both regression lines are shown along with those from another experiment (Figure 3.23 Di). One pair differed concerning the respective algebraic sign of correlation and the other pair was positively correlated in both cases.

NSI I8 showed a positive correlation for the analysis of stance and swing phase together (R = 0.51) and a negative correlation for the analysis of swing phase (R = -0.26) (Figure 3.23 E, Ei). The regression lines were significant, but differed concerning the respective algebraic sign of correlation (Figure 3.23 Ei).

3.6 Contribution of NSIs to alterations in stepping velocity in the single middle leg preparation

In the present study, the role premotor NSIs play in the generation of MN activity during stepping was addressed in general and during alterations in stepping velocity as an adaptive motor task. In order to investigate a possible contribution of NSIs to variations in stepping velocity, two different aspects of membrane potential modulation were examined. First, the correlation between the modulation amplitude and stepping velocity was quantified. Therefore, the maximum depolarization (peak potential) and the maximum hyperpolarization (trough potential) occurring within each step cycle of the stepping sequences within one recording from a given NSI type were plotted against the mean belt velocity as a measure of the mean stepping velocity. A second analysis was dedicated to reveal alterations in the time course of membrane potential in relation to variations of the mean belt velocity. For this purpose, averaged time courses of membrane potential of a given NSI recording during steps of different velocities were compared. Stepping velocity was classified as being fast, medium, or slow. A fast step was defined as a step with high mean belt velocity and short stance phase duration. A step with low mean belt velocity and long stance phase duration was defined as a slow step. Medium steps were defined to correspond approximately to the respective mean of a given recording for mean belt velocity and stance phase duration. The averaged time courses of NSI membrane potential were superimposed and aligned at the time of the last FETi spike of a burst, i.e., the time of swing phase end, to provide a detailed view on the transition from swing to stance and the initiation of stance phase. The averaged time courses were also superimposed and aligned at the time of the first FETi spike of a burst, i.e., the time of the transition from stance to swing phase, to provide a detailed view on the end of stance phase and early swing phase. Recordings from the individual NSI types were selected that included a large number of steps and a large range of mean belt velocity. The maximum belt velocity was also analyzed and generally led to the same results.

An example of two steps with different mean belt velocities (V mean: 4.4 and 2.5 cm/s) from a recording of NSI I1 is shown in Figure 3.24 (A). The relationship between mean belt velocity and peak and trough potential in I1 was analyzed (Figure 3.24 B). The peak depolarization during stance phase increased significantly with mean belt velocity (n = 25, black regression line (**)) for the recording exemplified in (A), as well as for the second I1 recording analyzed (grey regression line (*)). The trough membrane potential during swing phase remained rather constant and showed no systematic changes in parallel to the mean belt velocity in both recordings (dashed regression lines (n.s.)). In order to analyze variations in time course of membrane potential that accompanied alterations in mean belt velocity, several steps of different velocities were compared. The averaged membrane potential of fast (3.9 ± 0.48 cm/s, n = 4), medium (2.9 ± 0.79 cm/s, n = 3), and slow (2.1 ± 0.34 cm/s, n = 3) steps from the recording exemplified in Figure 3.24 (A) were aligned at the time of the last FETi spike (Figure 3.24 C, left). The overlay shows that I1 was depolarized faster and with larger amplitude during fast steps than during slower steps. The averaged membrane potentials were also aligned at the time of the first FETi spike (Figure 3.24 C, right). The amplitude of depolarization during stance phase was visibly highest for fast steps and lowest for slow steps. With the beginning of swing phase, the averaged membrane potentials of all three fast, medium, and slow steps hyperpolarized below RMP (-60 mV) with the same time course and amplitude.

Three steps with different velocities and stance phase durations (V mean: 2.0, 3.9, and 6.2 cm/s; V max: 6.9, 8.5, and 10.2 cm/s; stance duration: 0.67, 0.34, and 0.27 s) from a recording of NSI I2 are exemplified in Figure 3.25 (A). The relationship between mean belt velocity and peak and trough potential was analyzed for two I2 recordings (Figure 3.25 Ai). The peak potential increased significantly in correlation with mean belt velocity (for the recording exemplified in (A): n = 38, black regression line (***) and for the other recording: grey regression line (**)). The trough potential remained rather constant and showed no systematic changes with mean belt velocity in the recordings presented (dashed regression lines: (n.s.)). The averaged time courses of fast (6.1 ± 0.76 cm/s, n = 3), medium (4.2 ± 0.26 cm/s, n = 3), and slow (2.2 ± 0.17 cm/s, n = 3) steps indicated that the amplitude of depolarization was largest during fast steps

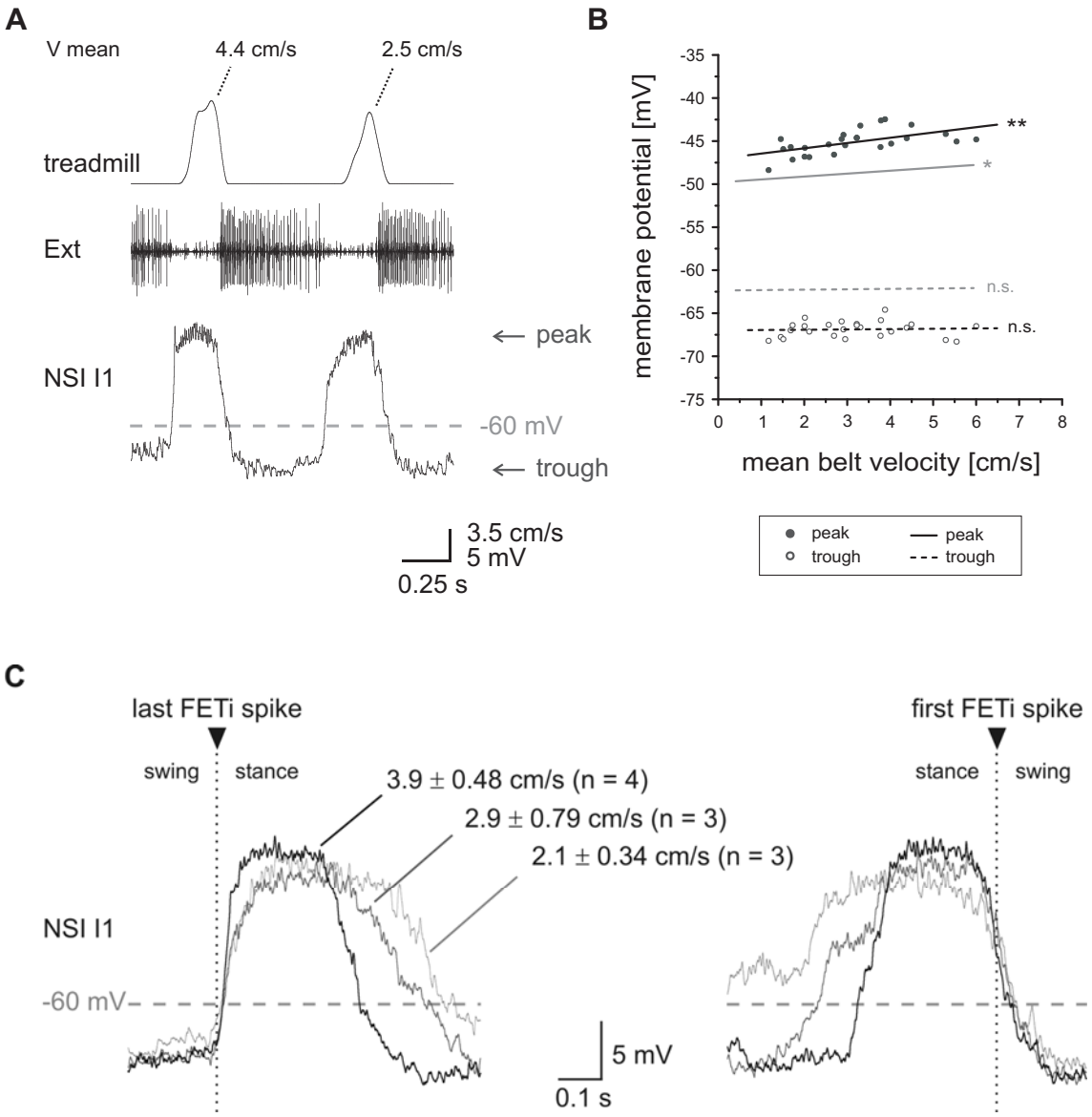

Figure 3.24: Modulation of NSI I1 in relation to stepping velocity. **A** Two steps with different mean belt velocities (V mean: 2.5 and 4.4 cm/s) along with the activity of extensor MNs (Ext; nerve recording) and I1 (intracellular recording). **B** In both recordings, the increase in peak potential was correlated with the increase in mean belt velocity (n = 25, black regression line (**); grey regression line (*)). The trough potential showed no systematic changes (dashed regression lines (n.s.)). **C** Averaged time courses of fast (3.9 ± 0.48 cm/s, n = 4), medium (2.9 ± 0.79 cm/s, n = 3), and slow (2.1 ± 0.34 cm/s, n = 3) steps aligned at the time of the last FETi spike of a burst showed a faster and larger depolarization in fast steps than in slower steps. The averaged time courses aligned at the time of the first FETi spike of a burst indicated the largest depolarization amplitude for fast steps and the smallest for slow steps. With the beginning of swing phase all three averaged membrane potentials hyperpolarized below RMP (-60 mV) with the same time course and amplitude. The stars mark the level of significance: (***) $P < 0.001$; (**) $0.001 \leq P < 0.01$; (*) $0.01 \leq P < 0.05$; (n.s.) not significant $P > 0.05$.

and smallest during slow steps, whereas the duration of the depolarization, i.e., the duration of stance phase, was longest for slow steps and shortest for fast steps (Figure 3.25 Aii, left). This became also obvious from the averaged time courses, which were superimposed and aligned at the time of the first FETi spike of a burst (Figure 3.25 Aii, right). With the beginning of swing phase, the averaged time courses of all three fast, medium, and slow steps hyperpolarized below RMP (-65 mV). Another recording from a type I2 NSI (RMP -60 mV), which showed two particularities, was analyzed. First, the peak depolarization towards the end of swing phase was larger than in other I2 recordings. Second, very high maximum belt velocities occurred (range: 4.9 to 14.8 cm/s). Three steps with different velocities from this recording are exemplified in Figure 3.25 (B) (V mean: 2.8, 4.1, and 5.2 cm/s; V max: 9.5, 12.8, and 13.2 cm/s; stance duration: 0.51, 0.46, and 0.37 s). The relationship between mean belt velocity and peak and trough potential for this recording was analyzed (Figure 3.25 Bi). The peak potential increased with mean belt velocity (n = 48), but was not significantly correlated (n.s.; P = 0,056). However, a significant correlation between peak potential and belt velocity for this recording was obtained with the maximum belt velocity (not shown). Interestingly, the trough potential was significantly correlated with mean belt velocity and showed a negative slope (dashed regression line (*)). The averaged time courses of fast (5.4 ± 0.3 cm/s, n = 9), medium (3.7 ± 0.24 cm/s, n = 9), and slow (2.3 ± 0.45 cm/s, n = 9) steps again indicated that I2 was depolarized strongest during fast steps (Figure 3.25 Bii, left). From the averaged time courses aligned at the time of the first FETi spike, i.e., the beginning of swing phase, it became obvious that the hyperpolarization in the first half of swing phase was strongest in fast steps (Figure 3.25 Bii, right). This indicates a stronger disinhibition of extensor MN activity within the step cycle of a fast step compared to slower steps. At least, this can be concluded from the level of hyperpolarization, since I2 provides inhibitory drive onto extensor MNs. However, this I2 recording was the only one that showed a significant negative correlation of trough potential and mean belt velocity.

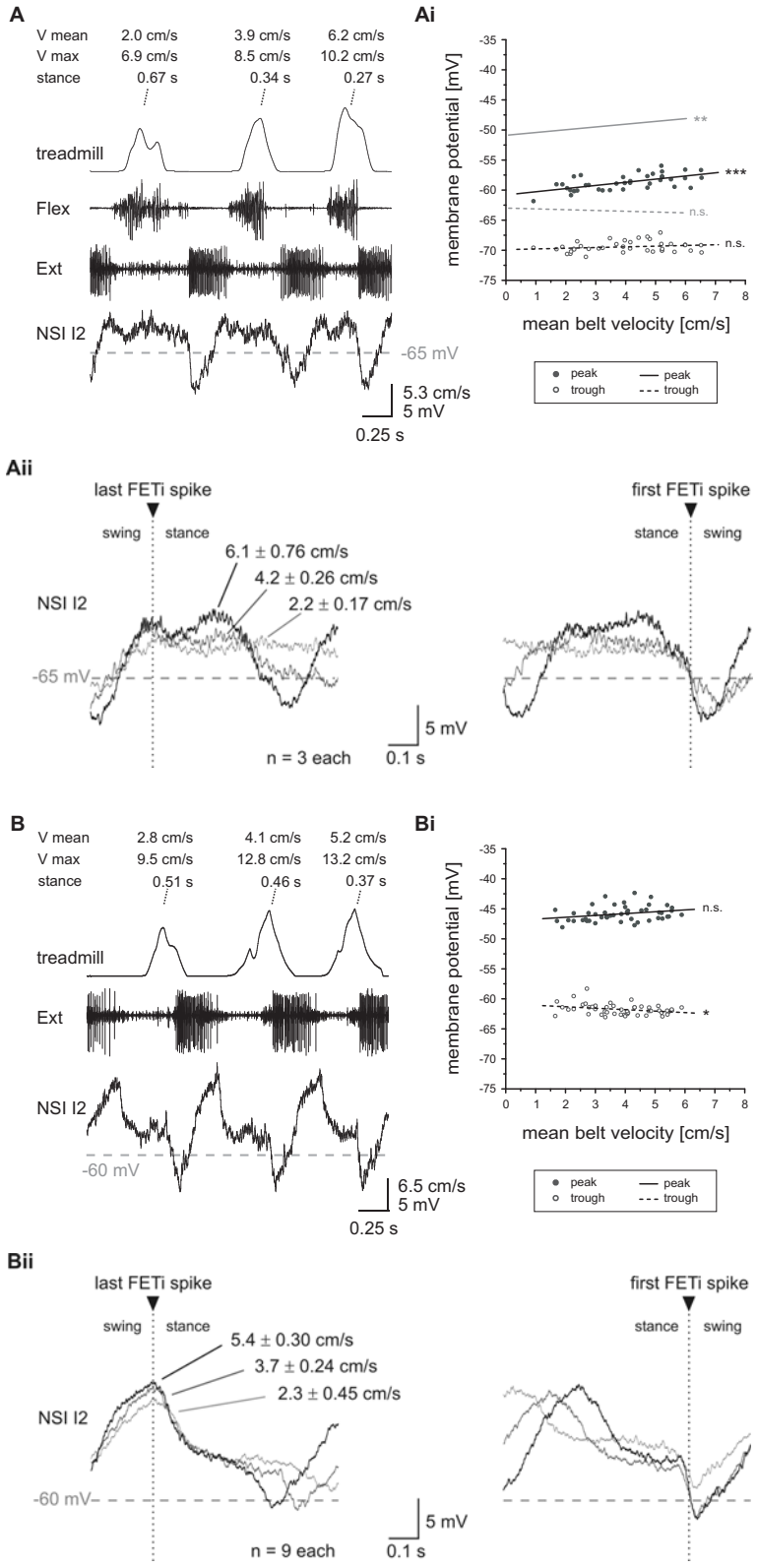

Figure 3.25: Modulation of I2 NSIs in relation to stepping velocity. **A** Three steps with different velocities and stance phase durations (V mean: 2.0, 3.9, 6.2 cm/s; V max: 6.9, 8.5, 10.2 cm/s; stance duration: 0.67, 0.34, 0.27 s) along with recordings from I2 (intracellular), extensor MNs (Ext; nerve recording) and flexor MNs (Flex; EMG). **Ai** The increase in peak potential

was correlated with the increase in mean belt velocity in both recordings (n = 38, black regression line (***); grey regression line (**)). The trough potential showed no systematic changes (dashed regression lines: (n.s.)). **Aii** The averaged time courses of fast (6.1 ± 0.76 cm/s, n = 3), medium (4.2 ± 0.26 cm/s, n = 3), and slow (2.2 ± 0.17 cm/s, n = 3) steps indicated the largest depolarization amplitude for fast steps and the longest duration of the depolarization for slow steps. With the beginning of swing phase the averaged time courses of all three fast, medium, and slow steps hyperpolarized below RMP (-65 mV). **B** Three steps with different velocities (V mean: 2.8, 4.1, 5.2 cm/s; V max: 9.5, 12.8, 13.2 cm/s; stance duration: 0.51, 0.46, 0.37 s) from another recording from a type I2 NSI (RMP -60 mV) along with extensor MN activity (Ext; nerve recording). **Bi** The peak potential increased with mean belt velocity (n = 48), but was not significantly correlated (n.s.; P = 0,056). The trough potential was significantly correlated with mean belt velocity and showed a negative slope (dashed regression line (*)). **Bii** The averaged time courses of fast (5.4 ± 0.3 cm/s, n = 9), medium (3.7 ± 0.24 cm/s, n = 9), and slow (2.3 ± 0.45 cm/s, n = 9) steps indicated again the largest depolarization amplitude during fast steps and the smallest during slow steps. Aligned at the time of the first FETi spike, the averaged time courses revealed a stronger hyperpolarization in the early swing phase in fast steps compared to slow steps, indicating a stronger disinhibition of extensor MNs. The stars mark the level of significance: (***) $P < 0.001$; (**) $0.001 \leq P < 0.01$; (*) $0.01 \leq P < 0.05$; (n.s.) not significant $P > 0.05$.

From a NSI E6 recording, two steps with different velocities (V mean: 5.3 and 3.1 cm/s) are exemplified in Figure 3.26 (A). The relationship between mean belt velocity and peak and trough potential of E6 NSIs was analyzed for two recordings (Figure 3.26 B). Neither peak nor trough potential showed significant correlation with mean belt velocity (n = 21, black regression lines (n.s.); grey regression lines (n.s.)). However, modulations of membrane potential at different stepping velocities were compared. The averaged time courses of fast (6.0 ± 0.78 cm/s, n = 3), medium (4.0 ± 0.82 cm/s, n = 3), and slow (3.1 ± 1.2 cm/s, n = 3) steps showed a similar depolarization at the initiation of stance, but then differed clearly in the course of the ongoing stance phase (Figure 3.26 C, left). The slower the stepping velocity was the later in stance the peak depolarization occurred. At the end of stance phase, the time course of repolarization was independent of stepping velocity (Figure 3.26 C, right). The same was true for the level of hyperpolarization reached during swing, which was only little below RMP (-68 mV).

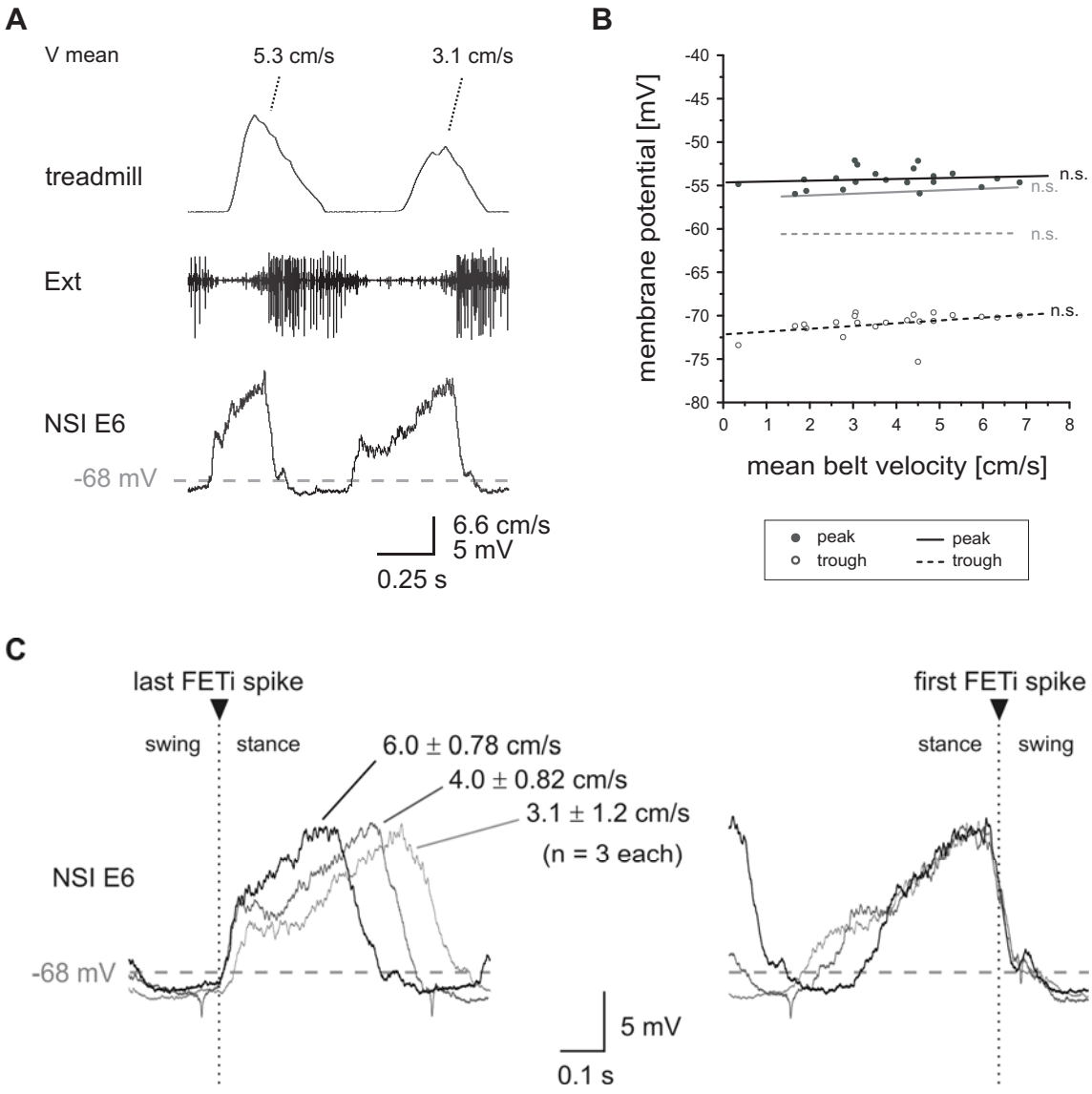

Figure 3.26: Modulation of NSI E6 in relation to stepping velocity. **A** Two steps with different velocities (V mean: 5.3 and 3.1 cm/s) along with the activity of extensor MNs (Ext; nerve recording) and E6 (intracellular recording). **B** In both recordings presented, neither peak nor trough potential showed significant correlation with mean belt velocity (n = 21, black regression lines (n.s.); grey regression lines (n.s.)). **C** Averaged time courses of fast (6.0 ± 0.78 cm/s, n = 3), medium (4.0 ± 0.82 cm/s, n = 3), and slow (3.1 ± 1.2 cm/s, n = 3) steps showed a similar initial depolarization at the beginning of stance. The peak depolarization occurred earlier in stance for fast steps and later in stance for slow steps. The time course of repolarization at the transition from stance to swing and the subsequent hyperpolarization during swing was similar for all stepping velocities. E6 was hyperpolarized only little below RMP (-68 mV). The stars mark the level of significance: (***) $P < 0.001$; (**) $0.001 \leq P < 0.01$; (*) $0.01 \leq P < 0.05$; (n.s.) not significant $P > 0.05$.

The relationship between mean belt velocity and peak and trough potential of NSI E1 was analyzed for two recordings (Figure 3.27 A). In both recordings, the peak depolarization increased significantly with mean belt velocity (n = 20, black regression line (***); grey regression line (*)). The trough membrane potential was not significantly correlated (dashed regression lines (n.s.)). The averaged membrane potentials of fast (5.9 ± 0.23 cm/s, n = 4), medium (3.7 ± 0.81 cm/s, n = 8), and slow 2.4± 0.33 cm/s, n = 6) steps showed that the time course of depolarization at the beginning of stance was the same for all velocities. Hence, the amplitude of depolarization was larger and exceeded RMP (-43 mV) only during fast steps (Figure 3.27 B, left). The repolarization occurred earlier during fast steps, indicating again the longer duration of stance phase during slower stepping velocities. With the beginning of swing phase, the averaged time courses for all three stepping velocities hyperpolarized to the same level (Figure 3.27 B, right).

From a NSI E5 recording, a stepping sequence with several steps of different velocities is shown in Figure 3.28 (A). Three steps with different mean belt velocities are highlighted (V mean: 2.2, 3.7 and 5.2 cm/s). A small tonic depolarization seemed to underlie during this stepping sequence. The membrane potential hyperpolarized during stance phase. Only during the fastest steps, the hyperpolarization reached a level below RMP (-50 mV). The relationship between mean belt velocity and peak and trough potential in E5 was analyzed (Figure 3.28 B). The peak depolarization occurring during swing phase was rather independent of mean belt velocity for both recordings presented (drawn regression lines (n.s.)). However, the trough membrane potential occurring during stance phase showed a negative slope in both recordings and was significantly correlated with mean belt velocity in one of them (n = 12, black dashed regression line (*) for the recording exemplified in (A); grey dashed regression line (n.s.)). The correlation with maximum belt velocity in this recording was even stronger ((***), data not shown). The averaged membrane potentials of fast (5.6 ± 0.43 cm/s, n = 3), medium (4.0 ± 1.0 cm/s, n = 9), and slow (2.1 ± 0.51 cm/s, n = 4) steps showed the strongest hyperpolarization during stance phase for fast steps (Figure 3.28 C, left). During slow steps, the hyperpolarization was the less pronounced. Apparently, the activity of extensor MNs is inhibited during stance phase, i.e., the phase of flexor activity, and the

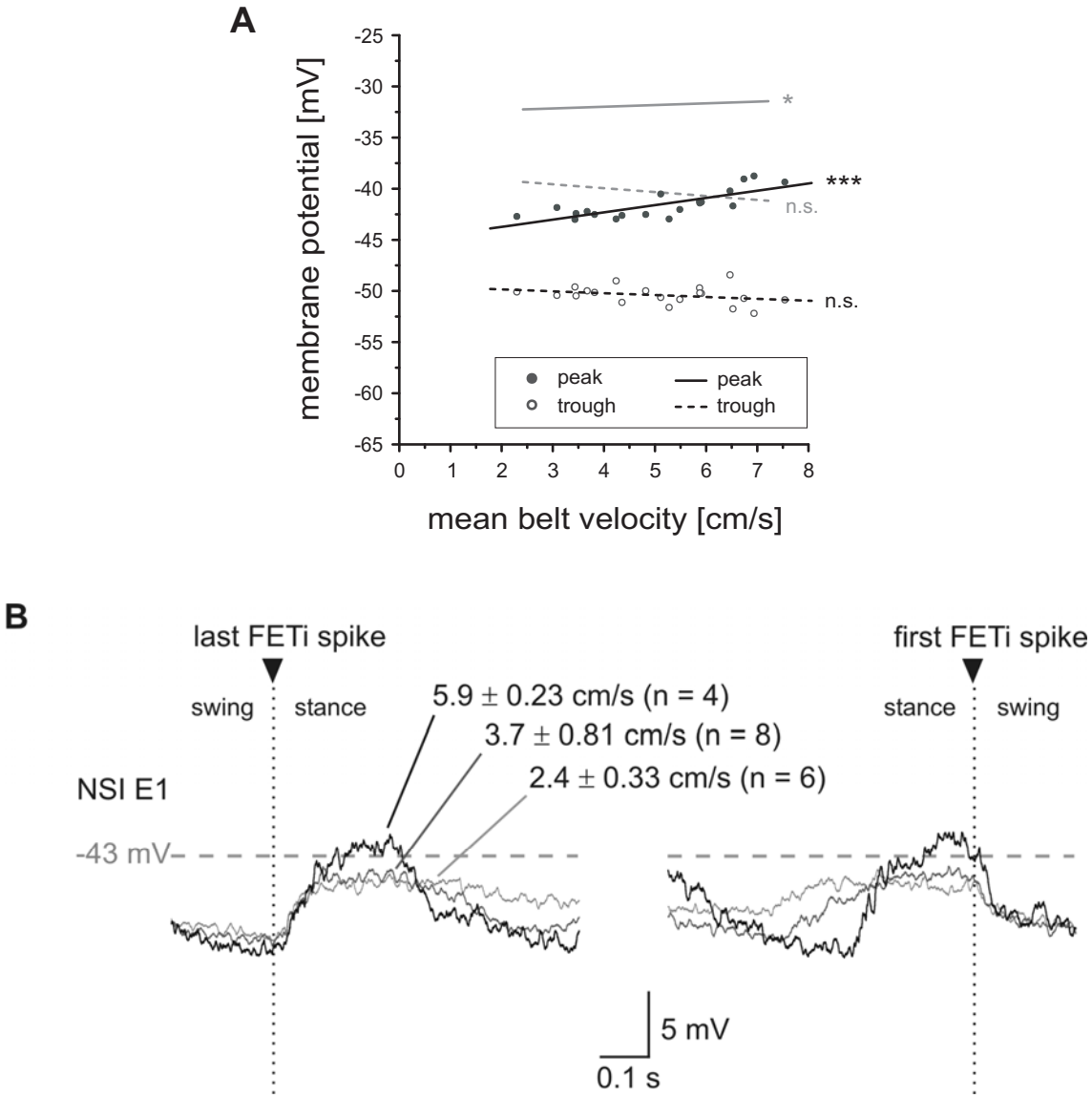

Figure 3.27: Modulation of NSI E1 in relation to stepping velocity. **A** In both recordings presented, the increase in peak potential was correlated with the increase in mean belt velocity (n = 20, black regression line (***); grey regression line (*)). The trough potential showed no correlation (dashed regression lines (n.s.)). **B** Averaged time courses of fast (5.9 ± 0.23 cm/s, n = 4), medium (3.7 ± 0.81 cm/s, n = 8), and slow (2.4 ± 0.33 cm/s, n = 6) steps showed a similar initial depolarization at the beginning of stance. The amplitude of depolarization was larger and exceeded RMP (-43 mV) during fast steps. Stance phase duration was longest during slow steps as can be seen from the prolonged depolarization. With the beginning of swing, all three averaged time courses hyperpolarized to the same level. The stars mark the level of significance: (***) $P < 0.001$; (**) $0.001 \leq P < 0.01$; (*) $0.01 \leq P < 0.05$; (n.s.) not significant $P > 0.05$.

strength of inhibition is related to stepping velocity. From the averaged membrane potentials aligned at the time of the first FETi spike, it became visible that the amplitude of depolarization during swing phase was very similar for all three fast, medium, and slow steps and thereby rather independent of stepping velocity (Figure 3.28 C, right).

The relationship between mean belt velocity and peak and trough potential in NSIs E2/3 (n = 41), E8 (n = 45), E4 (n = 22), E7 (n = 21) and I4 (n = 6) were also analyzed. Neither peak nor through potential showed a correlation with mean belt velocity (Figure 3.29), albeit the recordings presented provided a large number of steps and a wide range of mean belt velocity. For NSIs E7 and I4, only one recording of each type showed both a sufficient number of steps and a range of mean belt velocity large enough to enable a quantification of the relationship between modulation amplitude and stepping velocity. NSI I8 was not analyzed at all, because of the small number of steps and their similar velocities. The amplitude of membrane potential modulations of NSIs E2/3, E8, E4, E7 and I4 seemed not to contribute to alterations in stepping velocity. The analysis of membrane potential time course for the NSIs E2/3, E8, E4, E7 and I4 also failed to show systematic changes in parallel to the mean belt velocity.

The correlation coefficients for all regression lines presented in Figure 3.24 - Figure 3.29, resulting from the analysis of NSI peak and trough potential *versus* mean velocity, are summarized in Table 3.3.

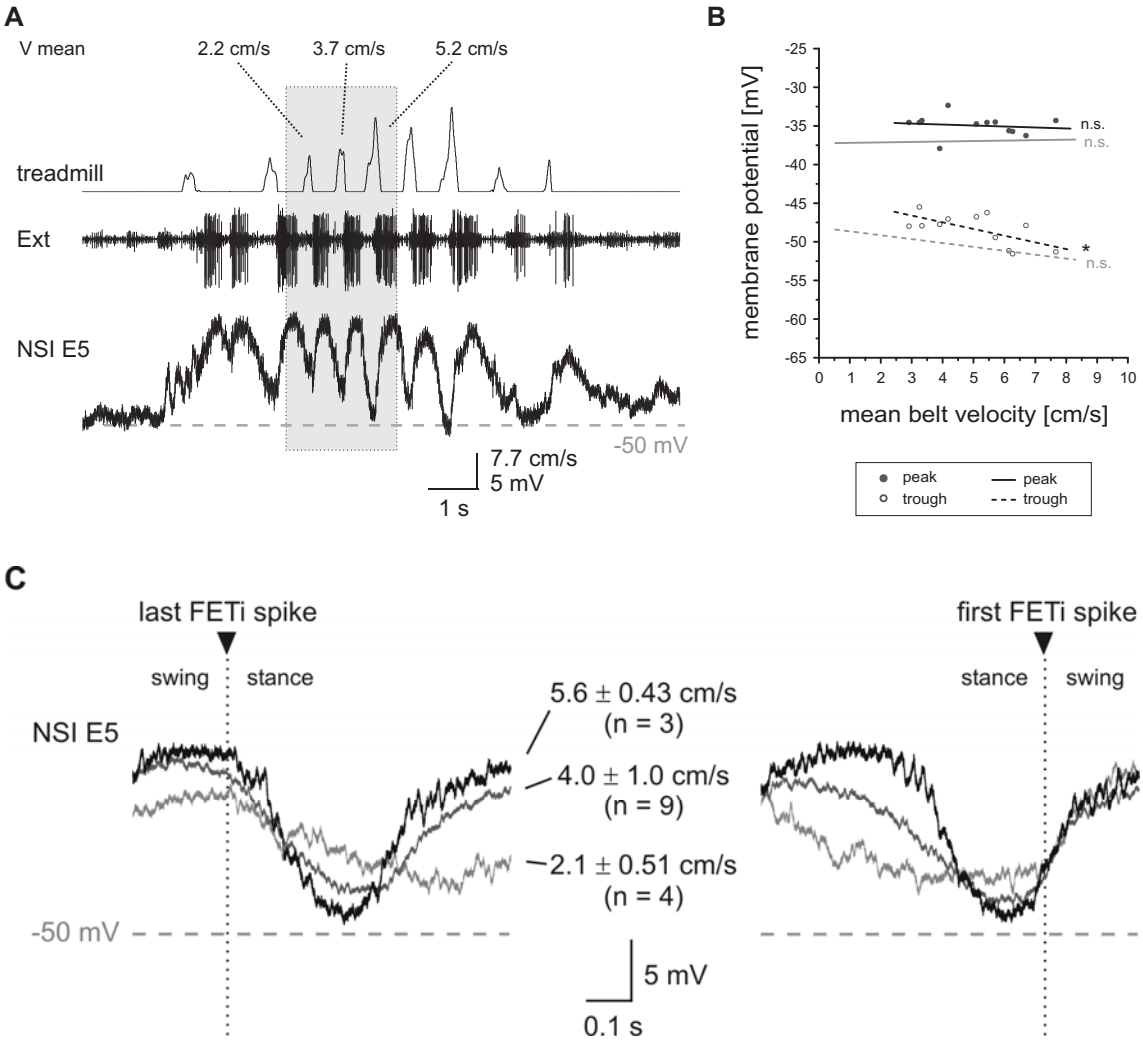

Figure 3.28: Modulation of NSI E5 in relation to stepping velocity. **A** A stepping sequence with steps of different velocities, three of which are highlighted (V mean: 2.2, 3.7 and 5.2 cm/s). A small tonic depolarization seemed to underlie during this stepping sequence. The membrane potential was hyperpolarized during stance phase and reached a level below RMP (-50 mV) only during the fastest steps. **B** In both recordings presented, the peak depolarization occurring during swing phase and the mean belt velocity were rather independent from one another (drawn regression lines (n.s.)). The trough potential occurring during stance phase showed a negative slope in both recordings and was significantly correlated with mean belt velocity in one of them (n = 12, black dashed regression line (*) for the recording exemplified in (A); grey dashed regression line (n.s.)). **C** The averaged membrane potentials of fast (5.6 ± 0.43 cm/s, n = 3), medium (4.0 ± 1.0 cm/s, n = 9), and slow (2.1 ± 0.51 cm/s, n = 4) steps showed the strongest hyperpolarization during stance phase for fast steps. From the averaged membrane potentials aligned at the time of the first FETi spike, it became visible that the amplitude of depolarization during swing phase seemed to be independent of stepping velocity. The stars mark the level of significance: (***) $P < 0.001$; (**) $0.001 \leq P < 0.01$; (*) $0.01 \leq P < 0.05$; (n.s.) not significant $P > 0.05$.

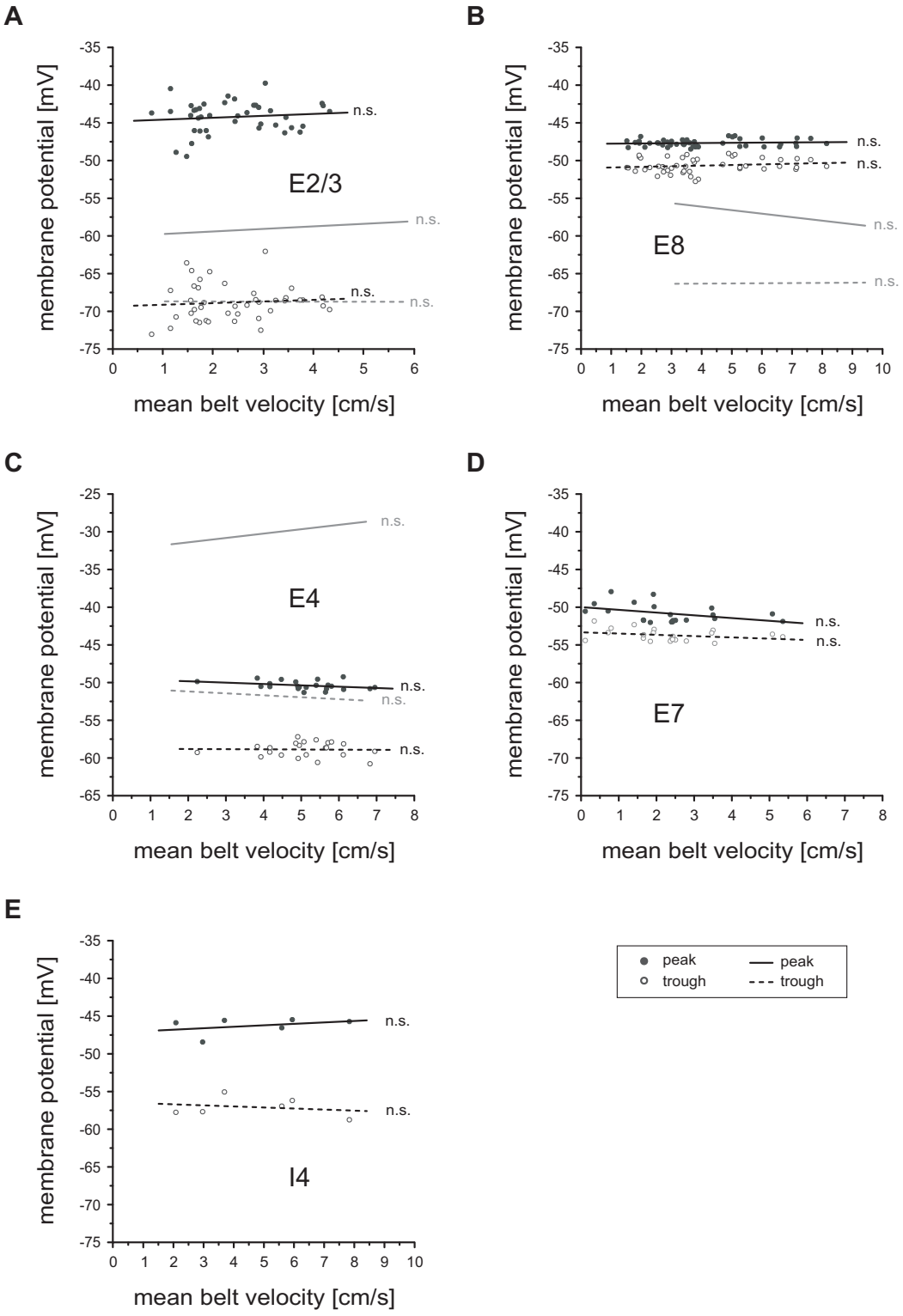

Figure 3.29: Modulation of NSIs E2/3, E8, E4, E7 and I4 in relation to stepping velocity. The membrane potential modulations of **A** E2/3 (n = 41), **B** E8 (n = 45), **C** E4 (n = 22), **D** E7 (n = 21) and **E** I4 (n = 6) seemed not to contribute to stepping velocity, since neither peak nor through potential showed a correlation with mean belt velocity. (n.s.) not significant $P > 0.05$.

Table 3.3: Correlation coefficients (R) for all regression analyses presented with NSI peak and trough potential *vs.* mean velocity. n: number of steps analyzed.

	black regression lines			**grey regression lines**		
	n	R peak	R trough	n	R peak	R trough
I1	25	0.57	0.053	11	0.603	0.128
I2 (A)	38	0.622	0.185	42	0.407	-0.136
I2 (B)	48	0.277	-0.302	-	-	-
E6	21	0.148	0.392	20	0.24	0.038
E1	20	0.771	-0.301	15	0.534	-0.304
E5	12	-0.14	-0.65	8	0.076	-0.68
E2/3	41	0.116	0.084	19	0.241	-0.026
E8	45	0.104	0.159	39	-0.222	0.011
E4	22	-0.33	-0.023	9	0.645	-0.257
E7	21	-0.407	-0.294	-	-	-
I4	6	0.368	-0.23	-	-	-

In summary, alterations in stepping velocity in relation to modulation of the peak depolarization could exclusively be observed in NSIs I1, I2 and E1, all of which showed an activation, i.e., depolarization of membrane potential, during stance phase. None of the NSIs that were activated, i.e., depolarized, during swing phase showed peak depolarizations modulated with variations in stepping velocity (Table 3.4). However, one of the NSIs activated during swing, i.e., NSI E5, showed a correlation between trough potential and stepping velocity in one experiment, indicating an inhibition during stance phase that became stronger with faster velocities. A similar observation was made in one I2 recording where both peak and trough potential increased in amplitude with stepping velocity during fast steps.

Table 3.4: Contribution of NSI types to alterations in stepping velocity. NSI types are listed depending on their contribution to the generation of stepping, i.e., whether they were activated during stance or during swing. Modulation of peak depolarization in relation to variation in stepping velocity either occurred (+) or not (-).

Activation during stance	**I1 +**	**I2 +**	**E1 +**	**E6 -**	**E7 -**	
Activation during swing	**I4 -**	**I8 -**	**E2/3 -**	**E4 -**	**E5 -**	**E8 -**

3.7 Correlation between extensor MN activity and stepping velocity in the single middle leg preparation

Subsequent to the investigation of NSI activity in relation to stepping velocity, the question arose how variations of locomotor speed are represented at the motoneuronal level. Therefore, the relationship between the instantaneous FETi spike frequency (1/interspike interval) and the belt velocity during stepping was analyzed. Two regression analyses were performed at a time for each recording. First, the mean FETi spike frequency was plotted *versus* the mean belt velocity. Second, the maximum FETi spike frequency was plotted *versus* the maximum belt velocity for a time independent description. Stepping sequences from fifteen experiments (animals) were analyzed with 484 overall steps (N = 15, n = 484). Recordings were selected that included a large number of steps and a large range of belt velocity. Step number, range of mean and maximum velocity, as well as the respective mean ± SD are listed in Table 3.5 for each of the 15 experiments. The overall mean velocity ranged from 0.5 to 8.3 cm/s (mean: 4.55 ± 1.61 cm/s, n = 484) and the overall maximum velocity ranged from 0.9 to 20.8 cm/s (mean: 9.41 ± 3.06 cm/s, n = 484).

One typical stepping sequence is exemplified in Figure 3.30 (A). The registered belt velocity of the treadmill during stepping is shown along with the extensor MN activity from the nerve recording. Additionally, the instantaneous FETi spike frequency (freq) is shown. The regression analyses for this stepping sequence are given in Figure 3.30 (Ai). There was no significant correlation in both cases, neither for the mean FETi spike frequency plotted against mean belt velocity nor for the maximum FETi spike frequency plotted against maximum belt velocity. These data are shown again together with the results from the analyses of the other 14 recordings in Figure 3.30 (B). By means of clarity, the results for the mean spike frequency plotted against mean belt velocity are extended in Figure 3.30 (C). For each of the 15 experiments, the regression coefficients for both analyses are given in Table 3.6.

Table 3.5: Step number, range and mean ± SD of mean velocity, as well as range and mean ± SD of maximum velocity for each of the 15 experiments analyzed.

n	mean velocity [cm/s]		maximum velocity [cm/s]	
	range	mean ± SD	range	mean ± SD
15	2.1 – 6.2	4.66 ± 1.31	4.6 – 14.0	9.15 ± 2.4
23	2.6 – 6.2	4.45 ± 0.88	3.5 – 14.2	7.69 ± 2.4
72	1.6 – 8.3	5.28 ± 1.51	2.8 – 14.8	9.46 ± 2.52
30	2.0 – 6.5	3.86 ± 1.07	4.4 – 12.1	8.89 ± 1.58
9	4.8 – 7.6	6.29 ± 0.88	8.7 – 12.2	10.33 ± 1.1
32	0.5 – 4.9	2.78 ± 1.36	0.9 – 9.8	5.31 ± 2.26
16	2.2 – 7.9	5.11 ± 1.56	5.0 – 20.8	10.93 ± 4.76
10	3.0 – 5.9	5.91 ± 1.8	6.8 – 16.5	11.57 ± 2.99
39	1.1 – 8.3	4.64 ± 1.65	3.3 – 14.7	9.45 ± 2.5
9	2.6 – 5.1	4.1 ± 0.87	4.6 – 9.5	6.93 ± 1.44
11	5.5 – 8.0	6.6 ± 0.84	10.9 – 15.7	13.53 ± 1.43
32	1.2 – 6.0	3.71 ± 1.46	3.1 – 15.0	8.94 ± 3.02
37	1.6 – 3.0	4.47 ± 1.44	5.8 – 17.4	10.18 ± 2.68
86	0.6 – 7.9	4.27 ± 1.66	1.7 – 17.8	10.4 ± 3.54
63	1.4 – 8.0	4.89 ± 1.35	4.5 – 14.3	9.53 ± 2.05

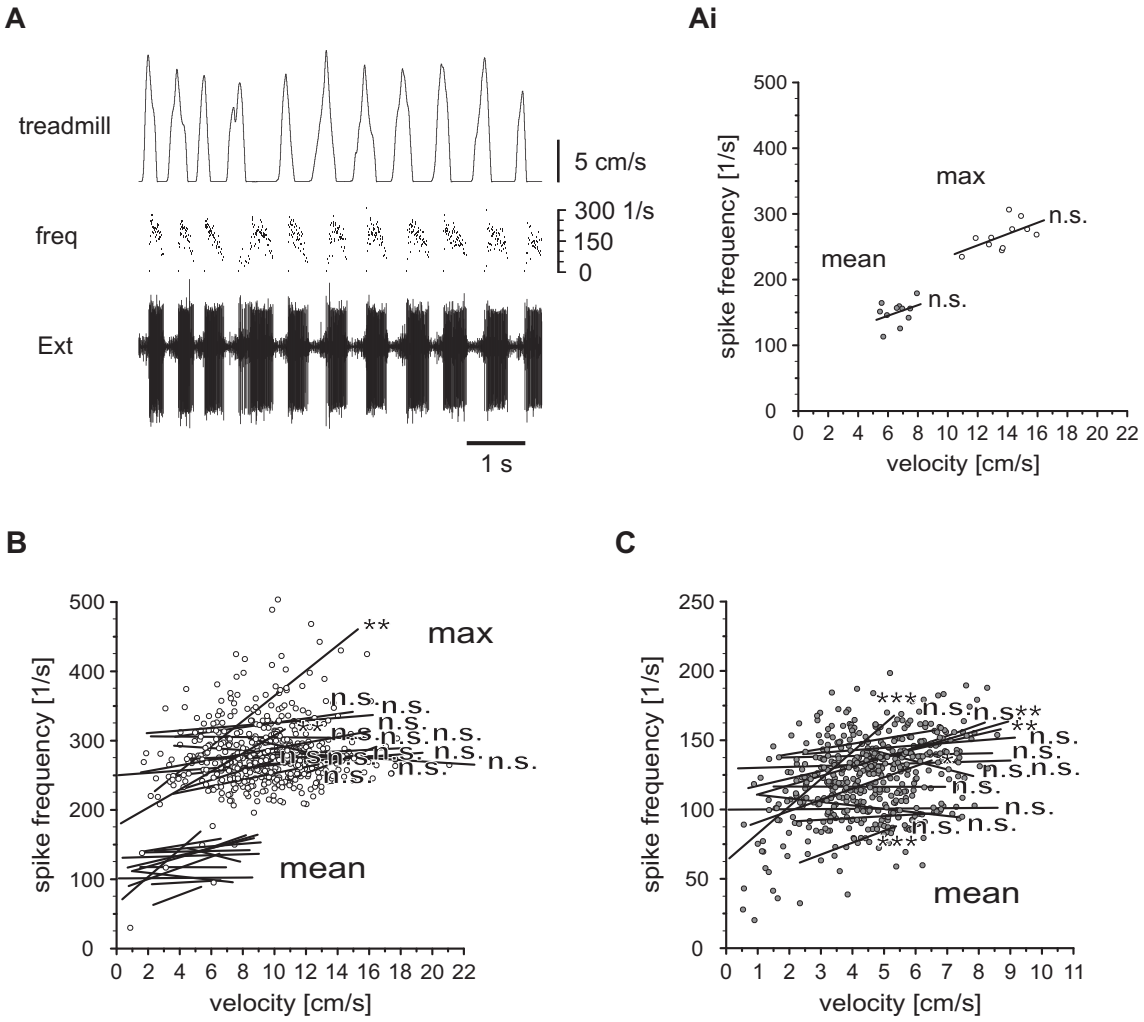

Figure 3.30: Extensor MN activity and stepping velocity. **A** Example of one typical stepping sequence. Treadmill belt velocity is shown along with extensor MN activity (Ext; nerve recording) and instantaneous FETi spike frequency (freq) during stepping. **Ai** Plot of FETi spike frequency against belt velocity for the stepping sequence exemplified in (A), with mean: mean spike frequency *versus* mean velocity, and max: maximum spike frequency *versus* maximum velocity. There was no significant correlation in this example. The data from (Ai) is shown together with data from 14 other recordings (**B, C**). By means of clarity, the results for mean spike frequency *versus* mean belt velocity are extended (**C**). In 10/15 experiments mean spike frequency was not significantly correlated with mean stepping velocity. In 13/15 experiments maximum spike frequency was not significantly correlated with maximum stepping velocity. 1/15 experiments showed a significant correlation between FETi spike frequency and stepping velocity in both cases (mean and maximum). Altogether, 484 overall steps from fifteen experiments (animals) were analyzed (N = 15, n = 484). The stars mark the level of significance: (***) $P < 0.001$; (**) $0.001 \leq P < 0.01$; (*) $0.01 \leq P < 0.05$; (n.s.) not significant $P > 0.05$.

To summarize the results, in ten out of fifteen recordings the mean spike frequency was not significantly correlated with the mean belt velocity and in thirteen out of fifteen recordings the maximum spike frequency was not significantly correlated with the maximum belt velocity. Altogether, only one out of fifteen recordings showed a significant correlation between the FETi spike frequency and the belt velocity in both cases.

Table 3.6: Correlation coefficients of instantaneous FETi spike frequency (mean or max, respectively) plotted *versus* stepping velocity (mean or max, respectively) for each of the 15 recordings analyzed. Bold values belong to the experiment exemplified in Figure 3.30 (Ai). The stars mark the level of significance: (***) $P < 0.001$; (**) $0.001 \leq P < 0.01$; (*) $0.01 \leq P < 0.05$; (n.s.) not significant $P > 0.05$.

n	**FETi mean freq *vs.* V mean**		**FETi max freq *vs.* V max**	
15	R = 0.230	n.s.	R = 0.234	n.s.
23	R = 0.043	n.s.	R = 0.602	**
72	R = 0.368	**	R = 0.204	n.s.
30	R = -0.002	n.s.	R = 0.142	n.s.
9	R = -0.319	n.s.	R = -0.224	n.s.
32	R = 0.668	***	R = 0.520	**
16	R = 0.069	n.s.	R = -0.173	n.s.
10	R = 0.323	n.s.	R = 0.036	n.s.
39	R = 0.046	n.s.	R = -0.014	n.s.
9	R = 0.936	***	R = 0.255	n.s.
11	**R = 0.371**	**n.s.**	**R = 0.586**	**n.s.**
32	R = 0.435	*	R = 0.135	n.s.
37	R = -0.284	n.s.	R = 0.078	n.s.
86	R = 0.016	n.s.	R = 0.139	n.s.
63	R = 0.371	**	R = 0.167	n.s.

3.8 Correlation between stance phase velocity and swing phase activation during single leg stepping

The preceding investigations raised the question whether there is an influence from one phase of the step cycle to the other, i.e., whether the activation strength of stance, measured as the mean belt velocity, influences the strength of swing activation, measured as time-to-peak of the instantaneous FETi spike frequency. The time-to-peak of the instantaneous FETi spike frequency (t-p) can be defined in two ways. First, as the time from the beginning of swing phase, i.e., time of the first FETi spike, until the peak frequency is reached (t-p1). Second, as the time from the end of stance phase, i.e., time of the last maximum of the treadmill trace (see chapter 2.6), until the peak frequency is reached (t-p2). To ensure that the peak spike frequency was set correctly, it was verified that the two interspike intervals neighboring the shortest interspike interval of a burst were in a similar range (see chapter 2.7). Both t-p1 and t-p2 were plotted against the mean velocity to analyze whether a correlation between the activation strength of swing phase motor output and the stepping velocity exists. Additionally, the time in between stance end and beginning of swing (t-p2–t-p1) was also plotted against the mean velocity. For these analyses, the same 15 recordings were taken as for the analysis in chapter 3.7. The range and mean ± SD of belt velocity was presented earlier (cf. Table 3.5).

A schematic drawing of one single step together with the extensor MN activity from the extracellular nerve recording and the instantaneous FETi spike frequency is shown in Figure 3.31 (A) to illustrate the definitions of t-p1, t-p2 and t-p2–t-p1:

t-p1: time from the first FETi spike (beginning of swing phase) to the peak frequency,

t-p2: time from the last maximum of the treadmill trace (end of stance phase) to the peak frequency, and

t-p2–t-p1: time from the last maximum of the treadmill trace (end of stance phase) to the first FETi spike (beginning of swing phase).

Figure 3.31 (B) exemplifies the results for one out of fifteen experiments with the respective regression lines for t-p1, t-p2 and t-p2–t-p1 plotted against the mean belt velocity. The regression line for t-p1 (light grey dotted line) showed a negative slope and was not significantly related to mean velocity. The regression line for t-p2 (dark grey dashed line) showed a negative slope and was not significantly related to mean velocity neither. The linear fit of t-p2–t-p1 plotted *versus* mean velocity, however, resulted in a significant correlation with a regression line of negative slope (black solid line, (*)).

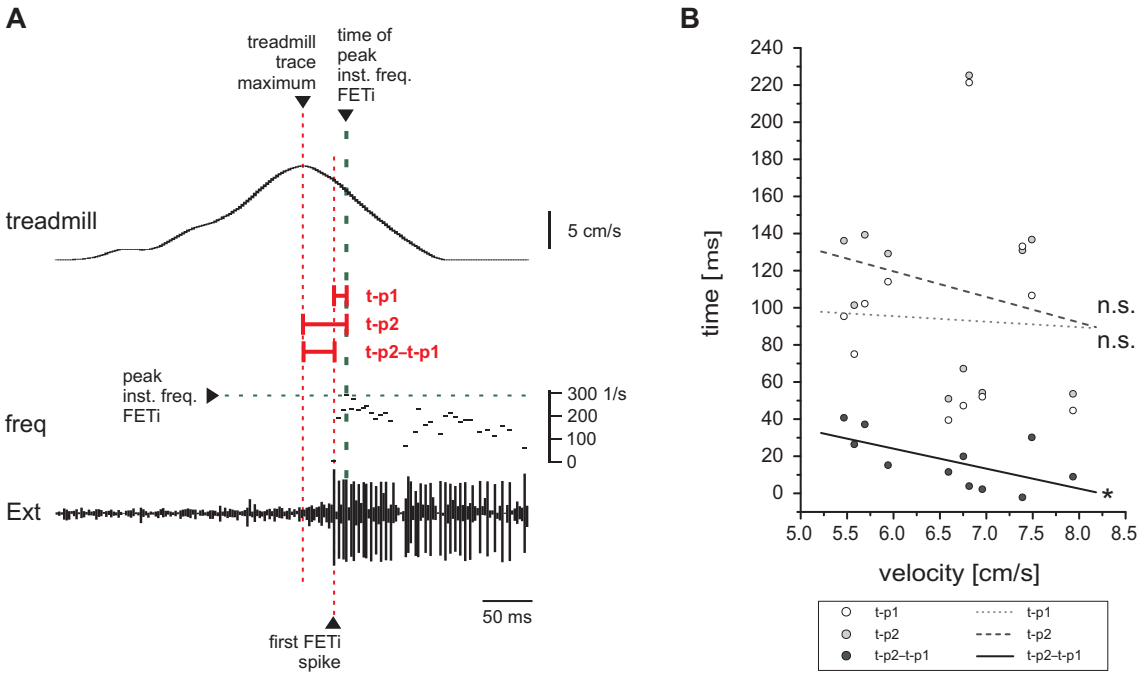

Figure 3.31: A Schematic drawing of one single step along with extensor MN activity (nerve recording) and instantaneous FETi spike frequency to illustrate the definitions of t-p1 (first FETi spike to peak frequency), t-p2 (last maximum of treadmill trace to peak frequency), and t-p2–t-p1 (end of stance to beginning of swing). **B** Data from one experiment (n = 11) with t-p1, t-p2 and t-p2–t-p1 plotted against mean belt velocity. Neither t-p1 (light grey dotted line (n.s.)), nor t-p2 (dark grey dashed line (n.s.)), but t-p2–t-p1 (black solid line, (*)) resulted in a significant correlation with mean velocity. Level of significance: (*) $0.01 \leq P < 0.05$; (n.s.) not significant $P > 0.05$.

The overall data from the 15 recordings are presented in Figure 3.32. The results are shown separately for t-p1, t-p2 and t-p2–t-p1 (Figure 3.32 A-Aii). There was no significant correlation between t-p1 and the mean belt velocity in fifteen out of fifteen experiments (Figure 3.32 A). The regression analysis of the pooled data for t-p1 also failed to show any correlation (thick dotted line; Figure 3.32 A). There was no significant correlation between t-p2 and the mean belt velocity in eleven out of fifteen experiments (Figure 3.32 Ai). The regression analysis of the pooled data for t-p2 showed a significant correlation with the mean velocity (thick dashed line; Figure 3.32 Ai). There was a significant correlation between t-p2–t-p1 and the mean belt velocity in ten out of fifteen experiments (Figure 3.32 Aii). The regression analysis of the pooled data for t-p2–t-p1 resulted in a significant correlation (thick solid line; Figure 3.32 Aii). Individual step numbers and correlation coefficients of all 15 experiments are shown in Table 3.7. Data from these analyses are presented as box plots in the bottom row of Figure 3.32 (B-Bii) in order to illustrate the distributions of t-p1, t-p2 and t-p2–t-p1, respectively. The bottom and top of the box show lower and upper quartile values, respectively. The horizontal black line within the box represents the median for each experiment. Additionally, in each case a square indicates the mean. The whiskers show 5th and 95th percentile, respectively. The median for t-p1 ranged from 13.6 to 95.4 ms (overall median of pooled t-p1 data: 38.5 ms), the median for t-p2 ranged from 56.6 to 149.7 ms (overall median of pooled t-p2 data: 95 ms), and the median for t-p2–t-p1 ranged from 15.2 to 63.8 ms (overall median of pooled t-p2–t-p1 data: 37.8 ms).

To summarize the results, the FETi time-to-peak measured from the beginning of swing phase (t-p1) showed no significant correlation with the mean velocity. The FETi time-to-peak measured from the end of stance phase (t-p2) showed a significant correlation with the mean velocity in four out of fifteen experiments, as well as in the pooled data of 484 overall steps. The time in between end of stance phase and beginning of swing phase (t-p2–t-p1) showed a significant negative correlation with the mean velocity in ten out of fifteen experiments, as well as in the pooled data.

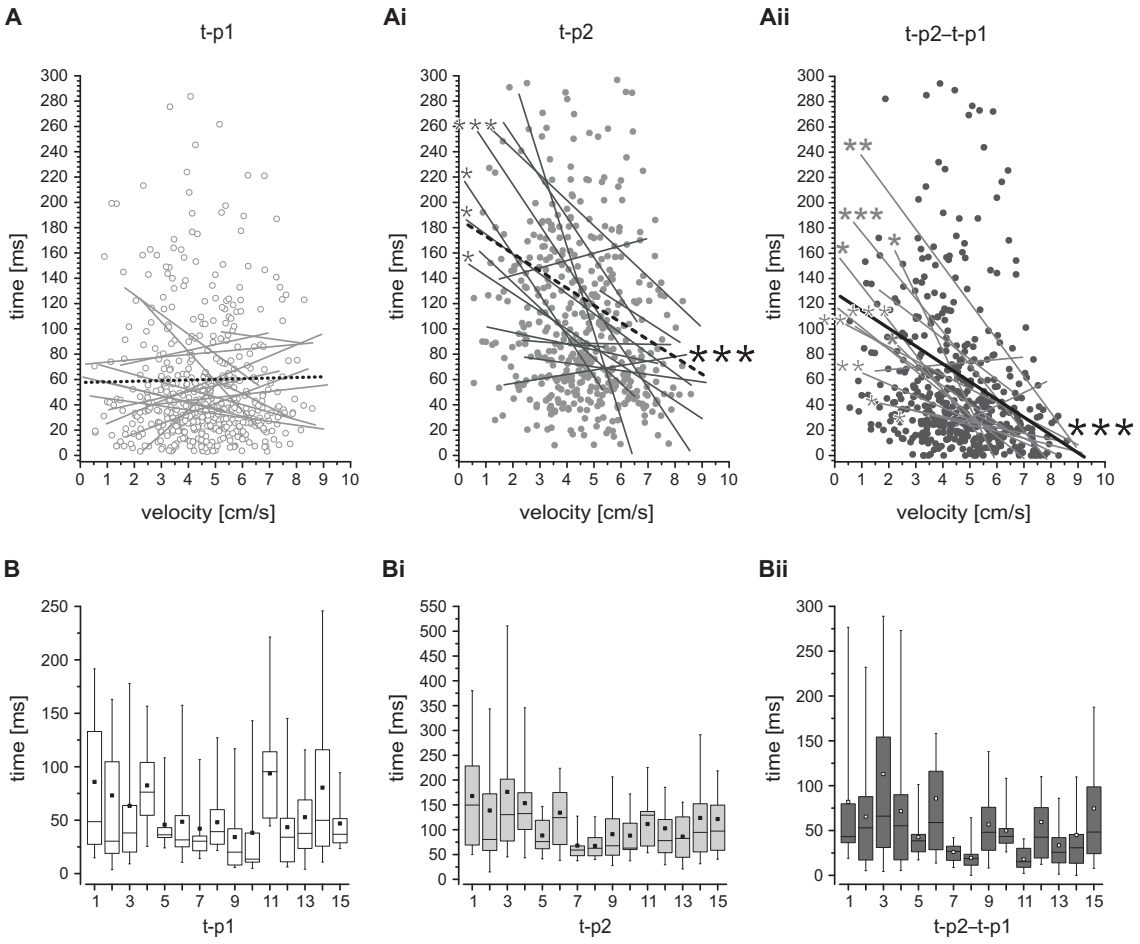

Figure 3.32: Regression analyses and box plots from 15 recordings are presented for t-p1, t-p2 and t-p2–t-p1. **A** t-p1 and mean velocity were not correlated (15/15). The pooled data for t-p1 also failed to show any correlation (thick dotted line (n.s.)). **Ai** t-p2 and mean belt velocity were not significantly correlated (11/15). The regression analysis of the pooled data for t-p2 showed a significant correlation with mean velocity (thick dashed line (***)). **Aii** There was a significant correlation between t-p2–t-p1 and mean belt velocity (10/15). The pooled data for t-p2–t-p1 showed a significant correlation (thick solid line (***)). Level of significance: (***) $P < 0.001$; (**) $0.001 \leq P < 0.01$; (*) $0.01 \leq P < 0.05$; (n.s.) not significant $P > 0.05$. **B-Bii** Data from the 15 recordings presented as box plots to illustrate the distributions of t-p1 (B), t-p2 (Bi), and t-p2–t-p1 (Bii), respectively. Line: median; boxes: 25th to 75th percentile; whiskers: 5th and 95th percentile; square: mean.

Table 3.7: Correlation coefficients of instantaneous FETi spike frequency time-to-peak (t-p) plotted *versus* mean stepping velocity for each of the 15 recordings. Bold values belong to the experiment exemplified in Figure 3.31 (B). Level of significance: (***) $P < 0.001$; (**) $0.001 \leq P < 0.01$; (*) $0.01 \leq P < 0.05$; (n.s.) not significant $P > 0.05$.

n	**t-p1 *vs.* V mean**		**t-p2 *vs.* V mean**		**t-p2–t-p1 *vs.* V mean**	
15	R = -0.243	n.s.	R = -0.336	n.s.	R = -0.21	n.s.
23	R = -0.187	n.s.	R = -0.382	n.s.	R = -0.517	*
72	R = 0.151	n.s.	R = -0.205	n.s.	R = -0.33	**
30	R = 0.116	n.s.	R = 0.08	n.s.	R = 0.028	n.s.
9	R = -0.367	n.s.	R = -0.007	n.s.	R = 0.355	n.s.
32	R = -0.147	n.s.	R = -0.418	*	R = -0.395	*
16	R = 0.346	n.s.	R = 0.157	n.s.	R = -0.555	*
10	R = 0.142	n.s.	R = -0.196	n.s.	R = -0.546	n.s.
39	R = -0.136	n.s.	R = -0.374	*	R = -0.46	**
9	R = 0.344	n.s.	R = -0.033	n.s.	R = -0.726	*
11	**R = -0.047**	**n.s.**	**R = -0.218**	**n.s.**	**R = -0.622**	*****
32	R = -0.183	n.s.	R = -0.282	n.s.	R = -0.268	n.s.
37	R = 0.181	n.s.	R = -0.142	n.s.	R = -0.436	**
86	R = 0.044	n.s.	R = -0.219	*	R = -0.371	***
63	R = -0.243	n.s.	R = -0.422	***	R = -0.413	***
484	R = 0.013	n.s.	R = -0.201	***	R = -0.266	***

4 Discussion

4.1 Afferent signals in the single middle leg preparation

Leg kinematics during middle leg stepping on a treadmill were investigated in the single leg preparation of the stick insect *Carausius morosus*. The results of the present motion tracking analysis show that the largest variation of angle during stance phase occurred in the FT-joint. The FT-angle decreased almost linearly during stance phase, which can account for a relatively constant velocity throughout one single stance phase movement. In contrast, the amplitude of CT-angle change was much smaller, i.e., approximately half as big. The CT-angle changed the direction of rotation in mid-stance, thereby producing two peaks during stance. Earlier findings by Akay et al. (2001) showed that movement signals from the CT-joint do not significantly affect tibial MN activity. In this context, the results of this study support the notion of the great importance that flexion signals from the FT-joint, monitored by its primary transducer the fCO, have in the control of tibial MN activity during the generation of single leg stepping (see also Weiland and Koch 1987). Hence, the single middle leg preparation is appropriate to study whether the activity of identified premotor NSIs in the generation of stepping corresponds to the findings on the generation of the „active reaction“.

4.2 Physiological properties of identified NSIs during single leg stepping

In the present study, the activity pattern of identified local premotor NSIs during single middle leg stepping was investigated and their contribution to the generation of motor output for stepping was revealed.

4.2.1 Activity pattern of NSIs in relation to step cycle in the single middle leg preparation

With the initiation of stepping, modulations of membrane potential were generated in all NSIs and were closely related to the step cycle. The activity pattern during stepping comprised distinct excitatory or inhibitory phasic input during at least one phase of the step cycle, i.e., stance or swing phase. Phasic excitation, for instance, visible as a depolarization of membrane potential, was seen during stance phase in the NSIs E1, E6, E7, I1 and I2, and during swing phase in the NSIs E2/3, E4, E5, E8, I4 and I8. The activity pattern of individual NSIs during stepping was thereby not predictable from the synaptic drive, i.e., excitatory or inhibitory, they provide onto MNs in the resting animal (cf. von Uckermann 2004). NSIs E2/3 and E8, which showed a very similar activity pattern, both provided excitatory drive onto extensor MNs during stepping. The same is true for NSI E5, whose activity pattern also resembled NSIs E2/3 and E8 qualitatively. NSIs E1, E6 and E7, all showed a depolarization of membrane potential during stance phase and, thereby, qualitatively the same contribution to the generation of motor output. However, E6 and E1 showed depolarizations of large amplitude during stance, whereas E7 showed a very little amplitude of membrane potential modulations during the step cycle in comparison. NSI E4 was found to reach its peak depolarization during single leg stepping shortly after the transition from stance to swing, followed by an ongoing repolarization throughout the rest of swing phase, and thus differed from the other excitatory NSIs. The two inhibitory NSIs I1 and I2 showed both a hyperpolarization of membrane potential during swing, indicating a release of extensor MN activity from inhibition. NSIs I4 and I8 both showed a qualitatively similar contribution to the stepping motor output, i.e., an excitation during swing phase. Most NSI types showed an inversion of membrane potential polarization from one phase of the step cycle to the other (cf. von Uckermann 2004). That means that a depolarization during stance was usually followed by a hyperpolarization during swing or *vice versa*. Those types of NSIs, which received phasic excitation on top of a tonic depolarization throughout a stepping sequence, subsequently showed a repolarization instead of a hyperpolarization during the following phase of the step cycle. These results corroborate the concept that

motor output for single leg stepping is produced by the parallel action of antagonistic pathways of information processing (reviewed in Bässler 1993b; Bässler and Büschges 1998). In six-legged walking, phase dependent depolarizations and hyperpolarizations were reported to result from and function within distributed, parallel, and partly antagonistic pathways underlying information processing in the FT-joint control network (Wolf and Büschges 1995; Kittmann et al. 1996; Büschges et al. 2001). The same could be true for the phase dependent depolarizations and hyperpolarizations, or repolarizations, respectively, of premotor NSIs in the generation of motor output for single leg stepping. From earlier findings it is known that each of these pathways bears a complex antagonistic interaction of excitation and inhibition at several consecutive levels (reviewed in Bässler and Büschges 1998; Büschges et al. 2000).

4.2.2 Amplitude of phasic membrane potential modulation of NSIs during single leg stepping

The amplitude of phasic modulation during single leg stepping varied markedly between the different types of NSIs. The maximum p-p amplitude of membrane potential modulation amounted to 16.9 ± 6.0 mV on average for all NSIs presented in this study and ranged from 5 mV (E7) to 34 mV (E2/3) for individual recordings. Hence, the p-p amplitudes observed in the stick insect were much higher than those reported for individual NSIs in the locust of 10 mV (Wolf and Büschges 1995) or during rhythmic leg movement in the cockroach of up to 10 mV (Pearson and Fourtner 1975). The lack of strong modulations in the case of NSI E7 suggests that its contribution to the local control of stepping might be less important. Of course, this does not exclude the possibility of a stronger involvement in the generation of walking in the six-legged animal. In this case, the weak modulation could be due to the absence of intersegmental sensory input. The p-p amplitude did not only depend on the type of NSI, but could also vary between different recordings from the same type of NSI with the actual recording site, in regard to the diameter of the impaled dendrite and the distance to active synapses.

4.2.3 Time course of NSI membrane potential modulation during single leg stepping

During stepping, not only the magnitude of phasic membrane potential modulation varied between the different types of NSIs, but also the time course of membrane potential. The maximum depolarization (peak potential), for instance, could either occur at the beginning, in the course of, or at the end of one phase of the step cycle, or right at the transition from one phase to the other. The same was true for the occurrence of the maximum hyperpolarization (trough potential). The time of peak and trough potential thereby substantially contributed to the patterning of motor output, since the membrane potential of individual types of NSIs correlated closely with the MN activity.

Interestingly, some types of NSIs were constantly depolarized at one level throughout a phase of the step cycle, e.g., E1, I1 and I8, instead of showing one peak depolarization. NSI I8, for instance, showed a plateau-like depolarization, which started at the beginning of swing phase and lasted until the beginning of stance phase, even if there was a pause in between end of FETi activity and beginning of stance. The maintained excitation could be due to sensory feedback from a local leg sensor, e.g., the fCO, and therefore last until a change is signaled, such as an initiation of leg flexion. That might indicate that the excitation would solely cease when a transition into the next phase of the step cycle is induced. Conceivably, I8 (and other NSIs being depolarized constantly throughout a phase) could be involved in the control of phase duration.

4.2.4 Tonic modulation of NSI membrane potential during single leg stepping

Besides the phasic modulation of membrane potential during stepping, a tonic excitation could be observed for individual types of NSIs, i.e., E4 and I4. However, in the single middle leg preparation used in this study, tonic depolarizations throughout a stepping sequence occurred to be less pronounced as described for mesothoracic NSIs during

stepping of a single ipsilateral front leg (Ludwar 2003). This observation leads to the notion that the tonic depolarization could result from the action of pathways for intersegmental coordination of stepping, thus, potentially also from intersegmental sensory information lacking in the preparation used here.

4.2.5 NSI activity pattern during single leg stepping compared to six-legged stepping

A detailed study on mesothoracic NSI E4 in the six-legged stick insect (Büschges et al. 1994) described an activity pattern during stepping comparable to the one revealed during single middle leg stepping, except for a time shift. In the six-legged animal, the peak depolarization occurred at the transition from stance to swing and not in the first third of swing, as during single leg stepping. This shift, however, might rather be due to the influence of local sensory signals than to the lack of intersegmental sensory information as inferred from earlier findings (Hess and Büschges 1999; Akay et al. 2001, 2004, 2007; Bucher et al. 2003; Ekeberg et al. 2004; Büschges and Gruhn 2008). Conceivably, the shifted pattern in E4 results from local sensory signals that coordinate the order of MN activity of the different joints during stepping, depending on the respective stepping situation, which are processed via the CPG networks with E4 being part of the latter (Büschges et al. 1994; Büschges 1995a; Büschges et al. 1995). Studies on six-legged locusts stepping on a double treadwheel provided descriptions of the activity pattern of individual mesothoracic NSIs, which were identified in both locusts and stick insects (Wolf and Büschges 1995). The activity pattern of, e.g., NSIs E5 and I4 during six-legged stepping did not significantly differ from the activity pattern during single leg stepping presented in this study.

4.3 NSIs as elements in the FT-joint control system of the stick insect middle leg

All NSIs were modulated around RMP during stepping and large depolarizations occurred as well as distinct hyperpolarizations. The mean RMP of all NSIs recorded amounted to -54.6 ± 8.6 mV (N = 55) and ranged from -33 to -78 mV for individual recordings. This range corresponds to NSI data in the locust (mean RMP -48 mV, range -35 to -60 mV; Burrows and Siegler 1978), but is more extended towards hyperpolarized levels. The entirety of NSIs fell into two main groups based on the RMP values. The first group contained NSIs, whose membrane potential during stepping was not only strongly, but also very symmetrically modulated around mean RMP. For NSIs in the first group, the mean RMP amounted to -56.9 ± 8.5 mV (N = 35) and ranged from -42 to -78 mV for individual recordings. These NSIs showed depolarizations and hyperpolarizations of the same amplitude. The maximum p-p amplitude for NSIs in the first group was 17.6 ± 6.2 mV on average (range: 6.5 to 34 mV). The membrane potential of NSIs in the second group was mainly modulated at levels being more depolarized than mean RMP. The mean RMP of NSIs in the second group was more positive than in the first group and amounted to -50.7 ± 7.3 mV (N = 20), with a range of -33 to -62 mV for individual recordings. The maximum p-p amplitude for NSIs in the second group was 15.6 ± 5.6 mV on average (range: 5 to 30 mV). The finding that most NSIs of the first group supported the ongoing motor output during stepping, whereas most NSIs of the second group opposed it, is likely to be coincidentally.

The main difference between the two groups might be the threshold for transmitter release. NSIs of the first group seemed to tonically release transmitter at RMP in quiescent animals. Otherwise, those NSIs could not have increased and decreased SETi spike frequency upon experimental alteration of their membrane potential by injection of positive and negative current pulses, even with smallest amounts of current, as it was observed for all NSI types of this group, e.g., I1 and E2/3 (cf. Büschges 1990). In the second group of NSIs, an injection of a depolarizing current pulse never failed to show an effect onto postsynaptic MNs, whereas mostly no effect was seen when these

neurons were shortly hyperpolarized (cf. Büschges 1990). In contrast to the first group of NSIs, whose thresholds of transmitter release apparently were lower than RMP, NSIs of the second group conceivably had thresholds a little above their RMP. These findings comply with data from NSIs in the locust where a proportion of NSIs was found to release transmitter tonically at RMP, while others did not (Burrows and Siegler 1978; Wilson and Phillips 1982).

Experiments, in which the membrane potential was artificially altered in the DCC-mode and the local input resistance was measured, revealed that the phasic excitatory and inhibitory modulations during stepping resulted from true excitatory and inhibitory synaptic input. Current injections into an individual NSI, i.e., type I1, immediately terminated stepping sequences. This indicates an important role of NSI I1 in the control of motor output for stepping. This is furthermore supported by similar findings on NSI I1 in the locust (Wolf and Büschges 1995).

4.4 Contribution of NSIs to the generation of motor activity in the single middle leg preparation

In the present study, the activity pattern of NSIs during stepping and during the „active reaction“ was studied and their contribution to both motor programs was compared. In both situations, the visible motor activity was generated by the premotor network with individual NSIs that supported the ongoing motor output and others that opposed it (cf. Driesang and Büschges 1996). The meaning of the terms supporting and opposing, in regard to the NSI activity for the investigated motor programs, will be explained using NSI E2/3 as example. NSI E2/3 supports the generation of the „active reaction“ as it showed a hyperpolarization during the first part of the „active reaction“, which is paralleled by the activation of flexor MNs and inactivation of extensor MNs and thereby corresponds to the MN activity of stance phase, and a depolarization during the second part of the „active reaction“, which is accompanied by the activation of extensor MNs and inactivation of flexor MNs and thereby corresponds to the MN activity during

initiation of swing phase (cf. Driesang and Büschges 1996). During single leg stepping, E2/3 was revealed to show a hyperpolarization of membrane potential during stance phase, i.e. flexor MN activity, and a depolarization during swing phase, i.e., extensor MN activity. Thereby, E2/3 supported the ongoing motor output, especially the extensor activity, in the generation of single leg stepping and in the generation of the „active reaction“. The same was true for NSIs E5 and E8. The inhibitory NSIs I1 and I2 also supported the motor output, since they showed the opposite activity pattern as described for excitatory NSIs, thereby removing inhibition from extensor MNs during swing phase. For NSIs that oppose the ongoing motor output, i.e., E1, E4, E6, E7, I4 and I8, the reversed situation is found concerning the activity pattern during tibial MN activity.

NSIs reported to support the „active reaction“ are E2/3, E5, E6, I1 and I2, whereas NSIs E1 and E4 were found to oppose the actual motor output (cf. Table 3.2; Driesang and Büschges 1996). In the course of the present study, the hitherto unknown contribution of NSIs E7 and E8 to the generation of the „active reaction“ could be revealed. NSI E7 opposed and E8 supported the visible motor output. The contribution of NSIs to a given motor program, e.g., “active reaction” or stepping, was always the same. No qualitative variability of contribution to one motor program occurred between different recordings from one respective type of NSI. During single leg stepping, NSIs E2/3, E5, E8, I1 and I2 were found to support the ongoing motor output and NSIs E1, E4, E6, E7, I4 and I8 to oppose it. Hence, these results reveal great accordance between the contribution of NSIs during stepping and their contribution to the generation of the „active reaction“.

These observations bear out the principle that parallel action of partly antagonistic pathways of information processing generates the motor output in a concerted and distributed manner (Bässler 1993b), during single leg stepping and during the generation of the “active reaction”. This principle was first proved for reflex pathways in stick insects (Bässler 1993b) and also appears to underlie the control of active motor programs such as stepping (see also Wolf and Büschges 1995). Earlier studies revealed that the quality of contribution of a given NSI type can differ from one motor task to another (Kittmann et al. 1996). Thus, the contribution of one type of NSI depends on the actual motor program generated and can be supporting for one motor program but

opposing for another. Strikingly, the comparison of NSI contribution to the generation of the „active reaction“ and to the generation of stepping presented in this study revealed great accordance. Hence, the results presented strongly support the notion that the motor response during the „active reaction“ represents a part of the control regime for the generation of single leg stepping (cf. Bässler 1988).

Only one NSI type, namely NSI E6, differed concerning the quality of its contribution between the generation of single leg stepping and the generation of the „active reaction“. During the „active reaction“ E6 supported the motor output in accordance to the activity of extensor MNs, i.e., E6 was depolarized during extensor MNs activity (cf. Driesang and Büschges 1996). However, during stepping E6 was depolarized during flexor MNs activity and thereby rather supported the generation of stance phase. Interestingly, E6 was thought earlier to possibly represent a kind of subtype of E5 NSIs. The characteristics of these NSIs could be determined in the course of development upon the biophysical requirements met, and therefore, phenotypes of E5 and E6 NSIs could occur together or only E5 characteristics could be expressed (U. Bässler, personal communication). In the case of E5 phenotype, the position information reported to be processed by E6 could be transmitted via other position-sensitive NSIs as E3, for instance, thus compensating the lack of E6. One argument supporting this possibility is that E5 NSIs were recorded in the locust mesothoracic ganglion many times, whereas E6 NSIs have not yet been reported (Büschges and Wolf 1995; Wolf and Büschges 1995).

4.5 Estimated number of premotor NSIs within one thoracic ganglion in insects

Albeit the progress in science and the development of new techniques there is no recent information available on the total number of local interneurons within one ganglion. An estimated number of 1200 local interneurons resulted from subtraction of identified neurons from the estimated number of 2000 neurons for one thoracic ganglion of the

locust (reviewed in Burrows 1996). Within this population of local interneurons, a number of 100 NSIs was roughly estimated for one thoracic hemiganglion of the locust, with approximately 70 of them thought to control one leg (Siegler 1985). This estimation is supported by evaluation of the ontogeny of nerve cells where the last cell division of a neuroblast gives birth to one glia cell and one local intraganglionic nonspiking neuron (Goodman et al. 1980). At least 30 types of NSIs are known that affect mainly MNs of the distal leg segments in the locust (Siegler and Burrows 1979; reviewed in Siegler 1985). That leads to an estimated number of 40 NSIs for the motor control of the proximal leg joints of one single leg. In the stick insect twelve different types of NSIs were characterized for the control of the FT-joint, which is one of the three proximal leg joints (Büschges et al. 1994). Even though NSI pools for the control of individual sets of MNs in the stick insect partly overlap (cf. Büschges 1995a), the existence of a large number of copies or even clusters of one NSI type which would be expressed altogether within one ganglion seems not very likely. However, the question remains open whether all identified types of NSIs are present altogether in each animal. In a few experiments, different types of NSIs were subsequently recorded and identified within one ganglion in the course of this study and in earlier studies, e.g., NSIs E8 and I2 (von Uckermann 2004), but for means of clarity more than two NSIs were never stained within one ganglion. One NSI type of the FT-joint control system known to exist in at least two copies or subtypes, respectively, is E4. Two E4 NSIs were stained together within one mesothoracic hemiganglion of the stick insect and were reported to differ concerning their branching patterns, since one of them showed midline dendrites which the other one didn't (Büschges et al. 1994; Büschges and Wolf 1995). These two types are reported to correspond to the NSIs named DCVII,1 (with midline dendrites) and DCVII,2 (without midline dendrites) in the locust (Wilson 1981), albeit DCVII,1 apparently excites flexor MNs and not extensors MNs in the locust (reviewed in Field and Matheson 1998).

4.6 Correlation between NSI membrane potential and extensor MN activity during single leg stepping

It was analyzed how tight premotor NSIs control the activity of the fast extensor MN (FETi) during stepping. For this purpose, the instantaneous FETi spike frequency was plotted as a function of membrane potential, in order to quantify the relation between the MN activity and the drive provided by individual NSIs. For each type of NSI the instantaneous FETi spike frequency was plotted *versus* the membrane potential during swing phase, i.e., the phase of FETi activity, as well as *versus* the membrane potential during the whole step cycle, i.e., stance and swing phase.

The regression analyses for swing phase showed different results for individual NSI types and between individual recordings for some types of NSIs, ranging from no significant correlation to a significant correlation with either a positive or a negative slope, respectively, whereas all regression analyses for the whole step cycle resulted in a strong correlation. This might partly be due to the general activity pattern of NSIs during stepping. First, NSIs inversed their polarization pattern from one phase of the step cycle to the other (see chapter 4.2.1). Second, the membrane potential excursion throughout the whole step cycle was always larger than the change in membrane potential occurring during one single phase in most cases, e.g., stance or swing. Thereby, subtle changes in membrane potential during one phase of the step cycle responsible for changes in MN activity could remain hidden in the analysis of the whole step cycle. Hence, for each NSI the results of both regression analyses, i.e., swing phase only and whole step cycle, respectively, must always be taken into account. By doing so, three different classes could emerge. A first class would consist of NSIs that show a strong correlation with a slope of the same sign in both cases as a result of all regression analyses performed for the NSI type in question. In this case, FETi spike frequency would relate to NSI membrane potential at any time throughout the step cycle indicating a direct effect and strong contribution of the respective NSI to extensor activity. These NSIs can be assumed to control FETi activity. These NSIs should also be involved in the fine tuning of extensor activity because of the close correlation between FETi spike

frequency and membrane potential throughout the step cycle. A second class would consist of NSIs that show strong correlations with a slope of the same sign in both cases as a result of most but not all regression analyses performed for the NSI type in question. These NSIs can also be assumed to contribute to the control of FETi activity. However, their contribution might be mediated less directly. A third class of NSIs would show no consistent results. These NSIs can be assumed not to support extensor activity. Indeed, all three functionally different classes resulted from the analyses presented.

The NSIs E2/3, E8, E4 and I2 were found to show strong correlations between the instantaneous FETi spike activity and the respective membrane potential. Five regression analyses were performed for each of these NSI types. The correlations were significant and the respective regression lines all showed slopes of the same sign in five out of five experiments. The excitatory NSIs E2/3, E8 and E4 showed positive correlations in all regression analyses, whereas the inhibitory NSI I2 showed negative correlations in the regression analyses. These results indicate not only a general activation of extensor activity in the case of E2/3, E8 and E4, and a release from inhibition in the case of I2, respectively, but also a role in the fine tuning of extensor activity since FETi spike frequency and membrane potential were related at any time throughout the step cycle.

The NSIs I1 and E5 also showed strong correlations between the instantaneous FETi spike activity and the respective membrane potential. For I1 the resulting correlations were all significant but only two out of three pairs of regression lines were consistent concerning the sign of their slopes in both cases. The third pair showed different signs of slope. Only two out of five regression analyses performed for E5 were positively correlated in both cases, whereas three out of five pairs differed concerning the sign of slope. Two of the latter regression lines resulting from swing phase analysis were not significant. Thus, regression analysis for NSI E5 resulted in a significant correlation between membrane potential and FETi activity in only three out of five experiments, and only two of these showed a positive correlation in both cases. That means that NSI E5 supported the extensor motor output during stepping in most but not all experiments. NSI I1 seemed to contribute to the motoneuronal output by disinhibition of extensor

MN activity, without any further control of output magnitude. This indicates an indirect contribution to extensor activity, possibly mediated trough a polysynaptic connection.

Regression analyses for the NSIs E1, E6, E7, I4 and I8 resulted in no consistent relation. For E1, E6 and I8 all pairs of regression lines showed opposite slopes, indicating that these NSIs do not support extensor activity. Opposing results were found in the two experiments performed for E7. Presumably, E7 plays a minor role in the control of FETi activity, as it was also indicated in the generation of motor output for stepping. The analyses performed for I4 differed in their results. The analysis of one I4 experiment resulted in a significant positive correlation in both cases suggesting a possible contribution to the control of extensor MN activity, such as the termination of swing and transition to stance phase. However, this was not confirmed by the second I4 experiment. If NSIs E1, E6, E7, I4 and I8 contribute to the control of extensor activity, their effect is likely to be mediated through a polysynaptic connection.

To summarize, the results suggest that extensor activity depends on the membrane potential of NSIs E2/3, E8, E4 and I2. It became apparent that the results from this analysis matched very well with the results described earlier in this study (chapter 3.2). The contribution of individual NSIs to the control of extensor activity was in accordance to their respective contribution to the generation of functional motor output for stepping. For instance, the NSIs E2/3 and E8, which were found to support the motor output of extensor MNs during stepping since they provide excitatory drive onto extensor MNs and were depolarized during swing phase, were found to be strongly involved in the control of extensor activity. NSI I1 was shown to support the extensor MN activity during the generation of stepping by disinhibition of extensor MNs and was found to contribute to the control of FETi activity by the same mechanism in this analysis. NSIs E1 and E6, for example, which were found to oppose the extensor activity during stepping since they provide excitatory drive onto extensor MNs but were depolarized during stance phase, did not support extensor activity in this analysis either.

4.7 Contribution of NSIs to alterations in stepping velocity in the single middle leg preparation

In order to address the role identified local NSIs play for the alteration of stepping velocity, two aspects of membrane potential modulations were examined in relation to variations in stepping velocity. First, the correlation between modulation amplitude and mean stepping velocity was quantified by plotting the peak and trough potentials occurring during stepping against the mean belt velocity as a measure of the mean stepping velocity. Second, alterations in time course of membrane potential in relation to variations of the mean belt velocity were investigated by comparison of averaged time courses of a given NSI recording during steps of different velocities.

The analyses presented here revealed that individual NSIs, i.e., I1, I2 and E1, contributed to the variation of stepping velocity by alteration of peak membrane potential, whereas other NSI types failed to show such velocity dependent modulations of peak amplitude. The investigation of NSI activity pattern during stepping showed that I1, I2, E1, E6 and E7 were activated during stance phase, whereas E2/3, E4, E5, E8, I4 and I8 were activated during swing phase (cf. chapter 3.2). From the combination of these results, the conclusion emerges that three out of five NSI types activated during stance are involved in the control of stepping velocity, whereas NSI types activated during swing do not underlie the control of stepping velocity (six out of six types). Two types of NSIs activated during stance, i.e., E6 and E7, showed no correlation between modulation amplitude and stepping velocity. NSI E7 showed very small modulations of membrane potential during the generation of motor output for stepping as described earlier (cf. chapter 4.2.2). Albeit the lack of amplitude modulation in relation to variations in stepping velocity, the time course of membrane potential in E6 NSIs appeared clearly to alter with stepping velocity. The time course of depolarization during stance phases of different velocities in E6 mirrored the activity of flexor MNs during variations of stepping velocity described recently (Gabriel and Büschges 2007), and suggests a possible contribution of E6 to the control of stance phase motor output.

The results presented on the correlation between time course of membrane potential of premotor NSIs and alterations in stepping velocity match earlier findings since it is known that changes in walking speed in insects result primarily from changes in cycle period, which in turn is generally achieved by a decrease in stance phase duration (Wendler 1964; Wilson 1966; Graham 1972; Burns 1973; Graham and Cruse 1981; Halbertsma 1983; reviewed in Orlovsky et al. 1999; Yakovenko et al. 2005). A correlation between modulation amplitude and stepping velocity was observed exclusively for individual NSI types that were activated during stance. Thereby, the previous finding from Gabriel and Büschges (2007) that the synaptic drive onto stance phase MNs, i.e., flexor MNs, is modified with changes in stepping velocity of the single leg is corroborated and extended to the premotor level. There are indications of an influence of sensory feedback, which arise from the fact that flexor MNs activity is reinforced during leg flexions in the active locomotor system (e.g., Bässler 1993a,b). Given that some of the synaptic drive onto flexor MNs arises from local sense organs, it is conceivable that changes in the effectiveness or gain of the underlying sensorimotor pathways, perhaps arising from descending inputs, may alter rate and amplitude of their activation (Bässler 1986a, 1988; Akay et al. 2001; cf. Yakovenko et al. 2005; reviewed in Büschges and Gruhn 2008).

Interestingly, for individual NSI types, i.e., I2 and E5, a correlation between trough potential and stepping velocity was found. In one I2 recording including very high stepping velocities, an increase in both the amplitude of peak and of trough potential was observed with increasing stepping velocity. The trough potential occurred in early swing, indicating a disinhibition of extensor MN activity. Thereby, the disinhibition was stronger during fast steps compared to slower steps. A similar observation was made for NSI E5, except for the difference that E5 received inhibition in relation to stepping velocity during stance phase and its excitatory drive provided onto extensor MNs during swing was independent of stepping velocity. These results indicate that during fast stepping velocities the stance part of the locomotor network is stronger activated and simultaneously the extensor part is inhibited to the same extent during stance phase.

4.8 Correlation between extensor MN activity and stepping velocity in the single middle leg preparation

In order to investigate the relationship between swing phase activity, i.e., extensor MN activity, and stepping velocity, the instantaneous FETi spike frequency was plotted against the belt velocity. Both the correlation between mean spike frequency and mean belt velocity as well as maximum spike frequency and maximum belt velocity was analyzed. In ten out of fifteen experiments there was no significant correlation between mean FETi spike frequency and mean belt velocity. In thirteen out of fifteen experiments there was no significant correlation between maximum FETi spike frequency and maximum belt velocity. Only one experiment out of fifteen showed a significant correlation between FETi spike frequency and belt velocity in both cases.

These results on tibial extensor MN activity contrast recent findings on the activity of the antagonistic flexor MNs where a strong correlation between flexor activity and stepping velocity could be shown (Gabriel and Büschges 2007). The results indicate that stepping velocity is independent of swing phase activity, i.e., extensor activity, and, hence, matches with the finding that the part of the premotor network which controls swing phase does not contribute to alterations in stepping velocity.

4.9 Correlation between stance phase velocity and swing phase activation during single leg stepping

Based on a model calculation, Cruse (2002) hypothesized that a local adaptation mechanism working on a step-to-step basis would lead to an influence from stance to swing phase, in the way that a muscle which was strongly excited during stance would automatically excite its antagonist during the subsequent swing. It was investigated in the present study whether there was an influence from one phase of the step cycle to the other, i.e., whether the activation strength of stance influenced the strength of swing

activation. Therefore, the relationship between the mean belt velocity resulting from stance phase activity and swing phase activation strength measured as time-to-peak of the instantaneous FETi spike frequency was analyzed.

No significant relation to mean velocity could be found when time-to-peak was measured from the beginning of the FETi burst (t-p1). Since the peak frequency usually occurred quite early in a FETi burst, a second analysis was performed where time-to-peak was measured from the end of stance phase (t-p2). As a result there was a significant correlation in four out of eleven experiments, as well as in the pooled data of fifteen experiments. However, the strongest relation resulted when the time in between end of stance phase and beginning of swing phase (t-p2–t-p1) was plotted *versus* mean belt velocity. In this case, ten out of fifteen significant correlations were found. The regression analysis of the pooled data also showed a strong correlation. The median values for the time in between end of stance and beginning of swing ranged from 15.2 to 63.8 ms (median of the pooled data: 37.8 ms; N = 15, n = 484).

The indicated values corresponded to earlier findings from Fischer et al. (2001), which described a pause of 29.8 ± 29.6 ms (mean ± SD) at the transition from stance to swing between the activity of flexor and extensor MNs. However, the results presented here differed in one aspect from the earlier findings. Fischer et al. (2001) described the duration of the pauses to be independent of cycle period. The findings present here, however, showed a strong negative correlation between the time from end of stance to beginning of swing and the mean belt velocity. This means, the pause between stance and swing phase activity becomes shorter with increasing speed and completely disappears during fast stepping sequences as was observed in the course of this study. This, again, matches with the earlier finding of the negative correlation between cycle period and velocity (cf. Wendler 1964; Halbertsma 1983; reviewed in Orlovsky et al. 1999; Yakovenko et al. 2005; Gabriel and Büschges 2007).

The results presented indicate that there is no velocity dependent influence between stance and swing phase generation, at least, not in the way that activation strength of stance would influence the subsequent activation strength of swing. These findings

suggest that the hypothesis formulated by Cruse (2002) on this concern does not apply for the control of stepping in the single middle leg preparation. This is further corroborated by the findings presented earlier in this study. First, stepping velocity was independent of extensor MN activity as found from the analysis of FETi spike frequency (cf. chapters 3.7 and 4.8). Second, albeit extensor MN activity was tightly controlled by individual premotor NSIs supporting the generation of motor output for stepping (cf. chapters 3.5 and 4.6), the investigation of NSI activity revealed that modulations of membrane potential in relation to stepping velocity occurred exclusively in NSIs that were activated during stance and not in those activated during swing (cf. chapters 3.6 and 4.7). Third, the finding that one of the NSIs activated during swing received inhibition in relation to stepping velocity during stance phase indicated that not only the stance part of the locomotor network is stronger activated during fast steps but also the swing part is stronger inhibited. These results on the different NSI activity patterns and functions are summarized schematically in Figure 4.1.

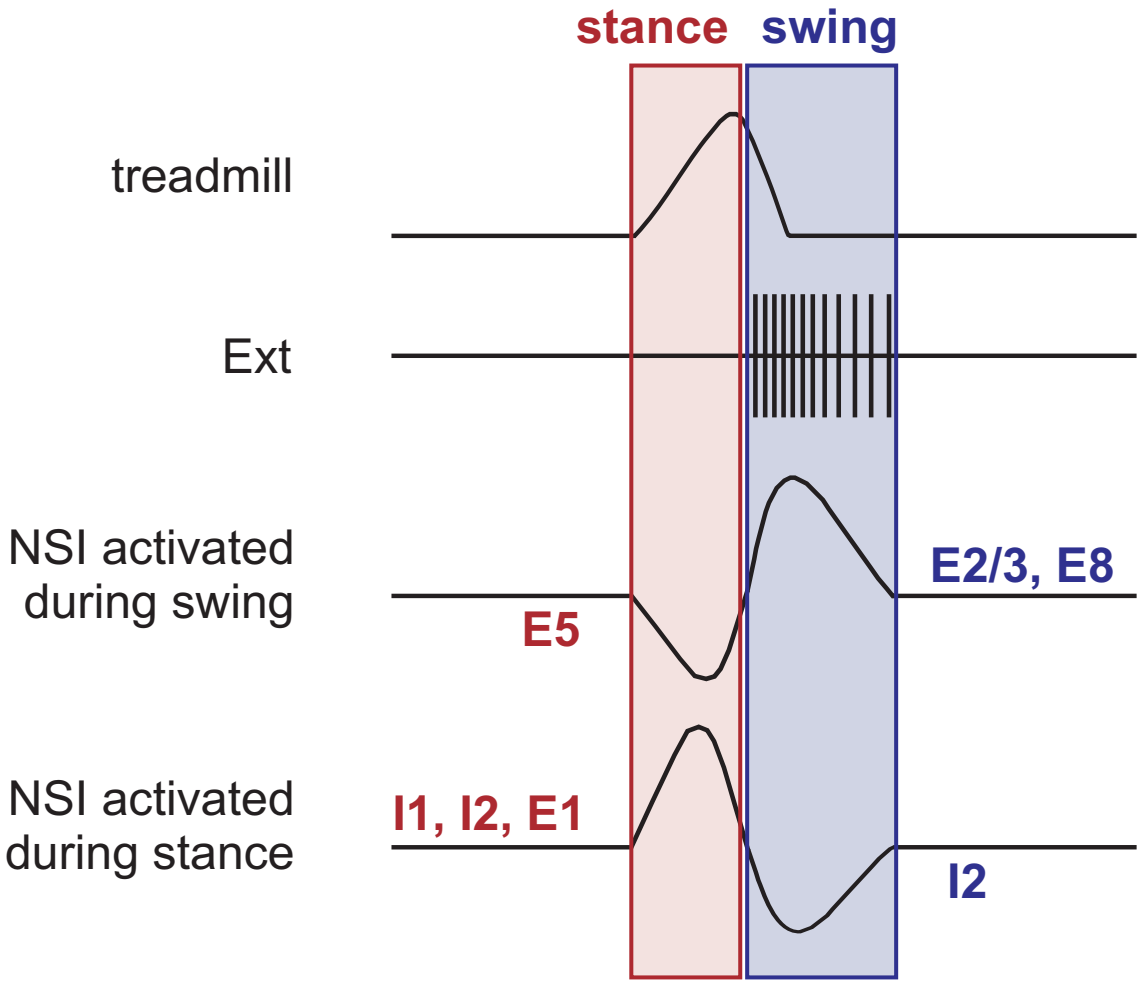

Figure 4.1: Simplified scheme summarizing the contribution of individual NSI types to the local control of locomotion. First, individual NSIs that support the generation of swing phase motor output tightly control the extensor MN activity by both the graduated depolarization of the excitatory NSIs E2/3 and E8, and the hyperpolarization of the inhibitory NSI I2 (disinhibition). Second, the stepping velocity is independent of extensor MN activity as resulted from the analysis of FETi spike frequency *versus* belt velocity. Third, modulations of membrane potential that are correlated to stepping velocity exclusively occur in NSIs that are activated (depolarized) during stance phase (NSIs I1, I2, E1) and not in those activated during swing phase. Fourth, the finding that NSI E5 receives inhibition in relation to stepping velocity indicates that not only the stance part of the locomotor network is stronger activated during fast steps but also the extensor (swing) part is stronger inhibited during stance phase. Fifth, the activation strength of stance does not influence the subsequent activation strength of swing, at least, not in the way that there would be a velocity dependent influence between stance and swing phase generation.

4.10 Conclusions on the role of NSIs during single leg stepping and outlook to possible future projects

The insights gained in the course of the present study on the activity of NSIs within the FT-joint control system of the stick insect raise the assumption of a premotor network being built from individual components with specific features rather than from homogenous neurons. Actually, there seem to be several functionally different and partly overlapping pools of NSIs. Apparently, some types control the actual magnitude of motor activity (e.g., E2/3, E8, I2), others seem to be involved in the generation of step phase transitions (e.g., E2/3, E4, I4) or the control of phase duration (e.g., I8, I1, E1), and again others play a role in the control of adaptive motor tasks, such as the control of stepping velocity (e.g., E1, I1, I2).

Several questions remain open that could be worth being addressed in future projects on premotor NSIs in the stick insect.

First, the role premotor NSIs play in the control of walking direction should be addressed. Earlier studies on the stick insect revealed that forward walking can be elicited by touching the abdomen of a stick insect and backward walking by pulling softly on the antennae (Graham and Epstein 1985; Akay et al. 2007). Recent preliminary data from the single middle leg preparation of *Carausius morosus* corroborated this finding and revealed that the stepping direction often changes spontaneously within one stepping sequence. In the single middle leg preparation, stepping is performed sideways on a treadband that is orientated perpendicular to the axis of the animal body. The walking direction, i.e., forward or backward, therefore is a fictive walking direction, but becomes obvious from the activity of the restrained TC-joint MNs, i.e., pro- and retractor coxae MNs. During forward stepping, retractor MNs are active together with flexor MNs during stance phase, whereas backward stepping is characterized by the activity of protractor MNs together with flexor MNs during stance. Forward and backward steps could easily be differentiated within the stepping sequences when activity of both pro- and retractor coxae MNs for the walking direction

and flexor and extensor tibiae MNs for the status of the step cycle is monitored by extracellular recordings. Simultaneous intracellular recording from identified premotor NSIs would allow for subsequent analysis of alterations in membrane potential modulation in relation to changes in stepping direction. Following the examination of the correlation between NSI activity and alterations in stepping velocity, it would be interesting to investigate how premotor NSIs contribute to changes in walking direction.

Second, eliciting stepping by artificial alteration of NSI membrane potential should be tested. NSI activity that was recorded during a stepping sequence could subsequently, during rest of the animal, be played back into the NSI in voltage clamp. It would be very interesting to investigate whether stepping could be elicited this way. To find out which are the crucial parameters of the activity pattern, the artificial stimulus could be changed in amplitude, shape or time course. It could further be analyzed which effect on the motor output a characteristic activity pattern from one NSI type has when played back to another NSI type. Different ramps or sine waves as a stimulus could also be tested. However, sine waves are said to be too unspecific for successful stimulation in most systems (B. Johnson, personal communication). By playing back recorded activity into NSIs in the resting animal, information could certainly also be gained about which NSI type is crucial for the generation of a functional motor output for stepping and whose activity can be compensated by other neurons of the premotor network.

Third, the molecular cell biology and intrinsic properties of NSIs should be investigated. Recently, an immunocytochemical project on the stick insect thoracic ganglia has been started in order to reveal transmitters and neuromodulatory substances (Gruhn, Meyen-Southard and Büschges, in preparation), but also intrinsic properties of NSIs should be addressed with the use of electrophysiological methods and drug application. A method for the pharmacological investigation of MN activity in the actively stepping animal has successfully been established (Schmidt and Westmark, described in Westmark 2007) which could now be used for the investigation of premotor NSIs. This method includes a mechanical removal of the ganglion sheath, the neurilem, which acts as a diffusion barrier for ions (Schofield 1979; Dörr et al. 1996) and pharmacological agents (Westmark 2007). This method enables pharmacological investigation of ion

conductances responsible for NSI activity. Especially, potassium and calcium channels with voltage dependent properties, known to be responsible for amplitude and pattern of membrane potential oscillations in interneurons of the crustacean stomatogastric ganglion (summary in Harris-Warrick 2002), would be interesting candidates for investigation in premotor NSIs of the locomotion generating network of the stick insect.

Fourth, a quite challenging enterprise would be to analyze the connectivity of premotor NSIs. Therefore, it would be very valuable to perform simultaneous intracellular recordings from two neurons within one hemiganglion. It should be considered to analyze the connectivity between NSIs and MNs first, since MNs bear the possibility to be recorded from the soma. The soma locations of the MNs driving the three main leg joints are well known (Bässler and Storrer 1980; Storrer et al. 1986; Debrodt and Bässler 1989; Goldammer 2008). A further advantage is that MN somata are comparably easy to access because of their size and lateral location in the ganglion (Storrer et al. 1986; Goldammer 2008). In the case of success, it could then be addressed to investigate the interconnectivity between premotor NSIs. This would be a great challenge as NSIs need to be recorded from their dendritic arborizations. Another possibility to address this issue could be the use of a staining dye able to pass synapses. Now that individual NSIs are not only characterized morphologically and during reflexes, but also during single leg stepping where they showed individual characteristics, these should be sufficient parameters for a reliable identification of the recorded neuron and the postsynaptic neuron(s). Another promising approach could be the use of a polar tracer, e.g., lucifer yellow, together with tetramethylrhodamine-dextran to investigate for the existence of electrical coupling between NSIs. The low molecular weight tracer lucifer yellow passes through gap junctions and dextrans do not, so the initially labeled cell would exhibit red fluorescence, whereas cells connected through gap junctions would have yellow fluorescence (Chandross et al. 1995). Electrical coupling was found in many other model systems, for example, in the crustacean stomatogastric ganglion (Mulloney 1987; Johnson and Harris-Warrick 1990).

The last two points are of particular interest as individual NSIs are known to affect antagonistic MN pools, e.g., NSI E4 was described to provide excitatory drive onto

protractor coxae, levator trochanteris and extensor tibiae MNs, as well as inhibitory drive onto the respective antagonists retractor coxae and depressor trochanteris MNs (Büschges 1995a). Until now, it is not known with certainty whether E4 also affects flexor tibiae MNs. NSI I2 is known to provide inhibitory synaptic drive onto extensor MNs and excitatory drive onto flexor MNs (Büschges 1990; Büschges and Wolf 1995), and a strong effect onto CT-joint MN activity could be observed in this study. Conceivably, NSI I2 could be a kind of counterpart to E4. A simplified scheme depicts the influence of NSIs onto tibial MNs, with individual types of NSIs as an example (Figure 4.2). The connections between NSIs and MNs are drawn as stippled lines since it is not known whether they are monosynaptic or not. Upon injection of depolarizing current into NSI I2 there is no apparent latency visible on the extracellular recordings between the inhibition of (slow) extensor MN activity and the excitation of (slow) flexor MN activity. Two types of underlying connections are conceivable. On the one side, NSI I2 could be connected monosynaptically with both antagonistic MNs, i.e., extensor and flexor. This in turn could imply the use of two different transmitters, one excitatory and one inhibitory, by one single neuron. Due to electrically isolated regions in NSIs that can be assumed from a model calculation based on anatomical studies (Rall 1981), and input and output synapses being intermingled on the fine dendritic branches of NSIs (Wilson and Phillips 1982), NSIs could be compartmentalized and consequently be simultaneously involved in the processing of different local circuits (Siegler and Burrows 1980; Wilson and Phillips 1983; Siegler 1984). In consequence, a neuron would no longer be the smallest functional unit within the nervous system (reviewed in Cohen and Wu 1990). On the other side, a disynaptic connection would also be conceivable, involving a spiking interneuron as it was suggested for NSI - MN connections in the locust (Burrows 1985). The NSI could excite a MN and a spiking interneuron, with the latter inhibiting the antagonistic MN (Burrows 1985). The latency of similar connections is reported to be in the same range as monosynaptic connections (Burrows 1979). Until now, the connection suggested for the locust could not be proved. Instead, numerous one-way inhibitory connections between NSIs providing excitatory drive onto MNs were found (summary in Burrows 1996).

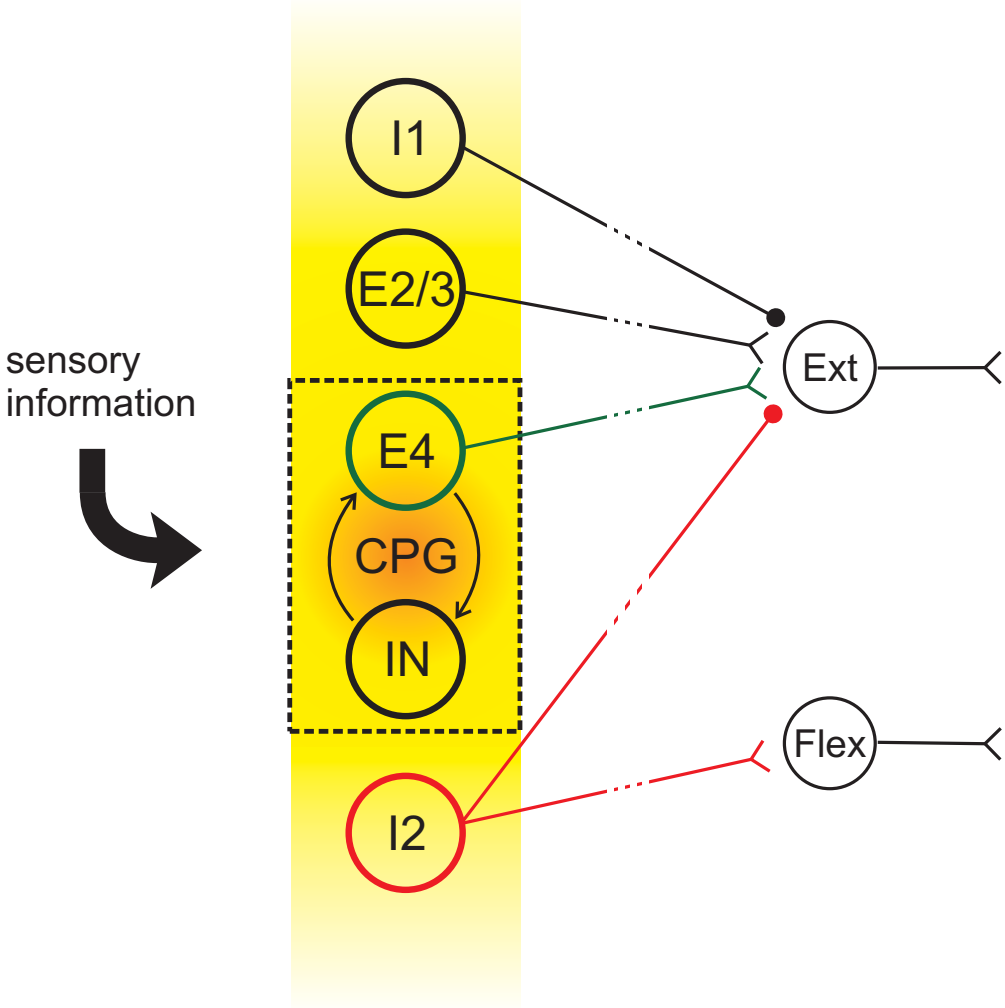

Figure 4.2: Simplified scheme depicting the influence of NSIs onto tibial MNs with individual NSI types as an example. NSI I1 provides inhibitory drive onto extensor MNs (Ext) and NSIs E2/3 and E4 excitatory drive. NSI I2 provides inhibitory drive onto extensor MNs and excitatory drive onto flexor MNs (Flex). The connections between NSIs and MNs are drawn as stippled lines since it is not known whether they are mono- or polysynaptic. Yellow square: premotor level of interneurons; dashed box: CPG for the FT-joint, including NSI E4 (Büschges 1995a) and another interneuron IN, integrating sensory information from various sources (review in Bässler and Büschges 1998). Inhibitory synapses are symbolized by circles and excitatory synapses as inversed arrowheads.

Bibliography

Akay T, Bässler U, Gerharz P and Büschges A. The role of sensory signals from the insect coxa-trochanteral joint in controlling motor activity of the femur-tibia joint. *J Neurophysiol* 85: 594-604, 2001.

Akay T. *The role of sensory signals for interjoint coordination in stick insect legs (Carausius morosus and Cuniculina impigra).* PhD thesis, University of Cologne, 2002.

Akay T, Haehn S, Schmitz J and Büschges A. Signals from load sensors underlie interjoint coordination during stepping movements of the stick insect leg. *J Neurophysiol* 92: 42-51, 2004.

Akay T, Ludwar BC, Göritz ML, Schmitz J and Büschges A. Segment specificity of load signal processing depends on walking direction in the stick insect leg muscle control system. *J Neurosci* 27: 3285-3294, 2007.

Ayers JL and Davis WJ. Neuronal control of locomotion in the lobster, *Homarus americanus*. I. Motor program for forward and backward walking. *J Comp Physiol* 115: 1-27, 1974.

Bässler U. Proprioreceptoren am Subcoxal- und Femur-Tibia-Gelenk der Stabheuschrecke *Carausius morosus* und ihre Rolle bei der Wahrnehmung der Schwerkraftrichtung. *Kybernetik* 2: 168-193, 1965.

Bässler U. Reversal of a reflex to a single motoneuron in the stick insect *Carausius morosus*. *Biol Cybern* 24: 47-49, 1976.

Bässler U and Storrer J. The neural basis of the femur-tibia-control-system in the stick insect *Carausius morosus.* I. Motoneurons of the extensor tibiae muscle. *Biol Cybern* 38: 107-114, 1980.

Bässler U and Wegner U. Motor output of the denervated thoracic ventral nerve cord in the stick insect *Carausius morosus*. *J Exp Biol* 105: 127-145, 1983.

Bässler U. *Neural basis of elementary behavior in stick insects*. Springer-Verlag, Berlin, Heidelberg, New York, 1983.

Bässler U. Afferent control of walking movements in the stick insect *Cuniculina impigra*. I. Decerebrated animals on a treadband. *J Comp Physiol A* 158: 345-349, 1986a.

Bässler U. Afferent control of walking movements in the stick insect *Cuniculina impigra*. II. Reflex reversal and the release of the swing phase in the restrained foreleg. *J Comp Physiol A* 158: 351-362, 1986b.

Bässler U. Functional principles of pattern generation for walking movements of stick insect forelegs: the role of the femoral chordotonal organ afferences. *J Exp Biol* 136: 125-147, 1988.

Bässler U. Variability of femoral chordotonal organ reflexes in the locust, *Locusta migratoria*. *Physiol Entomol* 17: 208-212, 1992.

Bässler U. The walking- (and searching-) pattern generator of stick insects, a modular system composed of reflex chains and endogenous oscillators. *Biol Cybern* 69: 305-317, 1993a.

Bässler U. The femur-tibia control system of stick insects - a model system for the study of the neural basis of joint control. *Brain Res Rev* 18: 207-226, 1993b.

Bässler U and Büschges A. Pattern generation for stick insect walking movements: multisensory control of a locomotor program. *Brain Res Rev* 27: 65-88, 1998.

Bässler U, Wolf H and Stein W. Functional recovery following manipulation of muscles and sense organs in the stick insect leg. *J Comp Physiol A* 193: 1151-1168, 2007.

Borgmann A, Scharstein H and Büschges A. Intersegmental coordination: the influence of a single walking leg on the neighbouring segments in the stick insect walking system. *J Neurophysiol* 98: 1685-1696, 2007.

Bucher D, Akay T, DiCaprio RA and Büschges A. Interjoint coordination in the stick insect leg-control system: the role of positional signaling. *J Neurophysiol* 89: 1245-1255, 2003.

Burns MD. The control of walking in Orthoptera. I. Leg movements in normal walking. *J Exp Biol* 58: 45-58, 1973.

Burrows M and Siegler MVS. Graded synaptic transmission between local interneurones and motor neurones in the metathoracic ganglion of the locust. *J Physiol* 285: 231-255, 1978.

Burrows M. Graded synaptic interactions between local premotor interneurons of the locust. *J Neurophysiol* 42: 1108-1123, 1979.

Burrows M. Local interneurones in insects. In: *Neurones without impulses*, edited by Roberts A and Bush BMH. Cambridge University Press, Cambridge, 1981, p. 199-221.

Burrows M. Nonspiking and spiking local interneurons in the locust. In: *Model Neural Networks & Behavior*, edited by Selverston AI. Plenum Publishing Corporation, 1985, p. 109-125.

Burrows M. Processing of mechanosensory signals in local reflex pathways of the locust. *J Exp Biol* 146: 209-227, 1989.

Burrows M. *The neurobiology of an insect brain*. Oxford University Press, New York, 1996.

Büschges A. Nonspiking pathways in a joint-control loop of the stick insect *Carausius morosus*. *J Exp Biol* 151: 133-160, 1990.

Büschges A, Kittmann R and Schmitz J. Identified nonspiking interneurons in leg reflexes and during walking in the stick insect. *J Comp Physiol A* 174: 685-700, 1994.

Büschges A, Schmitz J and Bässler U. Rhythmic patterns in the thoracic nerve cord of the stick insect induced by pilocarpine. *J Exp Biol* 198: 435-456, 1995.

Büschges A. Role of local nonspiking interneurons in the generation of rhythmic motor activity in the stick insect. *J Neurobiol* 27: 488-512, 1995a.

Büschges A. Plasticity of neuronal networks that control posture and movement of leg joints in insects. *Verh Dtsch Zool Ges* 88: 139-151, 1995b.

Büschges A and Wolf H. Nonspiking local interneurons in insect leg motor control. I. Common layout and species-specific response properties of femur-tibia joint control pathways in stick insect and locust. *J Neurophysiol* 73: 1843-1860, 1995.

Büschges A, Sauer AE and Bässler U. Flexibility of a proprioceptive feedback system results from its "parliamentary" (distributed) organization. In: *Prerational intelligence: adaptive behavior and intelligent systems without symbols and logic*, edited by Cruse H, Dean J and Ritter H. Kluwer Academic Publishers, Dordrecht, New York, London, 2000, p. 267-286.

Büschges A, Schmidt J and Wolf H. Sensory processing in invertebrate motor systems. *Encyclopedia of Life Sciences*, edited by Macmillan Publishers Ltd, Nature Publishing Group, 2001, p.1-7.

Büschges A, Ludwar BC, Bucher D, Schmidt J and DiCaprio RA. Synaptic drive contributing to rhythmic activation of motoneurons in the deafferented stick insect walking system. *Eur J Neurosci* 19: 1856-1862, 2004.

Büschges A. Sensory control and organization of neural networks mediating coordination of multisegmental organs for locomotion. *J Neurophysiol* 93: 1127-1135, 2005.

Büschges A and Gruhn M. Mechanosensory feedback in walking: from joint control to locomotory patterns. *Adv Insect Physiol* 34: 194-234, 2008.

Büschges A, Akay T, Gabriel JP and Schmidt J. Organizing network action for locomotion: insights from studying insect walking. *Brain Res Rev* 57: 162-171, 2008.

Chandross K, Chanson M, Spray D and Kessler J. Transforming growth factor-β1 and forskolin modulate gap junctional communication and cellular phenotype of cultured Schwann cells. *J Neurosci* 15: 262-273, 1995.

Clarac F and Chasserat C. Basic processes of locomotor coordination in the rock lobster. I. Statistical analysis of walking parameters. *Biol Cybern* 55: 159-170, 1986.

Clarac F, Cattaert D and Le Ray D. Central control components of a 'simple' stretch reflex. *Trends Neurosci* 23: 199-208, 2000.

Cohen L and Wu JY. One neuron, many units? *Nature* 346: 108-109, 1990.

Cruse H. What mechanisms coordinate leg movement in walking arthropods? *Trends Neurosci* 13: 15-21, 1990.

Cruse H. The functional sense of central oscillations in walking. *Biol Cybern* 86: 271-280, 2002.

Cruse H, Kühn S and Schmitz J. Adaptive control for insect leg position: controller properties depend on substrate compliance. *J Comp Physiol A* 190: 983-991, 2004.

Debrodt B and Bässler U. Recording from visible neurone somata in the desheathed metathoracic ganglion of the phasmid *Extatosoma tiaratum*. *Zool Jb Physiol* 93: 495-500, 1989.

DiCaprio RA and Clarac F. Reversal of a walking leg reflex elicited by a muscle receptor. *J Exp Biol* 90: 197-203, 1981.

Dörr H, Heß D and Gramoll S. Interstitial voltage and potassium concentration in the mesothoracic ganglion of a stick insect at rest and during neuronal activation. *J Insect Physiol* 42: 967-974, 1996.

Driesang RB and Büschges A. Physiological changes in central neuronal pathways contributing to the generation of a reflex reversal. *J Comp Physiol A* 179: 45-57, 1996.

Duysens J and Tax AAM. Interlimb reflexes during gait in cat and man. In: *Interlimb coordination: neural, dynamical and cognitive constraints*, edited by Swinnen SP, Heuer H, Massion J and Casaer P. Academic Press, London, 1994, p. 97-126.

Ekeberg Ö, Blümel M and Büschges A. Dynamic simulation of insect walking. *Arthropod Struct Dev* 33: 287-300, 2004.

El Manira A, DiCaprio RA, Cattaert D and Clarac F. Monosynaptic interjoint reflexes and their central modulation during fictive locomotion in crayfish. *Europ J Neurosci* 3: 1219-1231, 1991.

Field LH and Matheson T. Chordotonal organs of insects. *Adv Insect Physiol* 27: 1-230, 1998.

Fischer H, Schmidt J, Haas R and Büschges A. Pattern generation for walking and searching movements of a stick insect leg. I. Coordination of motor activity. *J Neurophysiol* 85: 341-353, 2001.

Forssberg H, Grillner S and Rossignol S. Phase dependent reflex reversal during walking in chronic spinal cats. *Brain Res* 85: 103-107, 1975.

Foth E and Bässler U. Leg movements of stick insects walking with five legs on a treadwheel and with one leg on a motor-driven belt. I. General results and 1:1-coordination. *Biol Cybern* 51: 313-318, 1985a.

Foth E and Bässler U. Leg movements of stick insects walking with five legs on a treadwheel and with one leg on a motor-driven belt. II. Leg coordination when step-frequencies differ from leg to leg. *Biol Cybern* 51: 319-324, 1985b.

Fouad K, Fischer H and Büschges A. Comparative locomotion systems. In: *Comprehensive Handbook of Psychology*, edited by Gallagher M, Nelson RJ and Weiner JB. Wiley & Sons, New Jersey, 2003, p. 109-137.

Gabriel JP, Scharstein H, Schmidt J and Büschges A. Control of flexor motoneuron activity during single leg walking of the stick insect on an electronically controlled treadwheel. *J Neurobiol* 56: 237-251, 2003.

Gabriel JP. *Activity of leg motoneurons during single leg walking of the stick insect: from synaptic inputs to motor performance.* PhD thesis, University of Cologne, 2005.

Gabriel JP and Büschges A. Control of stepping velocity in a single insect leg during walking. *Philos Transact A Math Phys Eng Sci* 365: 251-271, 2007.

Goldammer J. *Anatomie und Optophysiologie von Motoneuronen im Mesothorakal-ganglion von Carausius morosus - Neuronales Tracing und Calcium-Imaging*. Diploma thesis, University of Cologne, 2008.

Goodman CS, Pearson KG and Spitzer NC. Electrical excitability: A spectrum of properties in the progeny of a single embryonic neuroblast. *Proc Natl Acad Sci* 77: 1676-1680, 1980.

Graham D. A behavioural analysis of the temporal organisation of walking movements in the 1st instar and adult stick insect (*Carausius morosus*). *J Comp Physiol* 81: 23-52, 1972.

Graham D and Cruse H. Coordinated walking of stick insects on a mercury surface. *J Exp Biol* 92: 229-241, 1981.

Graham D and Epstein S. Behaviour and motor output for an insect walking on a slippery surface. II. Backward walking. *J Exp Biol* 118: 287-296, 1985.

Graham D. Pattern and control of walking in insects. *Adv Insect Physiol* 18: 31-140, 1985.

Graubard K. Synaptic transmission without action potentials: input-output properties of a non-spiking presynaptic neuron. *J Neurophysiol* 41: 1014-1025, 1978.

Grey MJ, Nielsen JB, Mazzaro N and Sinkjaer T. Positive force feedback in human walking. *J Physiol* 581: 99-105, 2007.

Grillner S. Neurobiological bases of rhythmic motor acts in vertebrates. *Science* 228: 143-149, 1985.

Grillner S and Wallén P. Cellular bases of a vertebrate locomotor system - steering, intersegmental and segmental co-ordination and sensory control. *Brain Res Rev* 40: 92-106, 2002.

Grillner S. The motor infrastructure: from ion channels to neuronal networks. *Nature Rev Neurosci* 4: 573-586, 2003.

Halbertsma JM. The stride cycle of the cat: the modelling of locomotion by computerized analysis of automatic recordings. *Acta Physiol Scand (Suppl)* 521: 1-75, 1983.

Harris-Warrick RM. Voltage-sensitive ion channels in rhythmic motor systems. *Curr Opin Neurobiol* 12: 646-651, 2002.

Heitler WJ and Pearson KG. Non-spiking interactions and local interneurons in the central pattern generator of the crayfish swimmeret system. *Brain Res* 187: 206-211, 1980.

Hellekes K. *Intra- und intersegmentaler Einfluss von Bewegungssignalen im Laufsystem der Stabheuschrecke Carausius morosus*. Diploma thesis, University of Cologne, 2008.

Hengstenberg R. Spike responses of 'non-spiking' visual interneurones. *Nature* 270: 338-340, 1977.

Hess D and Büschges A. Role of proprioceptive signals from an insect femur-tibia joint in patterning motoneuronal activity of an adjacent leg joint. *J Neurophysiol* 81: 1856-1865, 1999.

Johnson BR and Harris-Warrick RM. Aminergic modulation of graded synaptic transmission in the lobster stomatogastric ganglion. *J Neurosci* 10: 2066-2076, 1990.

Kittmann R, Schmitz J and Büschges A. Premotor interneurons in generation of adaptive leg reflexes and voluntary movements in stick insects. *J Neurobiol* 31: 512-531, 1996.

Ludwar BC. *Mechanisms for intersegmental leg coordination in walking stick insects*. PhD thesis, University of Cologne, 2003.

Marder E and Calabrese RL. Principles of rhythmic motor pattern generation. *Physiol Rev* 76: 687-717, 1996.

Marder E and Bucher D. Central pattern generators and the control of rhythmic movements. *Curr Biol* 11: 986-996, 2001.

Marquardt F. Beiträge zur Anatomie der Muskulatur und der peripheren Nerven von *Carausius (Dixippus) morosus* Br. *Zool Jb Abt Anat* 66: 63-128, 1940.

Mendelson M. Oscillator neurons in crustacean ganglia. *Science* 171: 1170-1173, 1971.

Mulloney B. Neural circuits. In: *The crustacean stomatogastric system*, edited by Selverston AI and Moulins M. Springer-Verlag, Berlin, 1987, p. 57-77.

Nothof U and Bässler U. The network producing the "active reaction" of stick insects is a functional element of different pattern generating systems. *Biol Cybern* 62: 453-462, 1990.

Orlovsky GN, Deliagina TG and Grillner S (Eds.). *Neuronal Control of Locomotion*. Oxford University Press, New York, 1999.

Pearson KG and Fourtner CR. Nonspiking interneurons in walking system of the cockroach. *J Neurophysiol* 38: 33-52, 1975.

Pearson KG and Collins DF. Reversal of the influence of group Ib afferents from plantaris on activity in medial gastrocnemius muscle during locomotor activity. *J Neurophysiol* 70: 1009-1017, 1993.

Pearson KG. Common principles of motor control in vertebrates and invertebrates. *Annu Rev Neurosci* 16: 265-297, 1993.

Pearson KG. Neural adaptation in the generation of rhythmic behavior. *Annu Rev Physiol* 62: 723-753, 2000a.

Pearson KG. Motor systems. *Curr Opin Neurobiol* 10: 649-654, 2000b.

Pearson KG. Generating the walking gait: role of sensory feedback. *Prog Brain Res* 143: 123-129, 2004.

Pflüger HJ. The control of the rocking movements of the phasmid *Carausius morosus* Br. *J Comp Physiol* 120: 181-202, 1977.

Rall W. Functional aspects of neuronal geometry: their significance for vertebrate and invertebrate nervous systems. In: *Neurones without impulses*, edited by Roberts A and Bush BMH. Cambridge University Press, Cambridge, 1981, p. 223-254.

Ritzmann RE and Büschges A. Insect walking: from reduced preparations to natural terrain. In: *Invertebrate Neurobiology*, edited by North G and Greenspan R. Cold Spring Harbor Laboratory Press, New York, 2007a, p. 229-250.

Ritzmann RE and Büschges A. Adaptive motor behavior in insects. *Curr Opin Neurobiol* 17: 629-636, 2007b.

Sachs L. *Statistische Auswertungsmethoden*. Springer-Verlag, Berlin, 1971.

Sauer AE, Driesang RB, Büschges A and Bässler U. Information processing in the femur-tibia control loop of stick insects 1. The response characteristics of two nonspiking interneurons result from parallel excitatory and inhibitory inputs. *J Comp Physiol A* 177: 145-158, 1995.

Sauer AE, Driesang RB, Büschges A and Bässler U. Distributed processing on the basis of parallel and antagonistic pathways. Simulation of the femur-tibia control system in the stick insect. *J Comput Neurosci* 3: 179-198, 1996.

Schmitz J. Properties of the feedback system controlling the coxa-trochanter joint in the stick insect. *Comp Biol Cybern* 55: 35-42, 1986.

Schmitz J, Büschges A and Delcomyn F. An improved electrode design for *en passant* recording from small nerves. *Comp Biochem Physiol A* 91: 769-772, 1988.

Schmitz J, Büschges A and Kittmann R. Intracellular recordings from nonspiking interneurons in a semiintact tethered walking stick insect. *J Neurobiol* 22: 907-921, 1991.

Schofield P. Ionic permeability of the blood-brain barrier system of an insect *Carausius morosus*. *J Exp Biol* 82: 385-388, 1979.

Siegler MVS and Burrows M. The morphology of local non-spiking interneurones in the metathoracic ganglion of the locust. *J Comp Neurol* 183: 121-147, 1979.

Siegler MVS and Burrows M. Non-spiking interneurones and local circuits. *Trends Neurosci* 3: 73-77, 1980.

Siegler MVS. Local interneurones and local interactions in arthropods. *J Exp Biol* 112: 253-281, 1984.

Siegler MVS. Nonspiking interneurons and motor control in insects. *Adv Insect Physiol* 18: 249-304, 1985.

Simmers AJ and Bush BMH. Non-spiking neurones controlling ventilation in crabs. *Brain Res* 197: 247-252, 1980.

Skorupski P and Sillar KT. Phase-dependent reversal of reflexes mediated by the thoracocoxal muscle receptor organ in the crayfish, *Pacifastacus leniusculus*. *J Neurophysiol* 55: 689-695, 1986.

Stein P, Grillner S, Selverston AI and Stuart D (Eds.). *Neurons, Networks, and Motor Behavior*. MIT Press, Cambridge, 1997.

Stein W and Sauer AE. Modulation of sensorimotor pathways associated with gain changes in a posture-control network of an insect. *J Comp Physiol A* 183: 489-501, 1998.

Storrer J, Bässler U and Mayer S. Motoneurone im Meso- und Metathorakalganglion der Stabheuschrecke *Carausius morosus*. *Zool Jb Physiol* 90: 359-374, 1986.

Takahata M, Nagayama T and Hisada M. Physiological and morphological characterization of anaxonic non-spiking interneurons in the crayfish motor control system. *Brain Res* 226: 309-314, 1981.

von Uckermann G. *Untersuchung zur Kontrolle der Extensor-Aktivität im Einbeinpräparat der Stabheuschrecke Carausius morosus*. Diploma thesis, University of Cologne, 2004.

Weidler DJ and Diecke FP. The role of cations in conduction in the central nervous system of the herbivorous insect *Carausius morosus*. *Z Vergl Physiol* 64: 372-399, 1969.

Weiland G and Koch UT. Sensory feedback during active movements of stick insects. *J Exp Biol* 133: 137-156, 1987.

Wendler G. Laufen und Stehen der Stabheuschrecke *Carausius morosus*: Sinnesborstenfelder in den Beingelenken als Glieder von Regelkreisen. *Z Vergl Physiol* 48: 198-250, 1964.

Wendler G. Erzeugung und Kontrolle koordinierter Bewegungen bei Tieren - Beispiele an Insekten. In: *Kybernetik*, edited by Hauske G and Butenandt E. Oldenburg-Verlag, München, 1977, p. 11-34.

Westmark S. *State-dependent long lasting modulation of leg motoneuron membrane potential during stick insect walking*. PhD thesis, University of Cologne, 2007.

Wilson D. Insect walking. *Annu Rev Entomol* 11: 103-123, 1966.

Wilson JA. Unique, identifiable local nonspiking interneurons in the locust mesothoracic ganglion. *J Neurobiol* 12: 353-366, 1981.

Wilson JA and Phillips CE. Locust local nonspiking interneurons which tonically drive antagonistic motor neurons: physiology, morphology and ultrastructure. *J Comp Neurol* 204: 21-31, 1982.

Wilson JA and Phillips CE. Pre-motor non-spiking interneurons. *Prog Neurobiol* 20: 89-107, 1983.

Wolf H and Büschges A. Nonspiking local interneurons in insect leg motor control. II. Role of nonspiking local interneurons in the control of leg swing during walking. *J Neurophysiol* 73: 1861-1875, 1995.

Yakovenko S, McCrea D, Stecina K and Prochazka A. Control of locomotor cycle durations. *J Neurophysiol* 94: 1057-1065, 2005.

Zill SN. Plasticity and proprioception in insects. II. Modes of reflex action of the locust metathoracic femoral chordotonal organ. *J Exp Biol* 116: 463-480, 1985.

Appendix

A Operating range data of all NSI recordings

	max hyperpolarization [mV]	RMP [mV]	max depolarization [mV]
E1	-52	-43	-39
	-53	-47	-43
	-45	-33	-30
E2/3	-56	-52	-46
	-71	-60	-54
	-70	-65	-57
	-61	-54	-45
	-74	-66	-40
	-70	-65	-51
	-53	-48	-40
	-51	-45	-36
	-47	-42	-30
E4	-62	-62	-47
	-55	-55.6	-40
	-62	-57	-48
	-54	-45	-29
	-66	-60	-36
E5	-51	-44	-35
	-60	-55	-45
	-64	-58	-50
	-53	-50	-33
	-62	-55	-45
	-60	-50	-43
	-53	-50	-33

	max hyperpolarization [mV]	**RMP [mV]**	**max depolarization [mV]**
E6	-72	-68	-52
	-64	-61	-39
	-84	-78	-65
	-64	-62	-47
	-73	-66	-60
	-62	-58	-54
	-56	-48	-44
E7	-43	-40	-38
	-54	-53	-47
E8	-55	-50	-40
	-52.5	-53	-46
	-71	-63	-52
	-68	-64	-55
	-60	-45	-30
	-75	-55	-50
	-74	-70	-54
I1	-68	-60	-43
	-64	-54	-47
	-47	-42	-32
I2	-61	-50	-43
	-62	-58	-54
	-64	-60	-42
	-65	-55	-49
	-72	-65	-54
	-68	-59	-48
	-55	-50	-45
	-61	-47	-36
	-67	-52	-41
I4	-59	-58	-43
	-54	-50	-37
I8	-50	-49	-40

B Reinforcement of ongoing movement

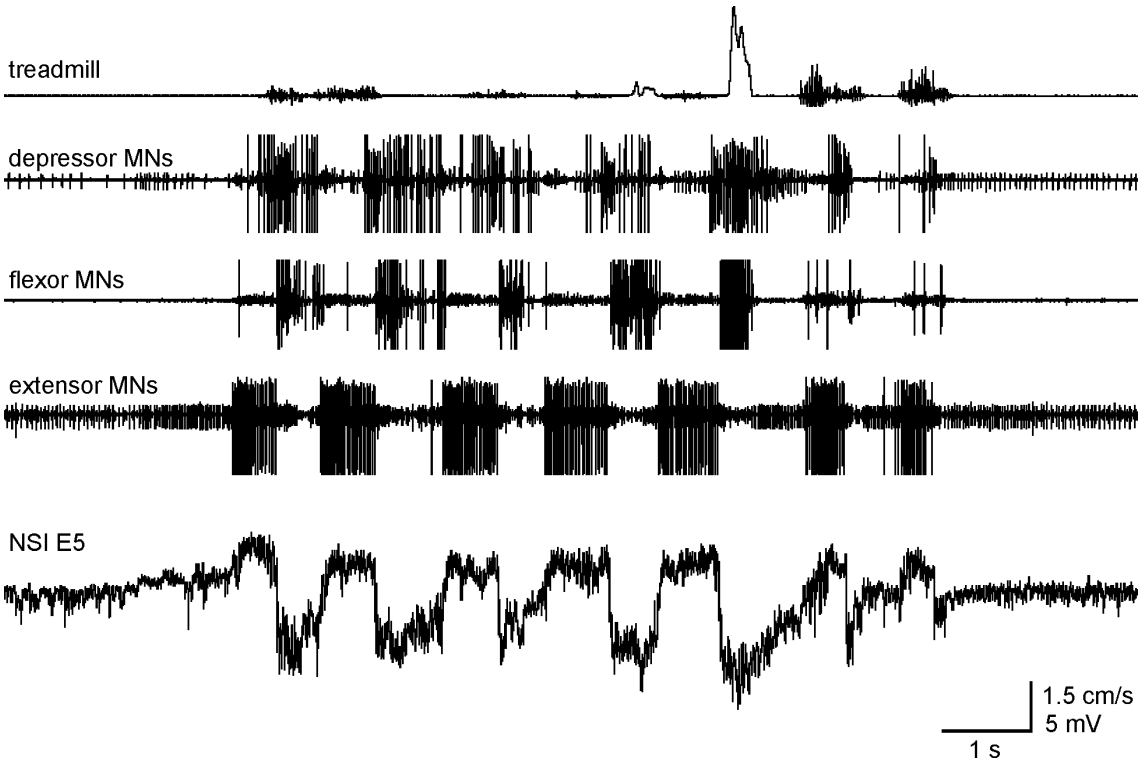

During one experiment, the animal did not perform true stepping sequences, possibly due to a mechanical damage of the leg. However, sequences of rhythmic stance and swing phase motoneuron (MN) activity could be observed (see extracellular MN recordings). When a step was performed (see treadmill trace), the neuronal stance activity was visibly reinforced, as can be seen from the extracellular recordings as well as from the intracellular recording from a nonspiking interneuron (NSI) of type E5.

C Oscillations in NSIs

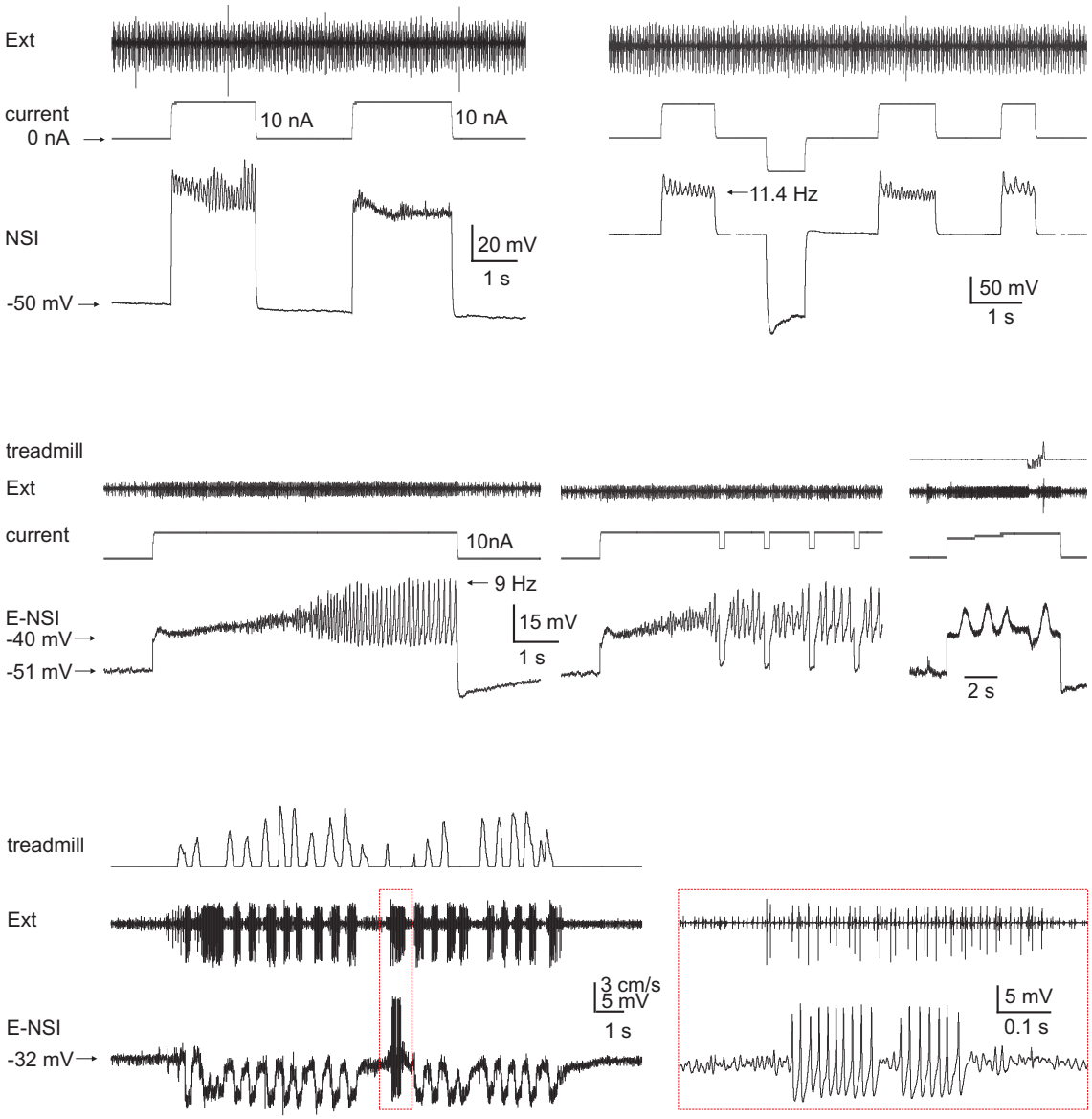

In the course of a few intracellular recordings from nonspiking interneurons (NSIs), membrane potential oscillations occurred that possibly resemble the resonant oscillation, regenerative potentials or Ca^{2+}-spikes, respectively, reported for NSIs in the locust (Laurent et al. 1993 *J Neurophysiol* 69:1484; Laurent 1993 *J Physiol* 470:45; Laurent 1990 *J Neurosci* 10:2268). These oscillations showed no direct influence on the activity of extensor motoneurons (Ext), as can be seen from the extracellular recording.

D Simplified scheme for supporting and opposing NSI activity

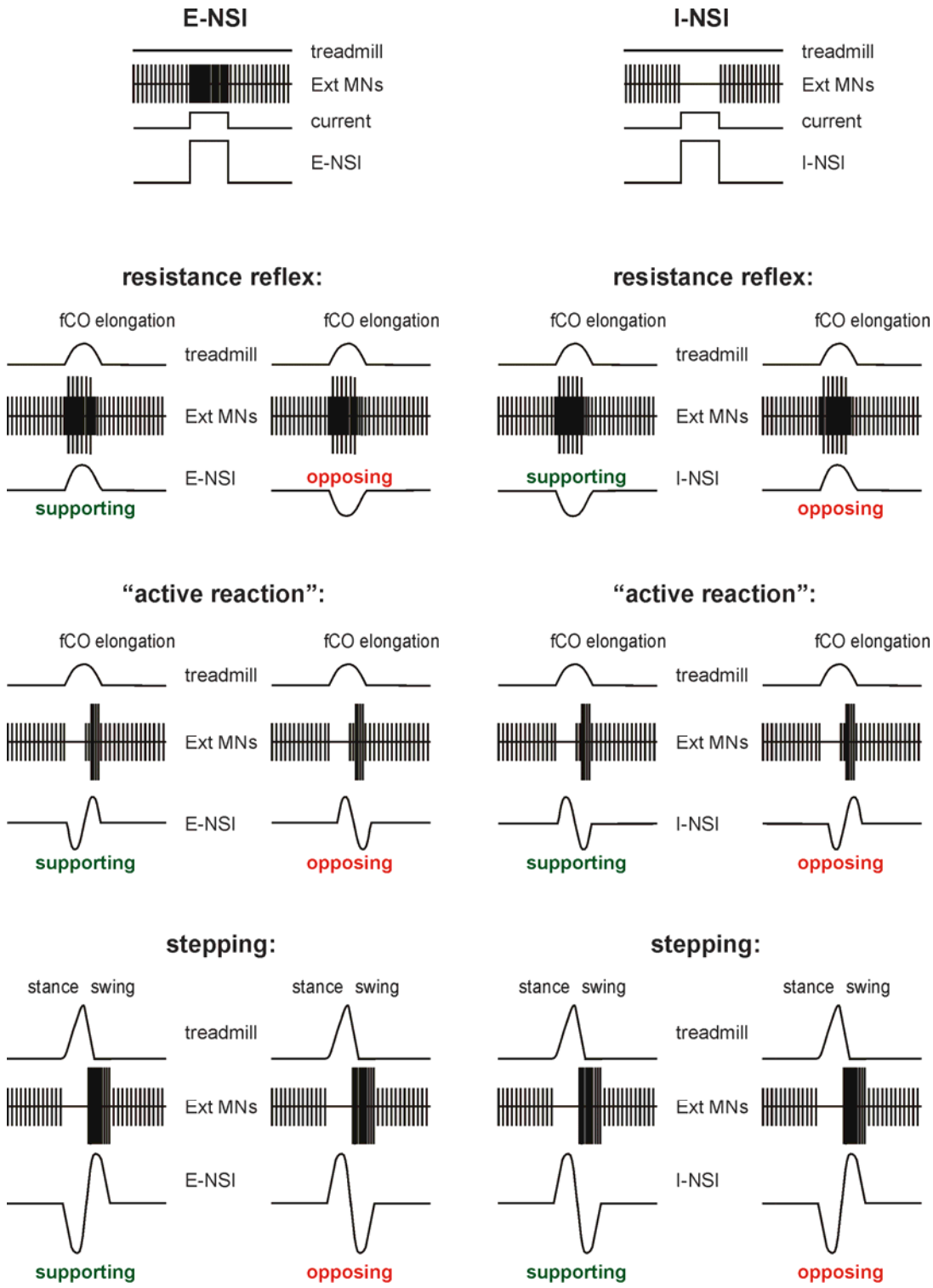

This scheme exemplifies the qualitatively different contributions of excitatory (E-) or inhibitory (I-) nonspiking interneuron (NSI) activity to a given motor program, being resistance reflex, "active reaction" or stepping. The scheme is strongly simplified and is not intended to mimic real time courses of NSI activity. For means of clarity and simplicity, only activity of extensor motoneurons (Ext MNs) is displayed, without showing activity of the antagonistic flexor MNs.

E Responses to fCO stimulation

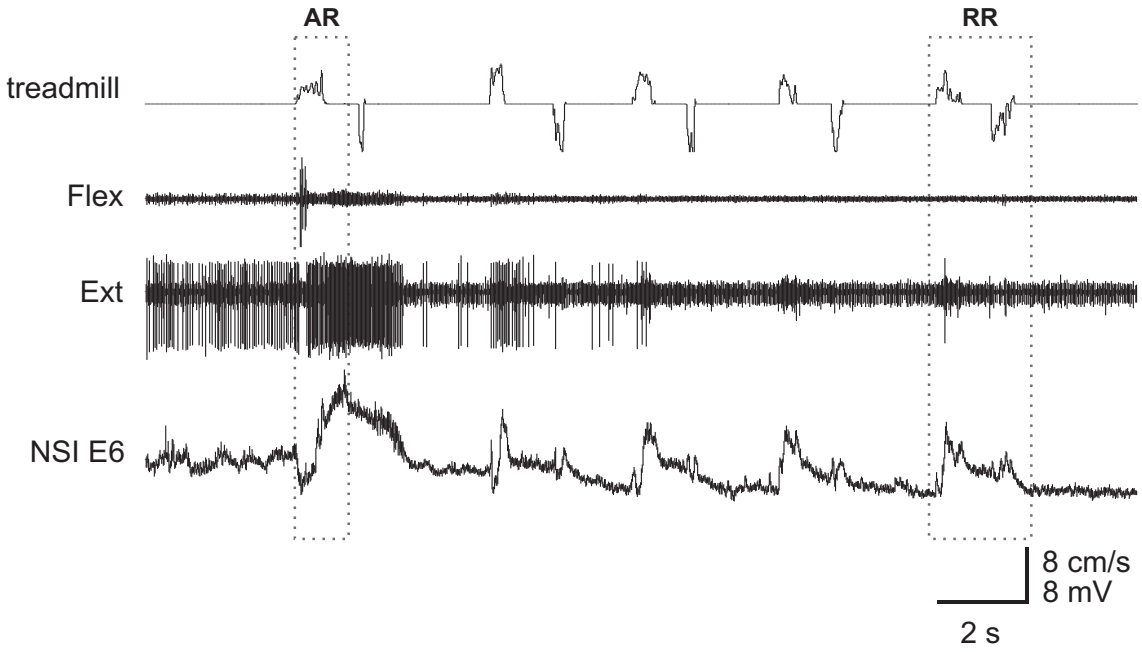

During one experiment, in which the activity of a nonspiking interneuron (NSI) of type E6 was recorded intracellularly and the femoral chordotonal organ (fCO) was stimulated several times subsequent to a period of extensor motoneuron (Ext) activity, the first fCO stimulus elicited an "active reaction" (AR), as described earlier for E6 (Driesang and Büschges 1996 *J Comp Physiol* 179:45). [The treadmill trace indicates application time and direction of fCO stimuli. During upward deflection of the treadmill trace the fCO was elongated and during downward deflection the fCO was relaxed.] In the following responses upon fCO stimulation, the time course of membrane potential varied qualitatively and finally resembled the activity pattern described for E6 during the resistance reflex (RR) (Büschges 1990 *J Exp Biol* 151:133). However, during the last fCO stimulus, no activity was elicited in the flexor motoneurons (Flex) and thereby the visible activity pattern did not fully correspond to a resistance reflex. Similar intermediate responses of NSIs upon fCO stimulation were described earlier for NSIs E3 and I1 (Driesang and Büschges 1996 *J Comp Physiol* 179:45).

F NSIs and the control of extensor MN activity

E2/3

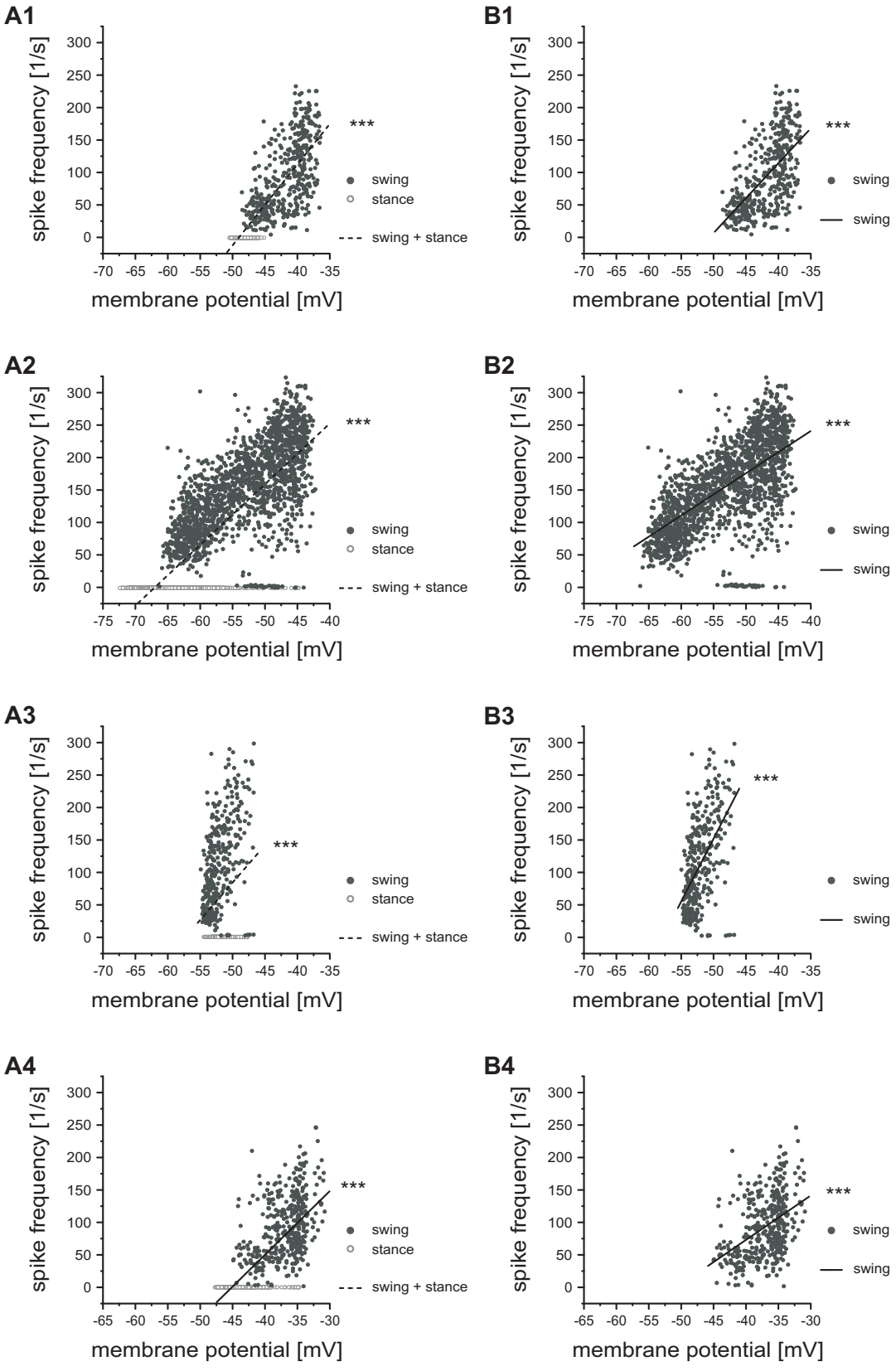

E8

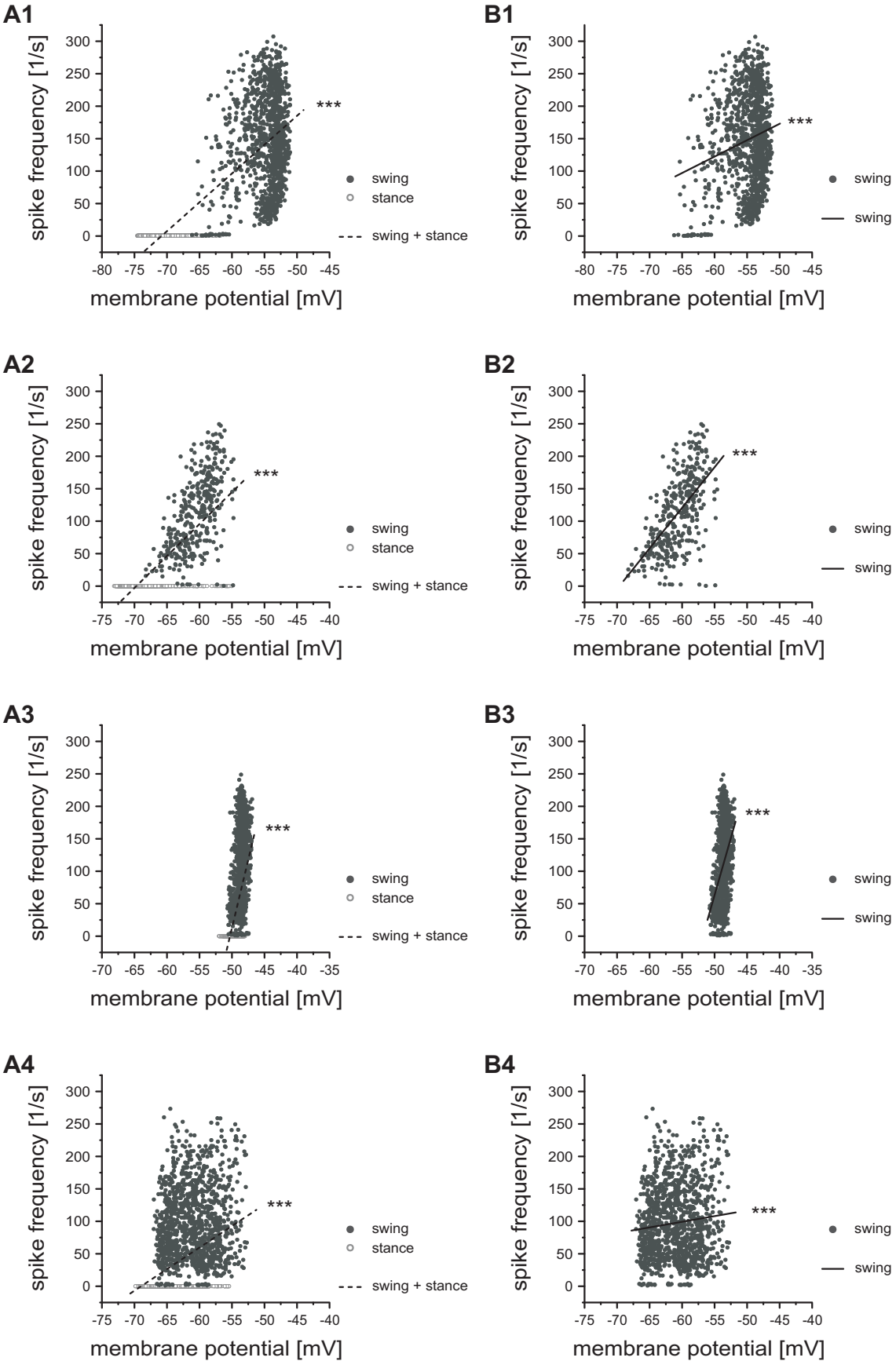
A1
B1
A2
B2
A3
B3
A4
B4
spike frequency [1/s]
membrane potential [mV]
***
swing
stance
swing + stance
swing

E4

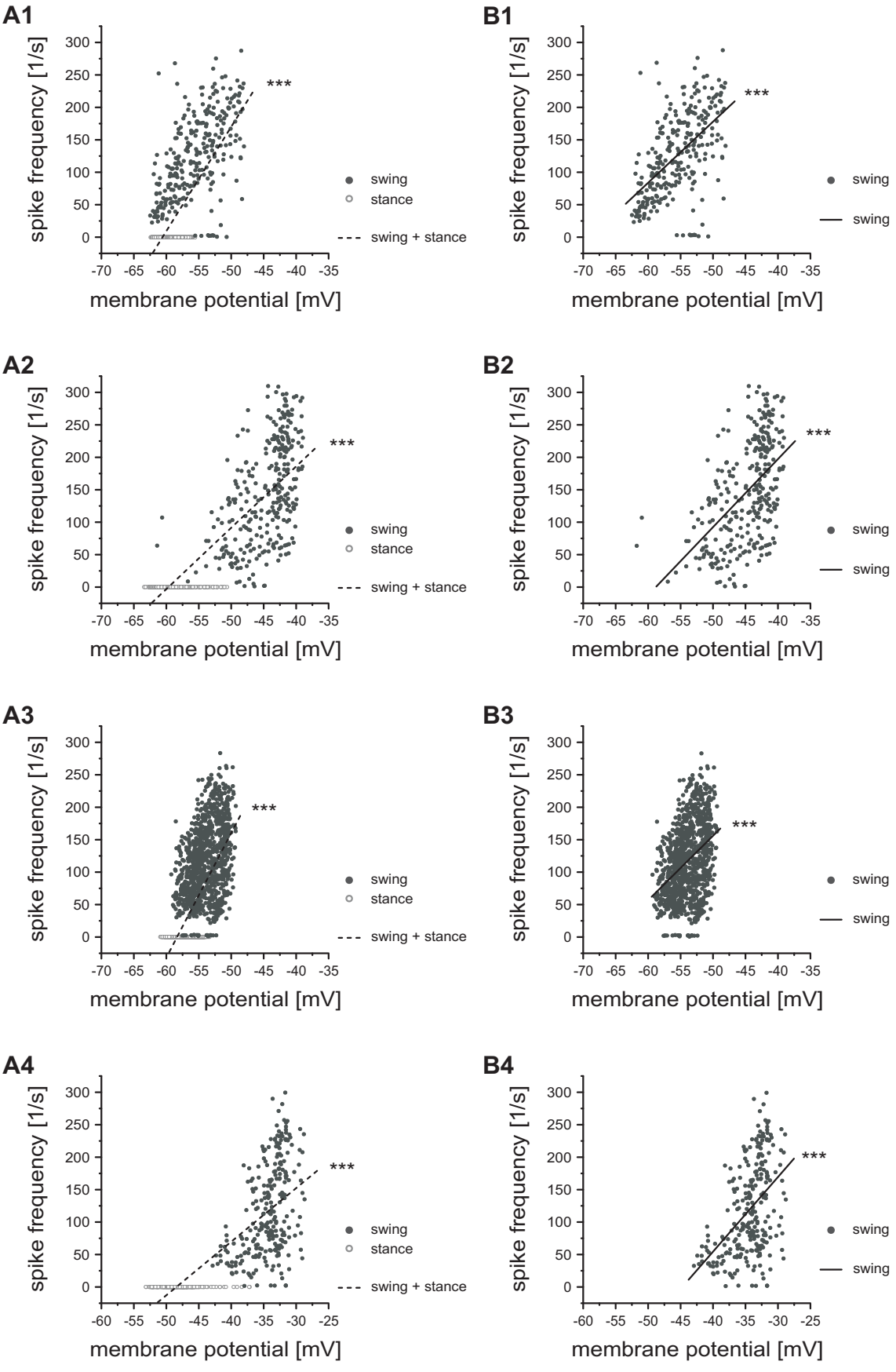
A1
B1
A2
B2
A3
B3
A4
B4
spike frequency [1/s]
membrane potential [mV]
***
swing
stance
swing + stance
swing

I2

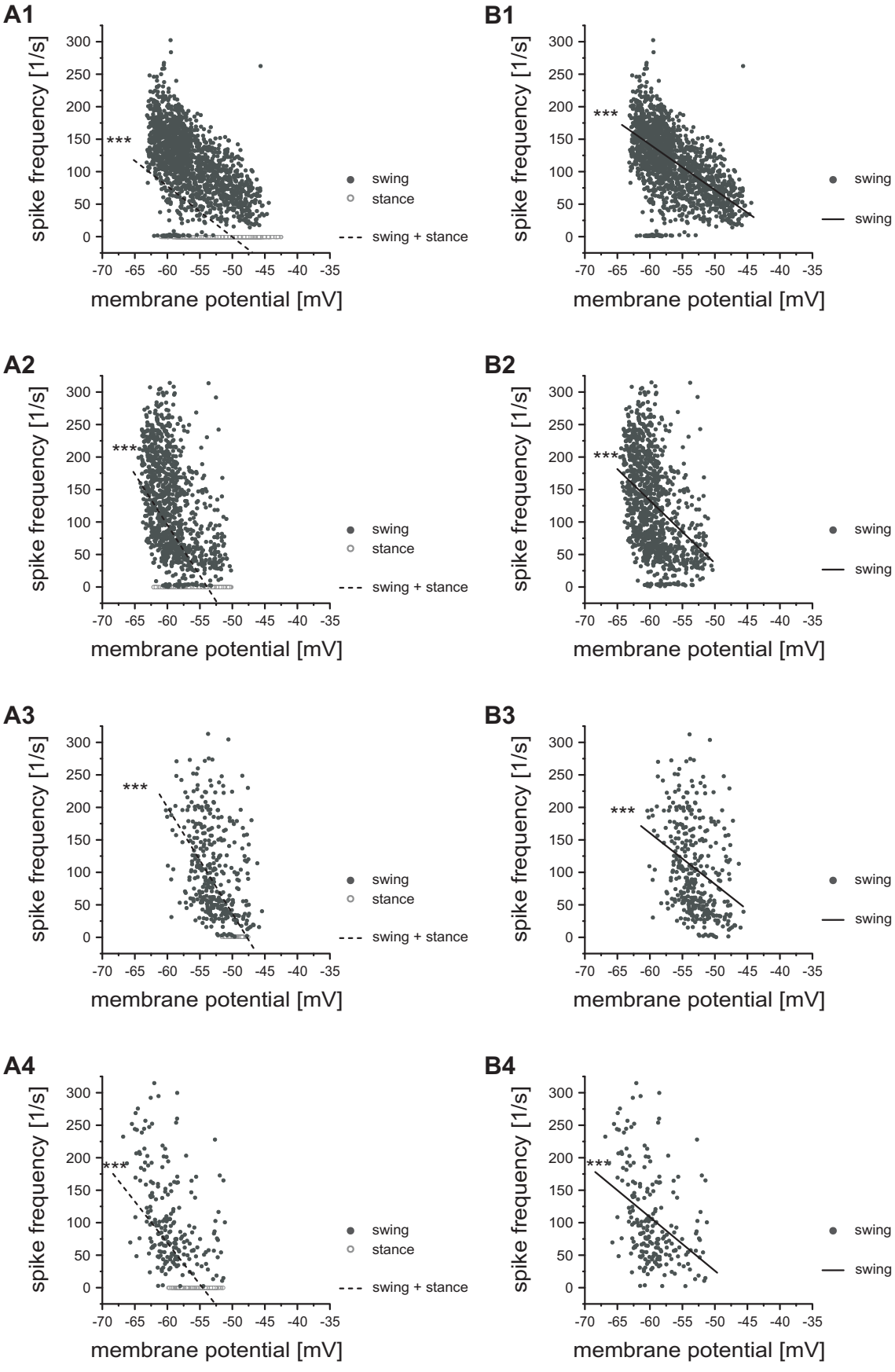
A1
B1
A2
B2
A3
B3
A4
B4
spike frequency [1/s]
membrane potential [mV]
***
swing
stance
swing + stance
swing
swing
0
50
100
150
200
250
300
-70
-65
-60
-55
-50
-45
-40
-35

I1

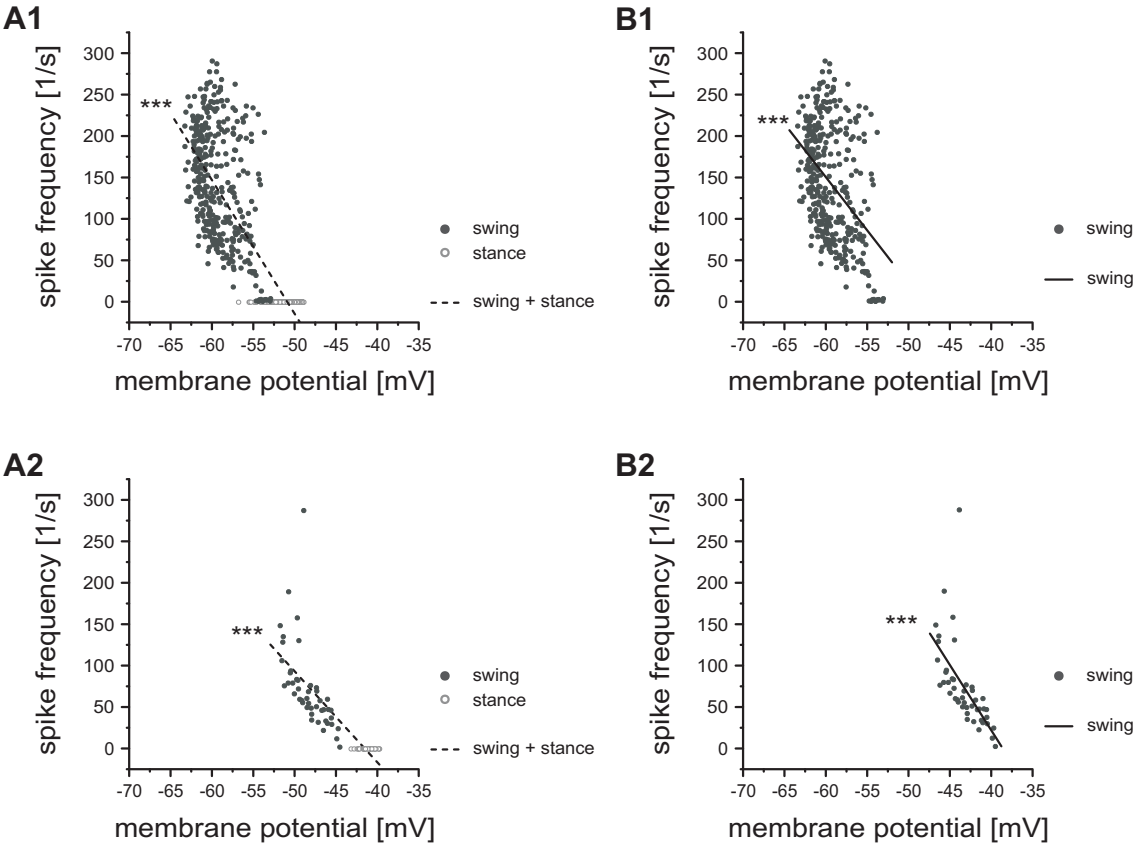
A1
B1
A2
B2
spike frequency [1/s]
membrane potential [mV]
***
swing
stance
swing + stance
swing

I4

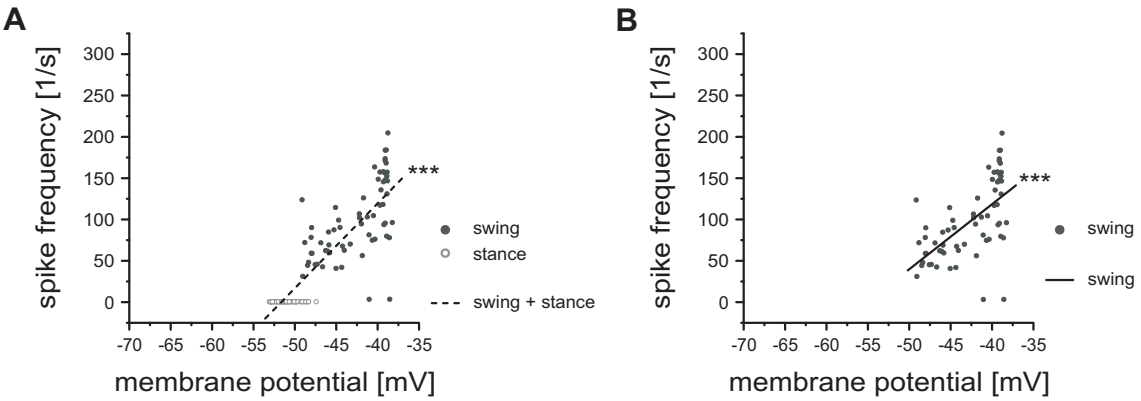
A
B
spike frequency [1/s]
membrane potential [mV]
***
swing
stance
swing + stance
swing

E5

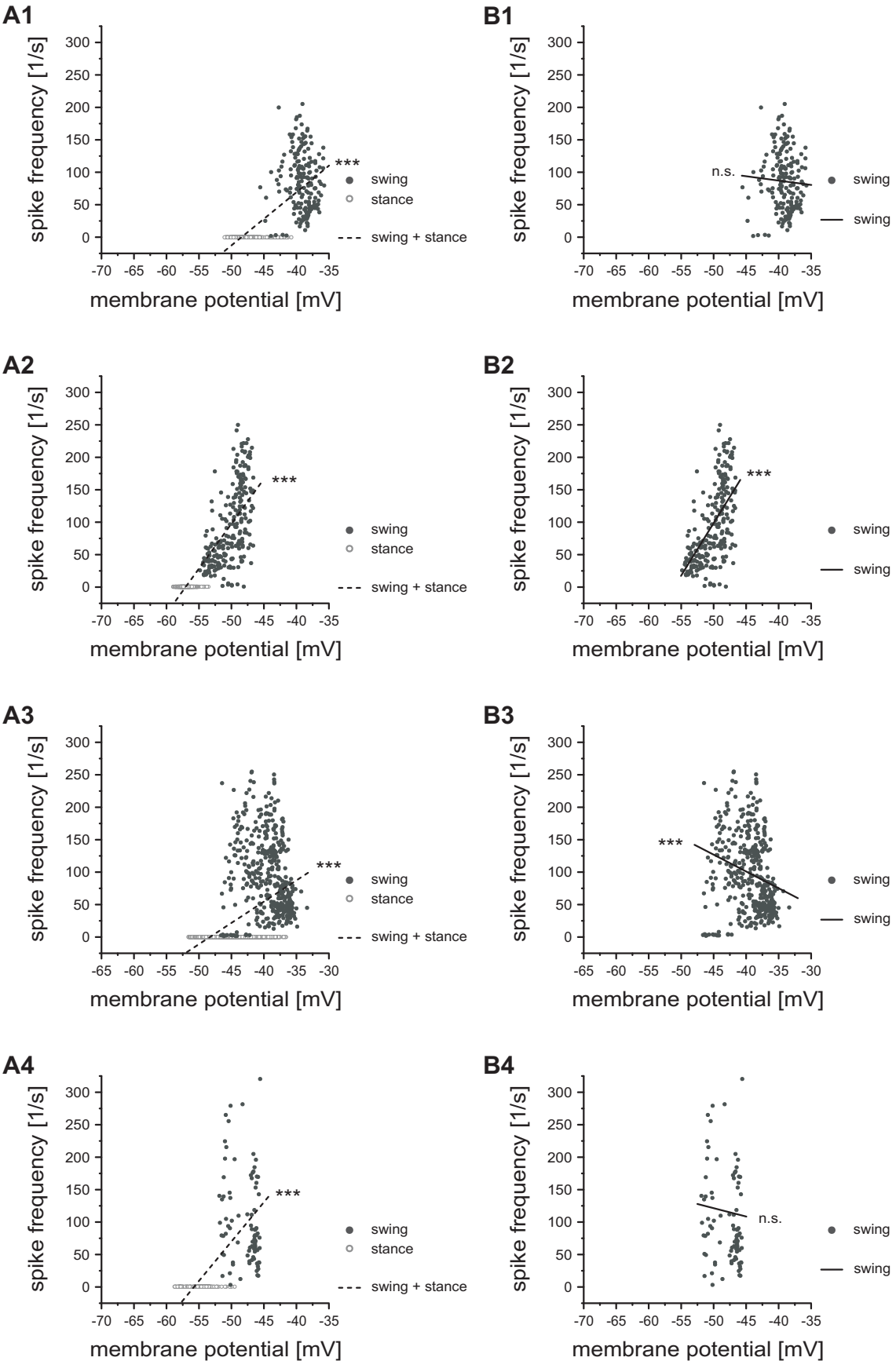
A1
B1
A2
B2
A3
B3
A4
B4
spike frequency [1/s]
membrane potential [mV]
***
n.s.
swing
stance
swing + stance

E6

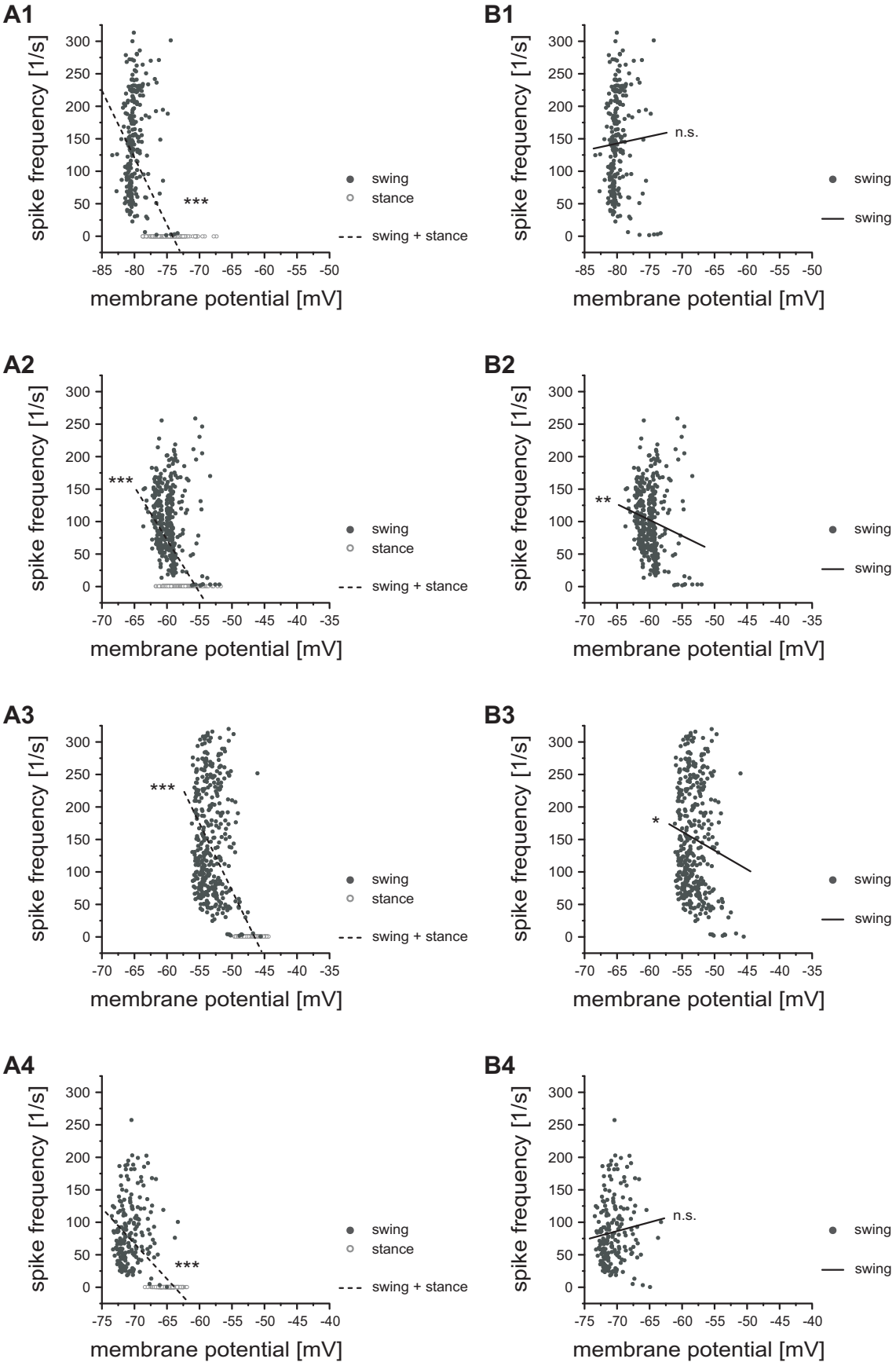
A1
B1
A2
B2
A3
B3
A4
B4
spike frequency [1/s]
membrane potential [mV]
swing
stance
swing + stance
***
**
*
n.s.

E1

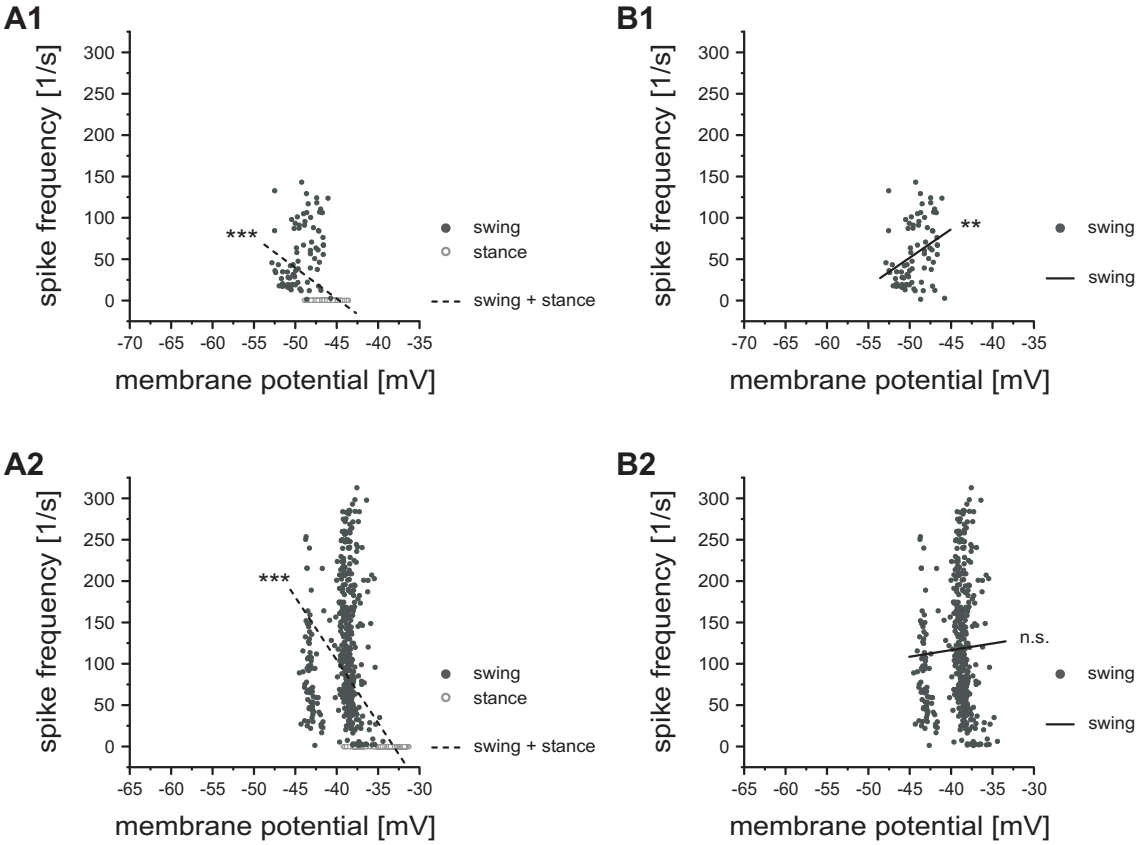
A1
B1
A2
B2
spike frequency [1/s]
membrane potential [mV]
***
**
n.s.
swing
stance
swing + stance
swing
swing

E7

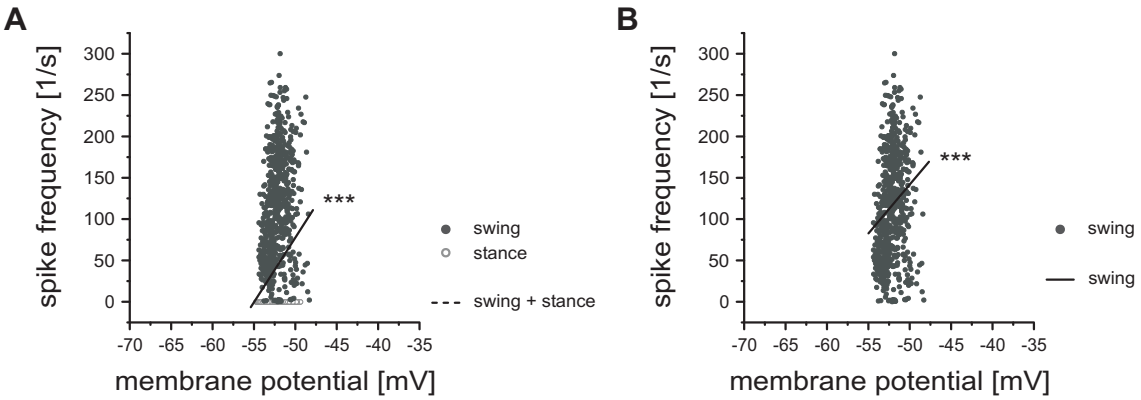
A
B
spike frequency [1/s]
membrane potential [mV]
***
swing
stance
swing + stance
swing
swing

G Instantaneous FETi mean/max spike frequency versus mean/max stepping velocity

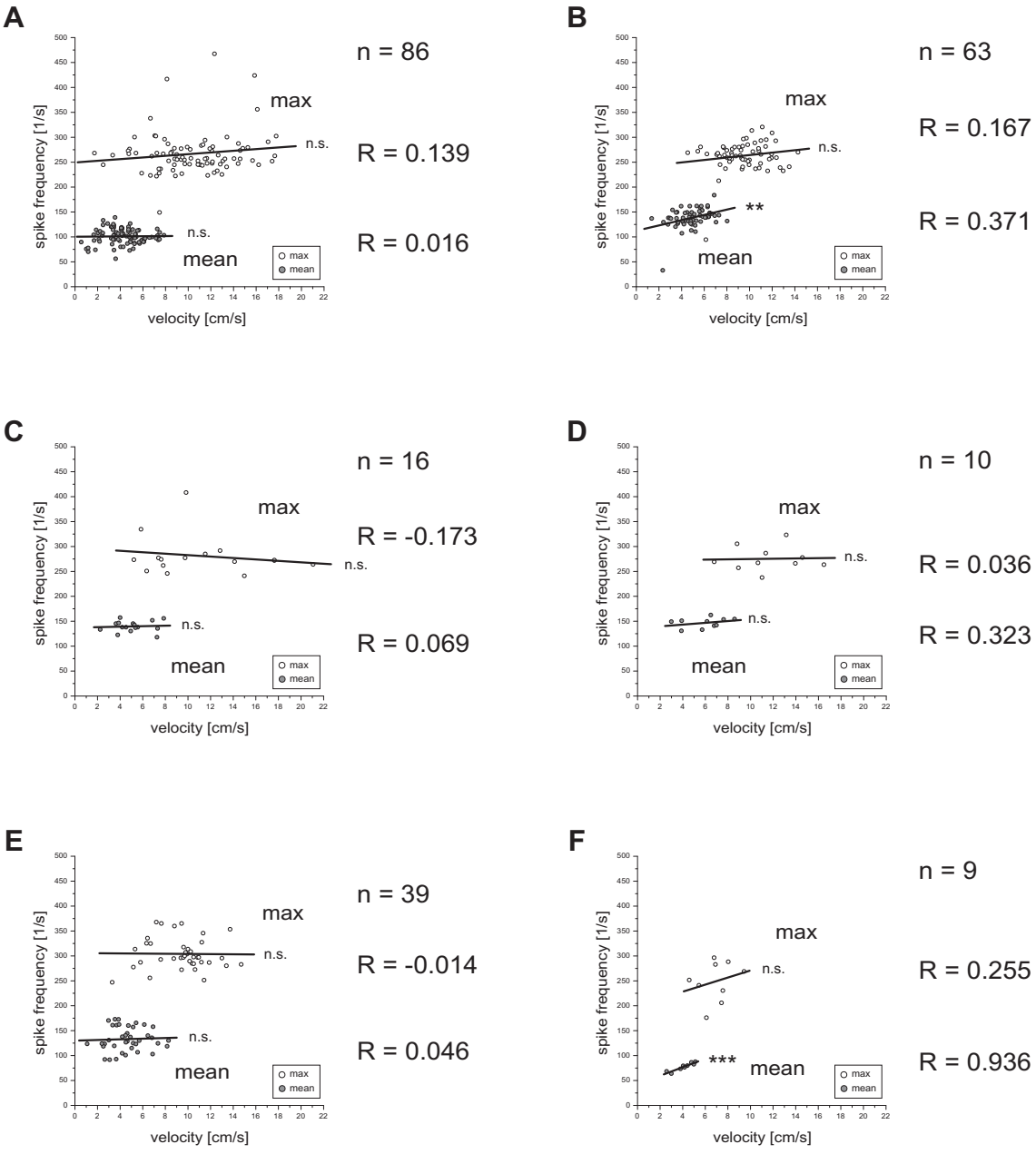

G

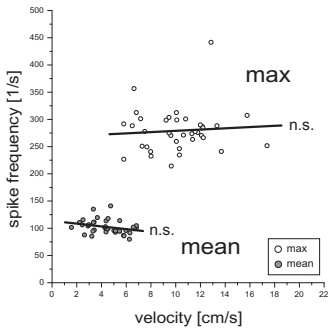

n = 37

R = 0.078

R = -0.284

H

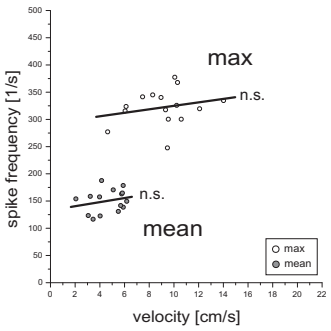

n = 15

R = 0.234

R = 0.230

I

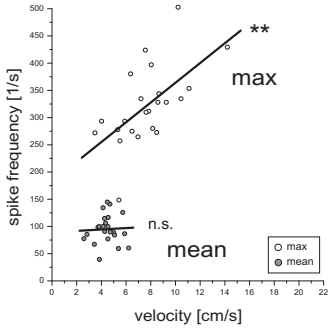

n = 23

R = 0.602

R = 0.043

J

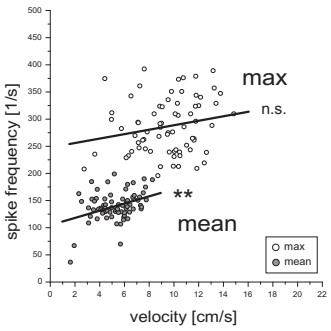

n = 72

R = 0.204

R = 0.368

K

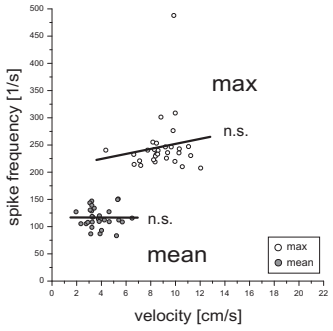

n = 30

R = 0.142

R = -0.002

L

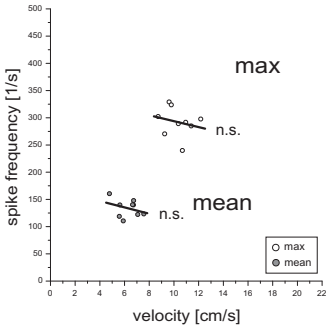

n = 9

R = -0.224

R = -0.319

M

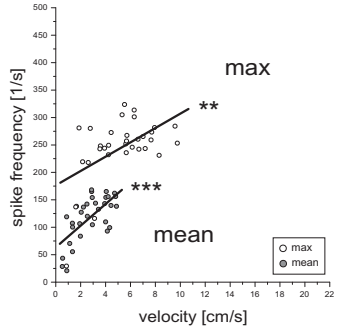

n = 32

R = 0.520

R = 0.668

N

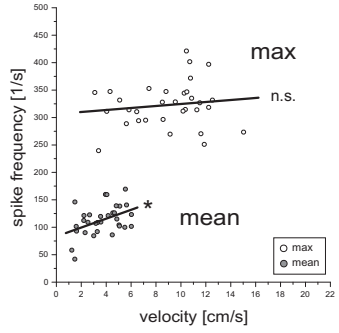

n = 32

R = 0.135

R = 0.435

H Instantaneous FETi spike frequency time-to-peak versus mean stepping velocity

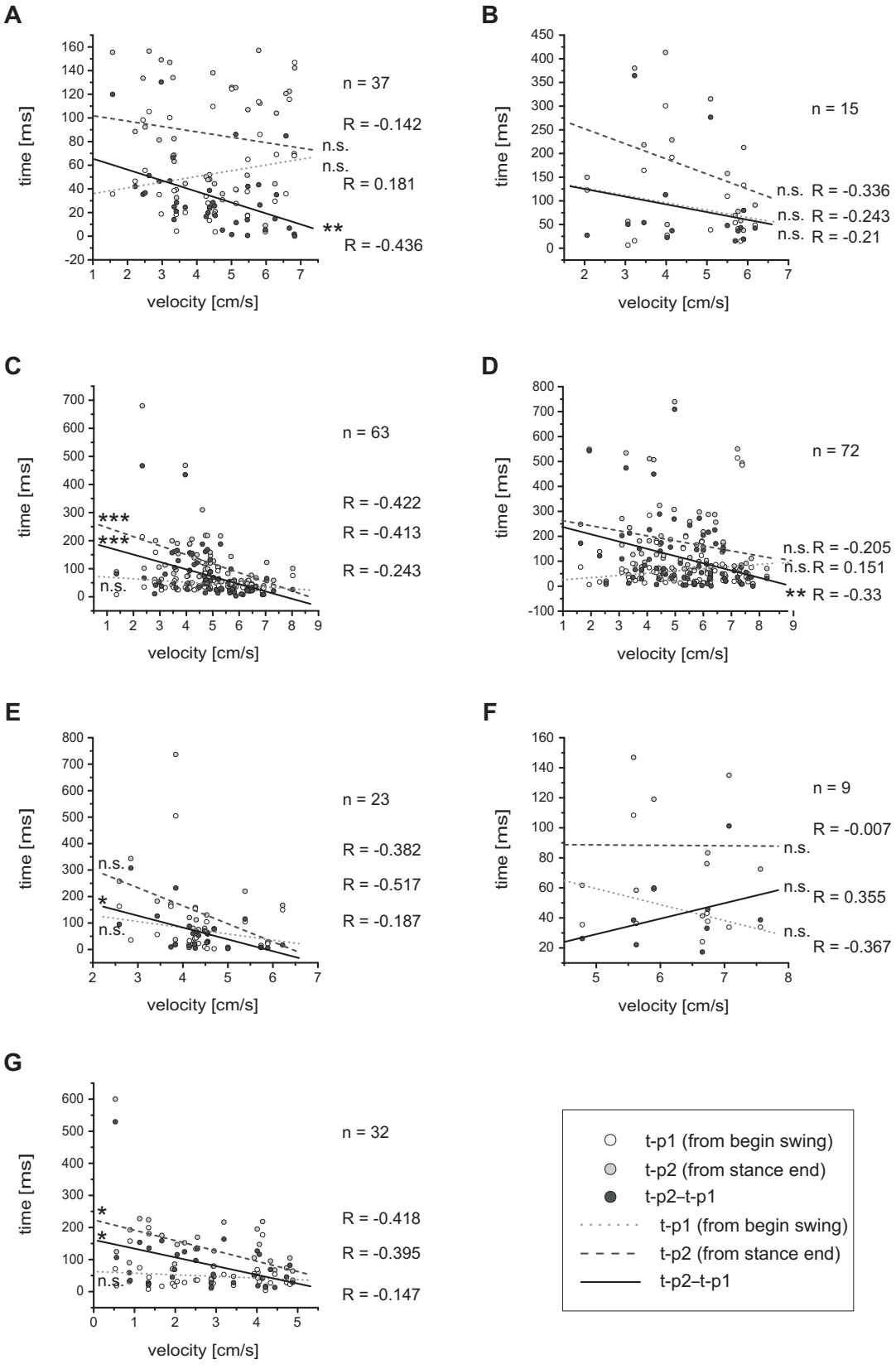

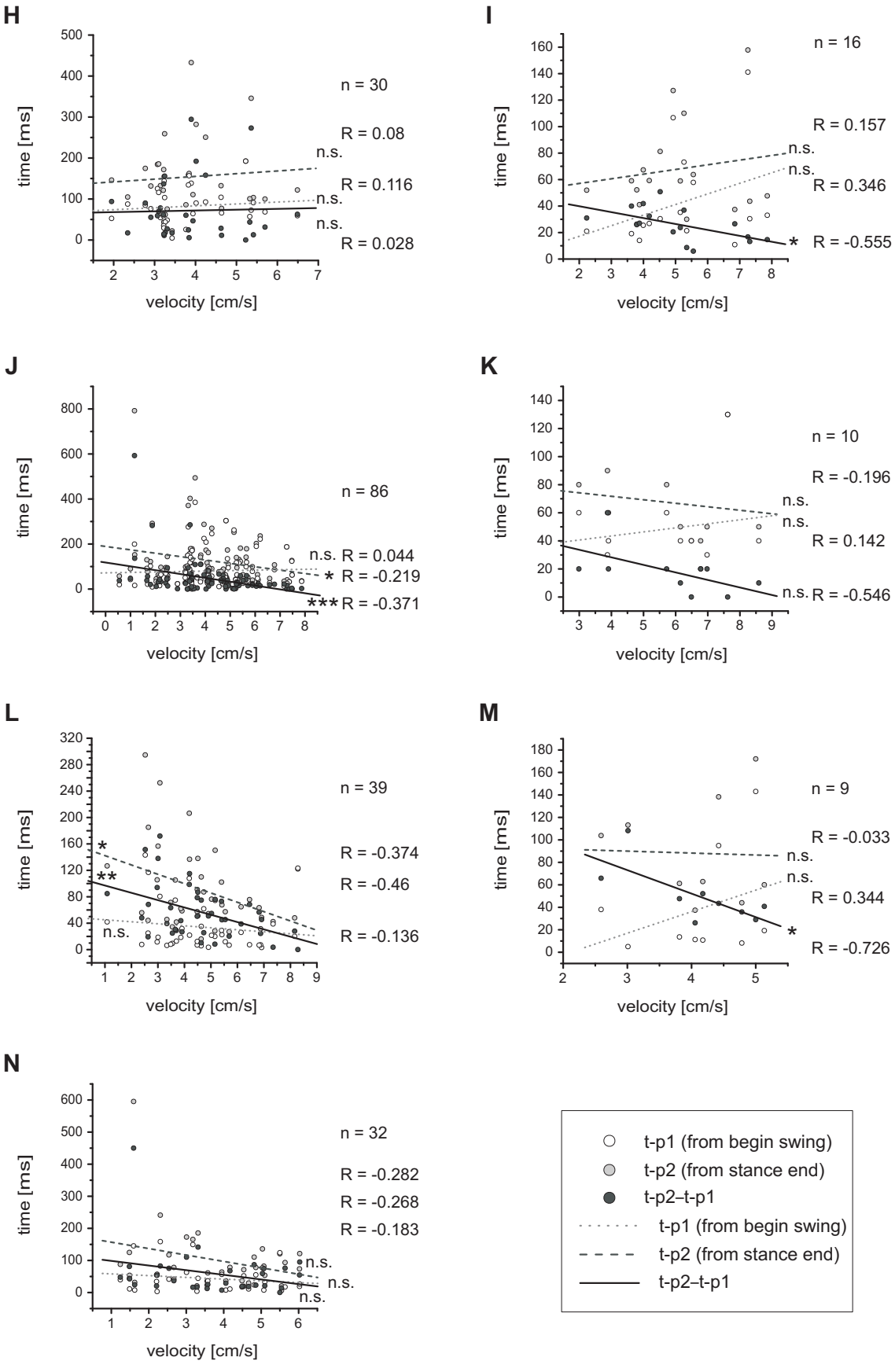
H
time [ms]
velocity [cm/s]
n = 30
R = 0.08
n.s.
R = 0.116
n.s.
n.s.
R = 0.028
I
n = 16
R = 0.157
n.s.
n.s.
R = 0.346
*
R = -0.555
J
n = 86
n.s. R = 0.044
* R = -0.219
*** R = -0.371
K
n = 10
R = -0.196
n.s.
n.s.
R = 0.142
n.s.
R = -0.546
L
n = 39
*
R = -0.374
**
R = -0.46
n.s.
R = -0.136
M
n = 9
R = -0.033
n.s.
n.s.
R = 0.344
*
R = -0.726
N
n = 32
R = -0.282
R = -0.268
R = -0.183
n.s.
n.s.
n.s.
t-p1 (from begin swing)
t-p2 (from stance end)
t-p2–t-p1
t-p1 (from begin swing)
t-p2 (from stance end)
t-p2–t-p1

Danksagung

An dieser Stelle möchte ich allen Mitgliedern und auch ehemaligen Mitgliedern der „AG Bü“ für die gute Arbeitsatmosphäre, die Hilfsbereitschaft und die vielen lustigen Abende in Grietherbusch, Günne, Göttingen und auch in Köln sehr herzlich danken.

Besonders bedanke möchte ich mich außerdem bei

… Prof. Dr. Ansgar Büschges für das faszinierende Thema, sowie die ausgezeichnete Betreuung und Förderung,

… Prof. Dr. Peter Kloppenburg für die freundliche Übernahme des Zweitgutachtens,

… Prof. Dr. Scott Hooper für die gelungene Zusammenarbeit am Extensormuskel,

… Dr. Hans Scharstein und PD Dr. Jochen Schmidt, die immer bereit waren sich Zeit für Diskussionen und Anregungen zu nehmen,

… PD Dr. Volker Dürr für den Journal Club,

… Hans-Peter für die netten Futterfahrten und kompetente Hilfestellungen technischer Art, Micha für seine großartige Hilfe beim Setup Ent-*brumm*-en und Ähnlichem, Sharon für ihre große Hilfsbereitschaft und die gut gepflegten Versuchstiere, Sherylane für die Bereitstellung von jeglichem Laborbedarf, sowie Frau Berlingen für den Beistand im Kampf mit Formularen & Co,

... Sonja für die großartige, mannigfaltige Unterstützung, die weit über die Bereitstellung eines Druckers hinausging, und für die Zollstocker Entspannungsoase mit karibischem Strand und Dachterrassendschungel,

… meiner Familie für ihr großes Interesse an meiner Arbeit und besonders meinen Eltern für ihren steten Rückhalt, finanzieller und moralischer Art.

Erklärung

Ich versichere, dass ich die von mir vorgelegte Dissertation selbständig angefertigt, die benutzten Quellen und Hilfsmittel vollständig angegeben und die Stellen der Arbeit − einschließlich Tabellen, Karten und Abbildungen −, die anderen Werken im Wortlaut oder dem Sinn nach entnommen sind, in jedem Einzelfall als Entlehnung kenntlich gemacht habe; dass diese Dissertation noch keiner anderen Fakultät oder Universität zur Prüfung vorgelegen hat; dass sie − abgesehen von den nachfolgend angegebenen Teilpublikationen − noch nicht veröffentlicht worden ist sowie, dass ich eine solche Veröffentlichung vor Abschluss des Promotionsverfahrens nicht vornehmen werde. Die Bestimmungen der Promotionsordnung sind mir bekannt. Die von mir vorgelegte Dissertation ist von Prof. Dr. Ansgar Büschges betreut worden.

Köln, den 22.04.2008

Teilpublikationen

Articles

Hooper SL, Guschlbauer C, von Uckermann G and Büschges A. Slow temporal filtering may largely explain the transformation of stick insect (*Carausius morosus*) extensor motor neuron activity into muscle movement. *J Neurophysiol* 98: 1718-1732, 2007.

Hooper SL, Guschlbauer C, von Uckermann G and Büschges A. Different motor neuron spike patterns produce contractions with very similar rises in graded slow muscles. *J Neurophysiol* 97: 1428-1444, 2007.

Hooper SL, Guschlbauer C, von Uckermann G and Büschges A. Natural neural output that produces highly variable locomotory movements. *J Neurophysiol* 96: 2072-2088, 2006.

Poster Abstracts

von Uckermann G and Büschges A. Role of premotor nonspiking interneurons in the control of stepping velocity in the stick insect *Carausius morosus*. International workshop funded by the DFG (Deutsche Forschungsgemeinschaft) "Load and force control in walking pattern generation of animals and robots: from sensors to local and global control function", Cologne, n° 9, 2008.

von Uckermann G and Büschges A. Reinforcement of movement and the neural control for single leg stepping in the stick insect. 100th Annual Meeting of the DZG (Deutsche Zoologische Gesellschaft), n° N22, 2007.

von Uckermann G and Büschges A. Contribution of nonspiking interneurons to the local control of single leg walking in the stick insect. Proceedings of the 31th Göttingen Neurobiology Conference and the 7th Meeting of the German Neuroscience Society, no T22-3B, 2007.

von Uckermann G and Büschges A. Do premotor nonspiking interneurons contribute to changes in stepping velocity in the stick insect? International Spring School "Interdisziplinäres Kolleg", Günne am Möhnesee, no 25, 2007.

von Uckermann G and Büschges A. Local premotor nonspiking interneurons in the control of stick insect single leg walking. Conference "Neurovisionen: Perspektiven in NRW", Düsseldorf, no 13, 2006.

von Uckermann G, Gabriel JP and Büschges A. The local control of tibial motoneuron activity during single leg walking in the stick insect. 98th Annual Meeting of the DZG (Deutsche Zoologische Gesellschaft), no 7_Po_02, 2005.

von Uckermann G and Büschges A. Nonspiking interneurons and the local control of extensor tibiae motoneuron activity during single leg walking in the stick insect. Proceedings of the 30th Göttingen Neurobiology Conference and the 6th Meeting of the German Neuroscience Society, no 82B, 2005.

Talk

von Uckermann G. Aktivität tibialer Motoneurone und die Kontrolle von Laufgeschwindigkeit im Einbeinpräparat der Stabheuschrecke. Workshop "Neurobiology Bonn - Cologne - Aachen", University of Bonn, 2007.